Papers Presented at the 17th Annual Canadian Meteorological and Oceanographic Society Congress Banff, Alberta

Atmospheric Sciences

Alberta
RESEARCH COUNCIL
Natural Resources Division

Cover Photo

Photograph of the INTERA/Alberta Research Council research aircraft. The specifically equipped Cessna Conquest aircraft was developed jointly by INTERA Environmental Consultants and the Alberta Research Council. The aircraft contains laser-based instruments to measure the sizes, concentrations, and shapes of liquid and ice cloud particles, and a computer for data storage and analysis.

Copies of this report are available from:

Atmospheric Sciences Department
Alberta Research Council
P.O. Box 5002
Red Deer, Alberta, Canada
T4N 5Y5

or: Publication Sales
Alberta Research Council
5th Floor, Terrace Plaza
4445 Calgary Trail South
Edmonton, Alberta
T6H 5R7

PREFACE

This report contains papers that were presented at the 17th Canadian Meteorological and Oceanographic Society Congress held in Banff, Alberta. These papers, by staff of the Atmospheric Sciences Department, represent some recent achievements and are indicative of the scope of the Atmospheric Sciences Program.

The Atmospheric Sciences Program falls within the broader mandate of the Alberta Research Council's Natural Resources Program. Advice on the general direction of research comes primarily from the Research Council's Atmospheric Sciences Program Committee and Alberta Agriculture's Advisory Committee on Weather Modification. Funding of the program was by Alberta Agriculture, Alberta Environment, Environment Canada and the Alberta Research Council. It is a pleasure to acknowledge these contributors together with all the highly skilled individuals who are part of the Atmospheric Sciences Program.

Assistance of reviewers, particularly those external to the Research Council, is also gratefully acknowledge. They were Drs. E. Reinelt, R. Charlton, E. Lozowski and K. Hage of the University of Alberta, Dr. G. Hillman from the Northern Forest Research Center (Environment Canada), and Mr. K. Grandia from INTERA Environmental Consultants.

Brian L. Barge,
Department Head and Program Manager,
Atmospheric Sciences.

Snow Climatology of the Southern Canadian Rockies

by

F.D. Barlow, F.E. Robitaille, J.W. Mason, C.M. Sackiw

Atmospheric Sciences Department
Alberta Research Council
Edmonton, Alberta

Paper presented at CMOS Congress - Banff, Alberta, May, 1983

Snow Climatology of the Southern Canadian Rockies

by

F.D. Barlow, F.E. Robitaille, J.W. Mason, C.M. Sackiw

Atmospheric Sciences Department
Alberta Research Council
Edmonton, Alberta

ABSTRACT

A preliminary analysis of the snow climatology of the Rockies south of Banff, Alberta is presented. this background study is part of a planned research effort to determine the modification potential of orographic cloud systems during the snow season. Its purpose is to assess the current snowfall climate data to determine the general character of snowfall within the possible study area.

Precipitation data from a variety of sources were analysed including A.E.S. climate stations and snow courses from Alberta, British Columbia and Montana. The temporal, altitudinal and spatial characteristics of snow are examined. A peak in snowfall amounts and frequency is found in January for the mountain A.E.S. stations. Snowpack water equivalent reaches an average maximum value in late spring. A strong correlation of snowfall with elevation is indicated by linear regression models. The spatial variability is quite complex with maximum annual snowfall amounts occurring along the Alberta-B.C. border regions. Recommendations for future research approaches are given.

1.0 INTRODUCTION

The winter snowpack of the southern Canadian Rockies is the principal water resource for irrigation agriculture in southern Alberta. Future expansion of this agriculture and accommodation of other water-based requirements depends on careful management of this regions's water resources (Environment Council of Alberta, 1982). Supplementing this water resource by increasing the snowpack storage may assist in such management.

The Alberta Research Council has initiated a preliminary project to examine the feasibility of supplementing the snowpack through the controlled use of cloud-seeding techniques. This project's initial aim is to measure and analyze the precipitation processes of the snow-producing orographic clouds. An instrumented research aircraft is being used to assess the efficiency of these cloud systems to determine if a potential "seeding window" exists (Vardiman and Moore, 1977). Preliminary analysis of upper-air data indicates that such a "window" of suitable temperature and moisture conditions may exist in the early fall or late spring (Renick et al, 1979).

The project study area straddles the Alberta-British Columbia border (Fig. 1). Knowledge of the characteristics of snowfall within this general area of the southern Canadian Rockies would assist in project design. Information on where and when snowfall occurs and which periods correspond to the "seeding window" would be particularly useful. In addition information on the spatial distribution of snow would be useful for the design of a network for any potential seeding program that may be initiated.

The general snow regime of the southern Canadian Rockies has not been previously analyzed. Detailed analyses of snowfall distribution over small areas have been done (Storr, 1973: Golding, 1974). The general climate of the contiguous mountain National Parks has also been summarized (Janz and Storr, 1977). On a larger scale, the frequency of extreme snowfall events for the province has also been investigated (Nkendirim and Benoit, 1975). The lack of snowfall analyses for the southern Canadian Rockies prompted this preliminary approach.

This paper first identifies and discusses the type and limitations of published snow data sources. An analysis of the temporal variation of snow follows. The important altitudinal variation of snow is then discussed. The analysis is completed with a brief examination of the regional variation of snowfall. Finally, recommendations on future assessment analysis needs are offered.

2.0 EVALUATION OF SNOWFALL DATA SOURCES

2.1 Data Sources

Two types of data were used for this preliminary analysis: monthly precipitation totals (cm) and seasonal snow depth measurements (mm water equivalent). Monthly snowfall values were abstracted from published monthly climate normals for Atmospheric Environment Service climate stations (Atmospheric Environment Service, 1951-1980). These averaged data represent the 30-year precipitation normal based on data from 1951 to 1980. Data synthesis techniques have been applied by A.E.S. in the normalizing procedure to accommodate missing data. This data set is considered to be the most complete, and is the principal data source for subsequent analysis.

Seasonal snow depth water equivalent values were abstracted from the published snow survey measurement programs of Alberta, British columbia and Montana. These measurements are generally made on a monthly basis from January to May (Alberta) or June (B.C. and Montana). Measurements are taken at the beginning of the month. An additional mid-May measurement may be included for some stations.

The sources, number of stations, years of record and average site elevation are summarized in Table 1. Mountain climate stations are defined as those stations located within the physiographic region of the Rocky Mountains or Foothills. An additional 25 prairie climate stations are identified for mapping purposes.

SNOW DATA SOURCES

SOURCE	TYPE	SITES	Mean Record Length (Years to 1980)		Mean Elevation (m MSL)
AES Climate Stations	Monthly Snowfall (12)				
MTN/Foothills		57	30	Normals	1182
Plains		25	30	Normals	1024
Alberta Snow Survey	Seasonal (5) (Feb.-June)	28	9.3		1857
B.C. Snow Survey	Seasonal (7) (Jan.-June)	28	13.7		1619
Montana Snow Survey	Seasonal (7) (Jan.-June)	15	9.1		1606

2.2 Data Source Analysis

The map showing the network of AES climate stations and snow survey sites (Fig. 2) includes the 6000 ft. (1825 m) contour as an indicator of terrain height. Two general features are notable. A sparse, clustered network is indicated with an approximate

value of about one station per 800 sq. km. Secondly, most of the stations are at lower elevations with only a few above the contour. These characteristics underscore the difficulty in providing a detailed and confident assessment of the snow climate.

The data sources vary substantially as to length of record and seasonal coverage. The AES climate stations generally have a longer record length. Figure 3 indicates this by showing the number of A.E.S. stations as a function of measurement record length. A bi-modal distribution is evident with peaks of station installation activity being at 20 and 60 years benchmarks. For climate assessment, the AES network record length seems quite adequate.

The different requirements and seasonal character of the snow surveys result in a data set more limited and variable than that of the A.E.S. stations. This variability, evident in both record length and number of stations, is shown for the Alberta and B.C. snow survey sites (Fig. 4). The generally longer record of B.C. data, particularly in the early months of the survey, is apparent.

3.0 RESULTS

3.1 Seasonal Snow Variation

A plot of the calculated average monthly snowfalls for all 56 mountain climate stations within the project region shows that snowfall increases from a minimum in the autumn to a monthly maximum of 50 cm in January (Fig. 5). This mid-winter maximum may reflect the higher efficiency of precipitation processes with colder temperatures and sufficient atmospheric water supply. The plateau of 30 cm to 40 cm through the late winter and early spring months gives way to the rapid decrease in late spring. The significant spring contribution suggests that the spring temperature-moisture "seeding window" may occur during periods of high natural precipitation.

Snowfall frequency (Fig. 6) follows a pattern similar to that of snowfall amount. The January peak of about 10 snow-days is followed by a decline that accelerates rapidly during the late spring. The lower April snow-day frequency, combined with the higher snowfall amount, suggests that in the late spring fewer but larger snowfalls occur.

Snow water equivalent data give a more limited view of actual snowfall, but they do provide relevant information on the seasonal character of snowpack water storage. The seasonal variation of the combined Alberta, B.C. and Montana data (Fig. 7) shows that over half (approximately 250 mm) of the maximum snowpack accumulates before the measurement program begins in January. Additional contributions throughout the winter-spring period results in a peak snowpack of 500 mm on May 1. A rapid depletion of the snowpack in late spring, which results in an increase in water flow, is also evident.

3.2 Snow Variation With Elevation

The complex topography and higher elevations of the mountain regions substantially affect snowfall characteristics. The cooler temperatures at higher elevations enhance snowfall occurrence and snowpack persistence. Station data were examined as to their variability with elevation to determine the relative importance of this factor. A plot of average annual snowfall against station elevation for the mountain AES climate stations (Fig. 8) shows a strong trend to increased snowfall amounts at higher elevations. Snowfall at lower elevation sites (e.g. 700 m MSL) may be less than one-half the annual snowfall at higher sites (e.g. 1500 m MSL). Included in Figure 8 is the calculated linear regression relation which predicts snow depth from elevation. The high, significant correlation coefficient (0.73) suggests that about 50% of the annual snowfall variation is explained by station elevation.

The seasonal variation of snowfall with elevation as measured by the correlation coefficient is more pronounced (Fig. 9). The twin peaks of high correlations in the early autumn and late spring may reflect the role of cooler temperatures at higher elevations during those periods. Snow at higher elevations would settle and remain first, and melt last, at higher elevation sites. The mid-winter low correlation reflects the ubiquitous cold temperatures within the region. The still-significant correlation during the warmer season may reflect the influence of complex topography and cooler temperatures at higher elevations.

The elevation-snow relation obtained snow survey data is less well-defined than that for average annual snowfall. Greater variability is indicated, particularly with the inclusion of the Montana data (Fig. 10). The Montana values seem to be consistently higher than those for Alberta and B.C., and may reflect differences in network criteria, data measurement procedures and quality control. The correlation coefficient of 0.59 (0.38 with Montana) suggests that only about 35% of the snow depth variation can be explained by site elevation. The complex effects of topography on snow storage may overshadow the effect of elevation on snow precipitation patterns.

3.3 Snow Spatial Variation

An analysis of the climate station data was conducted to examine the gross spatial characteristics of the regional snowfall. The sparse measurement network and complex terrain makes any data interpolation between points questionable but some patterns may be apparent. Figure 11 shows the computer-contoured average annual snowfall in the project region. This contouring includes prairie stations and is based on a one-pass weighted-average data smoothing.

The map shows that maximum snowfall amounts occur over the mountain regions, as expected. A fairly steep gradient over the drier Columbia river valley is indicated. Snowfall amounts gradually decrease across the Alberta foothills and into the lower prairie regions. The effect of the limited and irregular network is suggested by the apparent lower values over the divide southwest of Banff. This feature may be due more to network sparseness rather than any real precipitation patterns.

The variability of snowfall frequency is indicated by the annual number snowfall days (Fig. 12). Two data-smoothings were performed to minimize the significant variability of this data. A maximum frequency over the higher mountain regions is indicated. The complex pattern suggests a general tendency for the number of snowfall days to decrease eastwards across the prairies.

The high correlation of snowfall amount with site elevation may mask other factors influencing snow distribution. The previously noted snow-elevation regression model approach was used to "subtract" the elevation influence from the annual station values. Elevation-predicted annual snowfall amounts were determined for each station and the ratio of the actual to predicted values calculated. The contour plotting of these actual/predicted ratios is illustrated in Figure 13 (two smoothings). The plotted ratio can be used to suggest whether other factors may be responsible for snowfall variation. Values in excess of one indicate larger than expected snowfall values. Conversely, values less than one suggest less than expected snowfall values.

A general trend of underestimation towards the southwest and overestimation in the northeast is suggested. The excessive values for the southern part of the region may reflect the area's closer proximity to maritime moisture sources. The lower-than-expected values for the north may indicate dryer continental climate patterns.

4.0 CONCLUSION

This brief preliminary analysis has outlined some of the general characteristics of the snow climate of the southern Canadian Rockies. The seasonal strong season character of snowfall with a mid-winter peak has been indicated. The maximum snowpack depth in late spring, and subsequent rapid melt, has also been delineated. A strong correlation with site elevation provided equations for predicting snowfall and average snowpack water equivalent. The spatial distribution of snowfall has been shown to be quite variable with maximum values being indicated along the higher elevations.

These results give a preliminary overview of the snowfall climate of the snowpack study region. The temporal trend of snowfall and snowpack water equivalent suggests that a substantial contribution is made during the late winter and spring. The spring "seeding window" (Renick **et al,** 1979) may then occur during this period of substantial natural precipitation. This suggests that a potential for snowpack augmentation within the study area may occur during the spring months.

The study has also indicated the difficulty of assessing the snow climate due to the sparse network and limited snow survey record length. The importance of site elevation is also indicated. Based on these preliminary results, a measurement network for the region cannot be confidently specified.

A more detailed analysis of the precipitation data would provide a more confident climate assessment. Examination of daily records from the climate network would assist in this by identifying individual precipitation events. A time series analysis of the data may delineate any trends in the snow data. Finally, a cloud climatology of the region would provide relevant information on the snow-producing clouds of the region.

REFERENCES

1. Environment Council of Alberta, 1982, Irrigation Agriculture in Alberta, Edmonton, Alberta, 74 pp.

2. Golding, D.L., 1974, The Correlation of snowpack with topography and snowmelt runoff on Marmot Creek Basin, Alberta, Atmosphere, 12:1:31-38.

3. Janz, B. and D. Storr, 1977, The climate of the contiguous mountain parks. Banff, Jasper, Yoho, Kootenay. Atmospheric Environment Project Report No. 30.

4. Nkendirim, L.C. and P.W. Benoit, 1975, Heavy snowfall expectation for Alberta, The Canadian Geographer, 19:1:60-72.

5. Storr, D., 1973, Wind-snow relations at Marmot Creek, Alberta, Can. J. For. Res., 3:4:479-485.

6. Renick, J.H. , G.S. Strong and H. Sharp, 1979, A preliminary estimate of the winter orographic seeding potential in the Rocky Mountains of Alberta, Proceedings of the Seventh Conference on Inadvertant and Planned Weather Modification, American Meteorological Society, pp. 76-77.

7. Atmospheric Environment Service, Canadian Climate Normals, 1951-1980, British Columbia, Environment Canada, 268 pp.

8. Atmospheric Environment Service, Canadian Climate Normals, 1951-1980, Prairie Provinces, Environment Canada, 429 pp.

9. Alberta Environment, 1982, Snow Course Historical Data Summary (Mountain), Technical Services Division.

10. British Columbia Ministry of Environment, 1980, Snow Survey Measurements: Summary 1935-1980, Inventory and Engineering Branch, 219 pp.

11. U.S. Department of Agriculture, 1975, Summary of Snow Survey Measurements for Montana, Soil Conservation Service.

ACKNOWLEDGEMENT

The authors are most grateful to Mr. William Kuhnke, River Forecast Centre, Alberta, for his assistance in providing climate data. The assistance of Ms. M. Fong and Ms. L. Shannon is also acknowledged.

Figure 1. The Snow Project area. Research aircraft flights were made along specific tracks within the project boundary to obtain in situ observations of the cloud hydrometeors and thermodynamic structure.

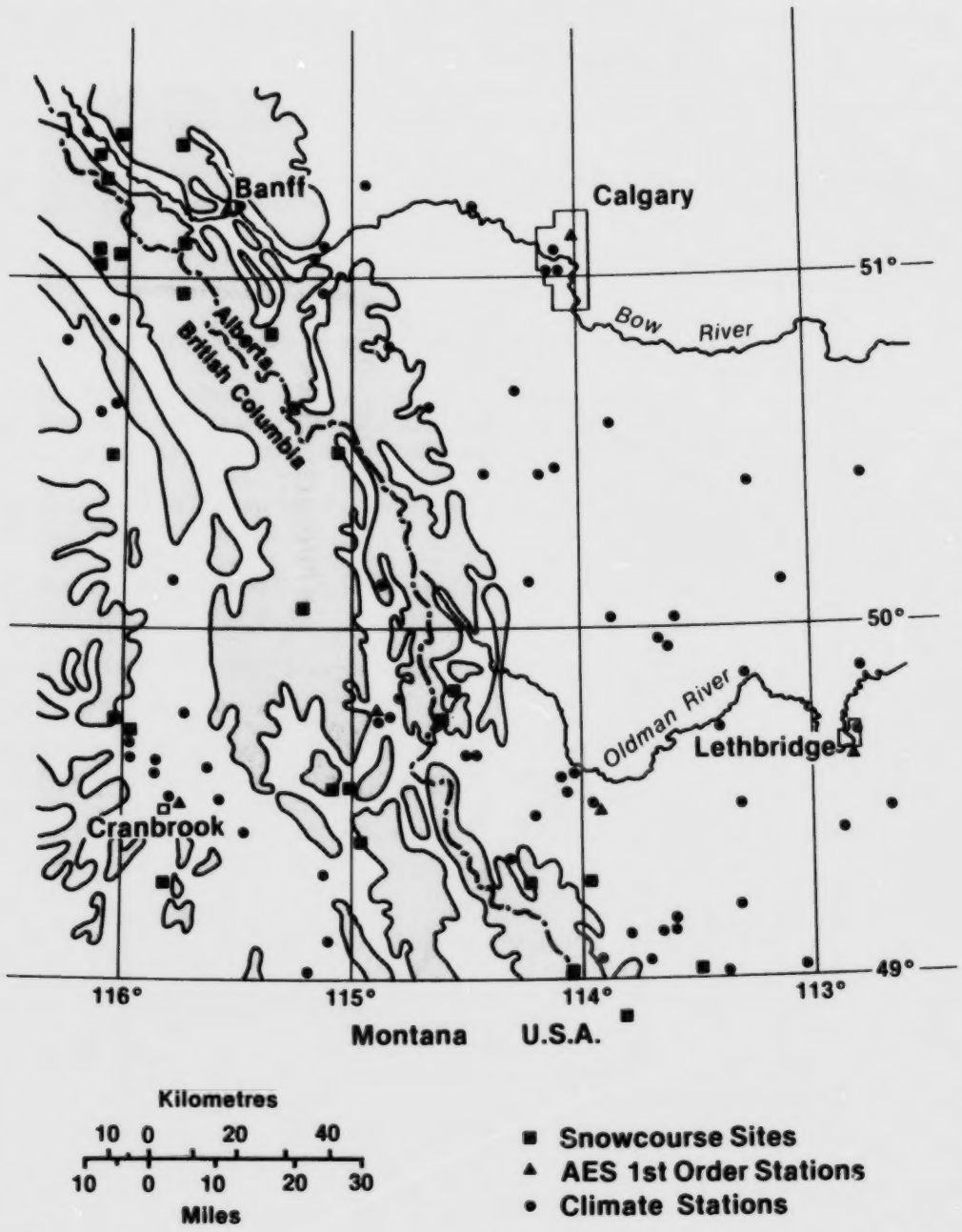

Figure 2. Network of A.E.S. climate stations and provincial snow survey sites in the southern Canadian Rockies area.

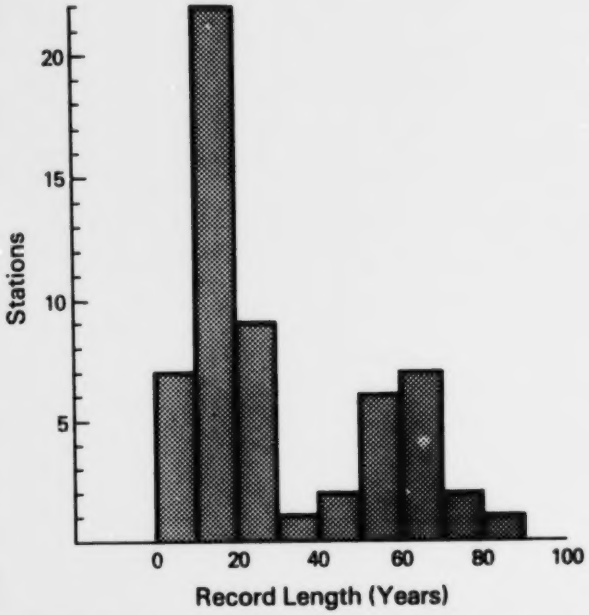

Figure 3. Frequency of record length for 57 A.E.S. mountain climate stations.

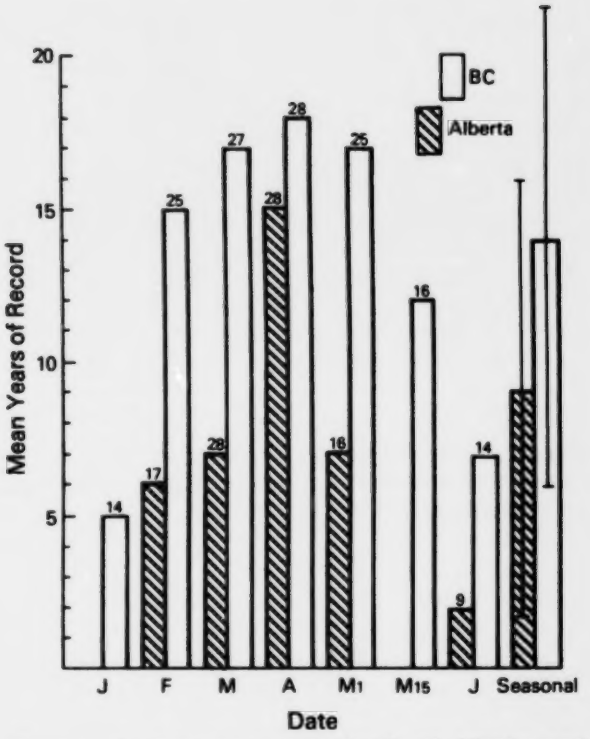

Figure 4. Average record length of Alberta and British Columbia snow survey courses throughout measurement season. The seasonal standard deviations is also given.

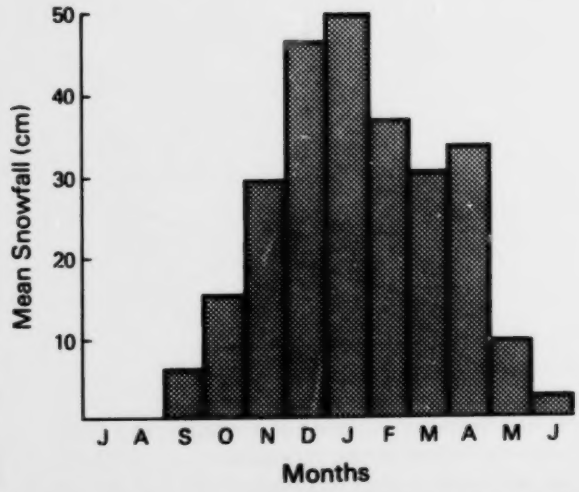

Figure 5. Average monthly snowfall over the year for 57 mountain A.E.S. climate stations.

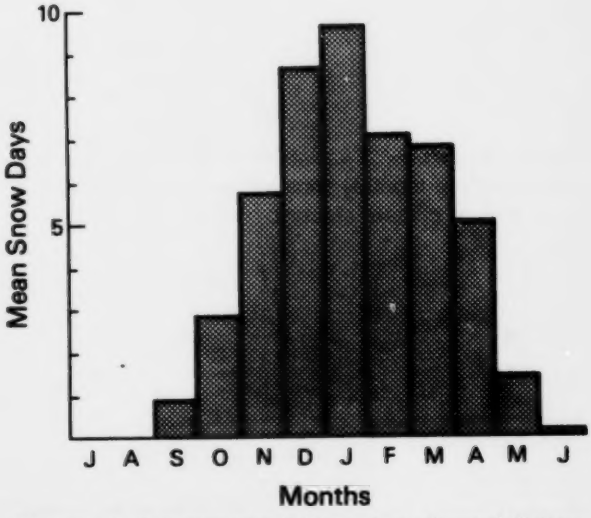

Figure 6. Average monthly number of snowfall-days over the year for 57 mountain A.E.S. climate stations.

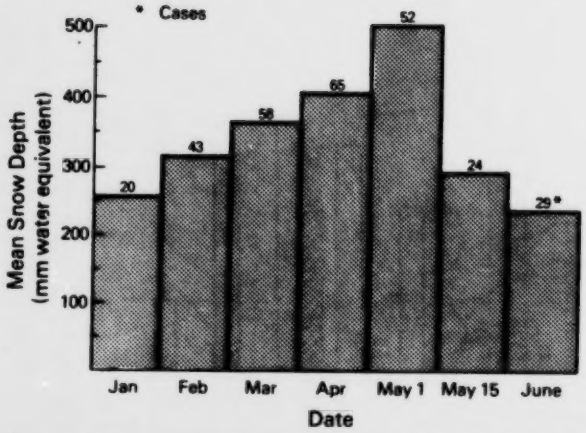

Figure 7. Average snow water equivalent over the measurement season for 70 Alberta, B.C. and Montana snow courses.

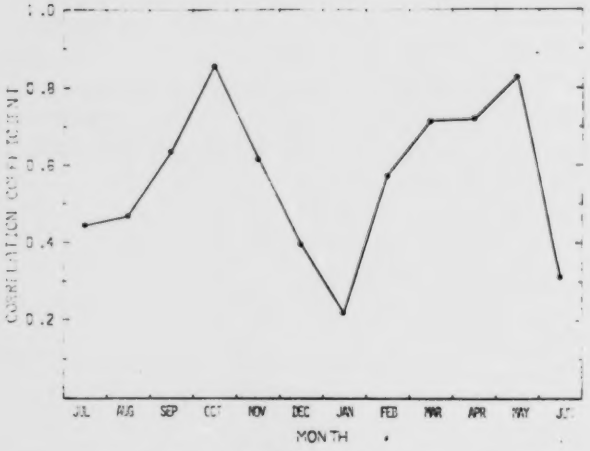

Figure 9. Seasonal variation of the correlation between average monthly snowfall and station elevation for 57 A.E.S. climate stations.

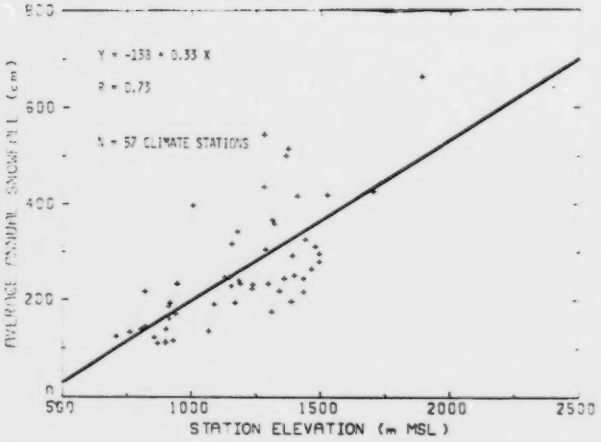

Figure 8. Variation of average annual snowfall with station elevation for 57 mountain A.E.S. climate stations. The calculated linear regression least squares fit and correlation coefficient are also shown.

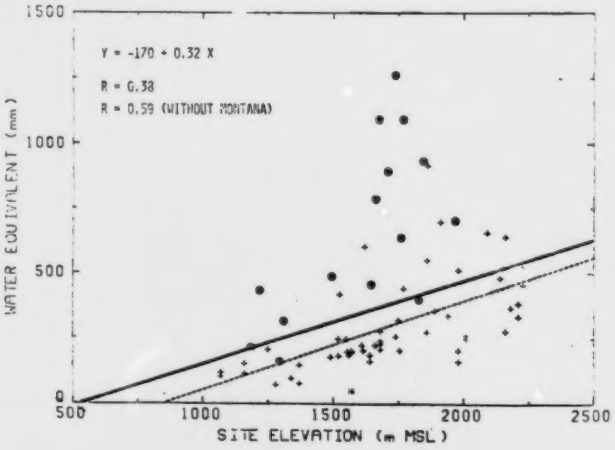

Figure 10. Seasonal variation of average snow water equivalent with elevation for 70 Alberta, B.C. and Montana snow courses. Linear regression lines and correlation coefficients calculated both with and without the Montana data are also shown.

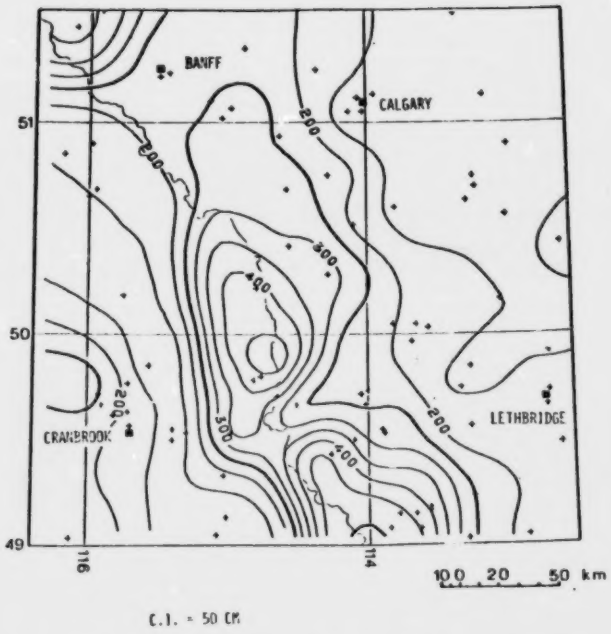

Figure 11. Average annual snowfall for general project area (82 A.E.S. climate stations).

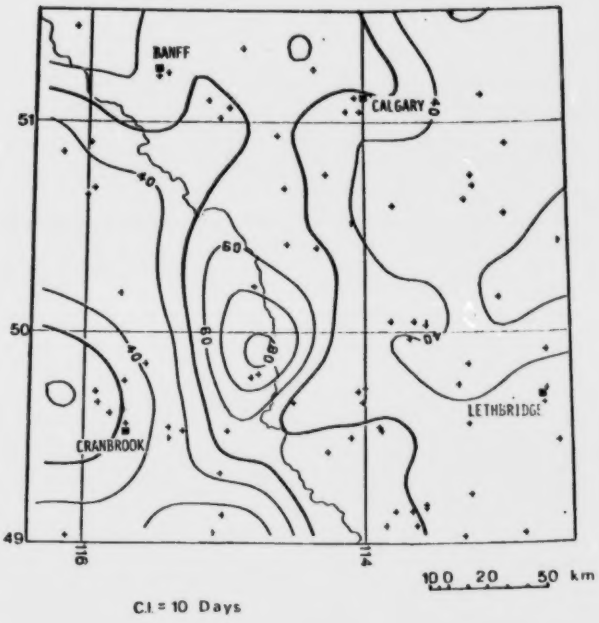

Figure 12. Average number of annual snow days for general project area (82 A.E.S. climate stations).

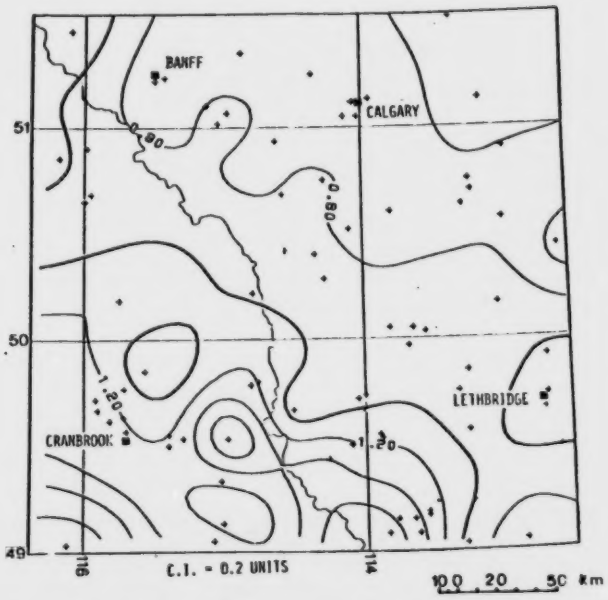

Figure 13. Ratio of actual annual snowfall to elevation regression model predicted annual snowfall for general project area (82 A.E.S. climate stations).

The Spatial/Temporal RESolution Study (STRESS) of Upper Air Data

C.M. Sackiw and G.S. Strong

University of Alberta
Department of Geography
Division of Meteorology

and

Atmospheric Sciences Department
Alberta Research Council
Edmonton, Alberta

Paper prepared for the 17th Annual Congress of the Canadian Meteorological and Oceanographic Society, Banff, Alberta, 03-05 May, 1983.

The Spatial/Temporal RESolution Study (STRESS) of Upper Air Data

C.M. Sackiw and G.S. Strong

University of Alberta
Department of Geography
Division of Meteorology

and

Atmospheric Sciences Department
Alberta Research Council
Edmonton, Alberta

ABSTRACT

Synoptic scale rawinsonde networks are capable of resolving atmospheric features larger than 1000-km in wavelength and with life cycles greater than 24-hours. For this purpose, instrumentation errors are usually ignored for upper air analyses and prognoses. The ability to diagnose and forecast mesoscale features such as thunderstorms, however, is often limited by the lack of upper air data at that scale. Even when these data are available, the analysis of pertinent features may be masked by data sampling uncertainties.

Convective weather is of major concern for Day-1 forecasting on the Prairies. Severe convective storms, particularly hailstorms, have been the main focus of Alberta Hail Project research for many years. A small scale upper air network appears to be necessary for investigating the interactions between synoptic scale processes and mesoscale thunderstorm systems. It was desirable to establish upper air data accuracy and resolution capability before such a network could be established. To this end, the Spatial and Temporal RESolution Study (STRESS) was commenced. This paper reports on preliminary STRESS analyses, using data from Alberta and Oklahoma.

1. INTRODUCTION

1.1 Problem definition —

The resolution of atmospheric processes using upper air data is limited by sampling uncertainties of the instrument sensors. The minimum environmental change that is detectable by the measurement system is twice the magnitude of the sampling uncertainty. Within the sampling constraints, the spatial and temporal resolution capability of a data network is then defined by the space and time sampling intervals. This assumes that the sampling intervals are reasonably uniform, rather than random. It should be noted that this paper considers only thermodynamic data. Errors in wind data are of a different nature and must be treated in another manner.

Sampling errors are not usually a serious problem for synoptic scale analyses and numerical prognoses over North America and Asia. In fact, Oort (1978) found that spatial gaps in the global rawinsonde network, even for the northern hemisphere (over oceanic areas for example), produced more error than those due to instrumentation or temporal gaps. Such gaps are not a major concern over North America alone, where the average rawinsonde spacing is 500 km or less, with soundings every 12 hours. These sampling intervals enable resolution of atmospheric phenomena of length scale larger than 1000 km and time scale greater than 24 hours; i.e., at least the synoptic scale. However, if one were to space instrumentation 5 km apart, the sampling error would probably be too large to attempt resolving features of length scales of about 10 km (cloud scale).

This problem is compounded by the use of different types of instrumentation, and by natural variations in the gradients of the measured variables (pressure, temperature, and moisture). Spatial resolution of upper air data is a crucial consideration for severe storm work, where one may wish to make meso-scale measurements at length scales in the order of 10 to 100 km. Similar consideration must be given to temporal resolution. For example, is there additional useful information provided by hourly serial releases as opposed to releases three hours apart? This leads to the following questions. What are the minimum or optimum time intervals for soundings? What optimum spacing between sites should be chosen when designing upper air and surface observing networks? Should the time/space intervals for soundings be modified according to weather conditions?

Sampling uncertainties result from:

1. instrument calibration errors;
2. upper air data acquisition system errors;
3. observer errors (where the system is not fully automatic);
4. mathematical interpolation (between discrete levels).

Once these error sources are identified, the next step is to determine the optimum space and time intervals for a network to resolve a given scale of atmospheric motion with the given system uncertainties. In reality, it may be necessary to study system accuracy and spatial/temporal resolution problems concurrently. Since data sampling uncertainties depend on other meteorological variables, one is forced to converge on the solutions gradually. For this reason, it is desirable to build flexibility into any data network.

1.2 Background Studies —

Gill and Hexter (1972) defined the following terminology pertaining to instrumentation:

a) Resolution — the smallest change in the environment that will cause a detectable change in the value displayed by the instrument.
b) Accuracy — the degree to which the instrument will measure the variable in terms of some accepted standard or true value.
c) Reference accuracy — the error limit that will not be exceeded during standard operating conditions; normally, manufacturer's performance specifications really mean reference accuracy rather than accuracy.
d) Repeatability — the closeness of agreement of numerous measurements for a particular input value under normal operating conditions, when approaching from the same direction.

Upper air data uncertainties and system irregularities have been investigated with respect to the repeatability of sonde measurements, but absolute values measured are rarely questioned. Laboratory experiments are designed to test absolute values of thermodynamic variables by simulating atmospheric conditions. Since more complex conditions occur in the environment these tests are beneficial only in studying how different sondes react to a given stimulus.

Table 1 lists RMS errors*1 in pressure, temperature, and humidity from several investigations, as well as some of the most recent specifications provided by manufacturers. For example, Hodge and Harmantas (1965) noted that, except for pressures less than 100 mb, the evaluation technique to extract temperatures at mandatory levels could produce errors of up to approximately 2°C. With the addition of more levels, this error would be reduced by more than half. Thus, using standard sondes, one can expect uncertainties at all levels of 1-2 mb for pressure data, 0.2 to 0.7°C for temperature, and 4-10% RH for humidity.

TABLE 1. Summary of RMS errors for upper air measurements of pressure, temperature, and humidity.

SOURCE	RMS Errors P(mb)	T (C)	HUMIDITY (%RH)
Case, 1962			
— Sfc — 400 mb	1.3	0.7	10.
400 - 100 mb	1.1		
100 - 10 mb	0.7		
Hodge and Harmantas, 1965			
— 2-sonde diff.	2.2	0.5	
— 1-sonde estimate	1.5	0.4	
Lenhard, 1970			
— single sonde			
Sfc - 200 mb	3	0.3	
200 - 100 mb	2		
100 - 50 mb	1.5		
Lenhard, 1973			
— using Hodge and Har. pres. error		0.2	
Richner / Phillips, 1981 — std. sonde	0.2% of pres. range (1080-5 mb)	0.4	4.
VIZ (1982) rawinsonde specifications:			
— standard sonde	0.2% of range	0.4	4.
— premium sonde	0.2% of range	0.1	2.
AIR Airsonde (1982)	1.0	0.2	0.1 °C wet bulb

*1 The RMS error, or standard error of estimate is defined as the positive square root of the mean-square error (Huschke, 1959).

2. UPPER AIR DATA REQUIREMENTS

Assuming no shortage of observing systems, the design of any data network must be based mainly on the scale of phenomena which one wishes to measure. However, the ability to accurately sample these phenomena will then be limited primarily by instrument error. Statistically, one requires at least three points to resolve a wave in two dimensions. Initially, one may choose to accept the manufacturer's claims of data accuracy and resolution. One should then consider the natural variations (of the phenomena) which occur in the atmosphere, and then design a network which provides the optimum data resolution.

If one wishes to verify that measured variations are real and not simply random data fluctuations, independent tests of instrument error are necessary. These uncertainties will encompass the four main error sources listed in Section 1.1. With these determined, tests of temporal and spatial resolution will provide the optimum spacing and time intervals for sampling the required phenomena.

2.1 Synoptic Scale Gradients —

In order to provide a suitable reference datum for the present study, it was necessary to confirm that synoptic scale features are adequately resolved by the existing upper air network over North America, with average station spacing of 500 km. Typical 700 and 500 mb geopotential height and temperature gradients were

analyzed for July, 1980. These results are summarized in Table 2. Summer months generally provide the weakest gradients, when phenomena at the lower range of the synoptic scale, such as large convective complexes, are common.

For Table 2, it was assumed that pressure height and temperature measures at each synoptic station are correct to 5 meters and 0.4°C respectively. Thus, uncertainties in the gradients (reduced to 100 km) are of the order of +/-1.4 m/100 km (from 1/5*((5)**2 + (5)**2)-**1/2) for geopotential height, and +/-0.1°C for temperature. These uncertainties reduce to +/-0.3 m/100 km and +/-0.02°C /100 km; i.e., mean error, E = error/-N**1/2 (Spiegel, 1961), for the average gradients.

Table 2 shows only maximum gradients between any two rawinsonde stations for each day, since the minima (absolute values) would be close to (or equal to) zero. For temperature gradients, the smallest daily maximum value for any given day (during July, 1980) is 0.5°C/100 km (2.5°C/500 km), with the average about double this. Thus, with sensor accuracy of 0.4°C RMS (VIZ radiosondes), one is assured of resolving length scales of 1000 km with 500-km spacings (i.e., the synoptic networks).

TABLE 2. Absolute values of maximum (synoptic scale) horizontal gradients of geopotential height and temperature at 700 and 500 mb over western Canada during July, 1980.

(1980)	HEIGHT GRADIENT (m/100 km)		TEMP. GRADIENT (°C/100 km)	
DAY	700 mb	500 mb	700 mb	500 mb
July 02	8	13	0.7	0.8
03	7	13	0.8	0.8
04	7	11	1.4	0.5
05	12	25	2.2	1.8
06	14	25	2.1	1.5
07	16	44	0.9	2.3
08	9	17	1.1	0.5
09	9	15	1.3	1.2
10	11	18	1.8	0.8
11	10	22	1.3	4.1
12	8	20	0.8	1.5
13	8	27	1.8	1.5
14	9	22	0.5	0.7
15	6	9	0.8	1.2
16	11	27	1.2	1.2
17	14	29	1.3	2.1
18	16	25	0.7	1.5
19	11	22	1.5	0.8
20	8	17	0.8	0.8
21	10	15	0.5	0.6
22	13	20	0.8	0.8
23	-	17	-	0.8
24	11	25	1.6	1.0
25	7	18	1.1	1.4
26	12	22	1.2	1.1
27	13	30	2.6	1.0
28	15	27	1.6	0.9
29	14	24	2.7	1.5
30	14	29	1.3	1.0
31	13	27	1.7	1.5
AUG. 01	11	20	1.3	0.5
Min.	6	9	0.5	0.5
Max.	16	44	2.7	4.1
MEAN	10.9	21.7	1.3	1.2
S.D.	2.9	7.0	0.6	0.7

This table provides a first approximation to the best spatial resolution possible with a given sensor. For the VIZ sonde for example, with 0.4°C temperature uncertainty, one is only assured of resolving 0.8°C temperature difference. Table 2 suggests that an optimum spacing of 160 km would ensure this accuracy, at least for the weakest gradient conditions of July, 1980; in other words, the minimum 0.5°C/100km converted to 0.8°C/160 km. On synoptically active days (i.e. days with gradients exceeding the means of Table 2) one might achieve 'useful' additional spatial resolution with spacings down to 80 km. The NSSL*2 rawinsonde network had an average site spacing of 85 km (Fankhauser, 1969) and data from active convective days have been utilized in many studies. Accepting the Airsonde manufacturer's sonde accuracy of 0.2°C as the temperature uncertainty, site spacings could be reduced to as low as 80 km in order to achieve the maximum possible resolution with the weakest gradients. For average (or stronger; e.g., severe storms) gradient conditions, one might consider spacings as close as 40 km if operating costs were not a factor. These values represent the best results achievable, since it is assumed that all radiosondes in the network are identical in design and calibration. One also assumes totally automated systems so that there is no observer bias.

Similar deductions can be made from the geopotential height gradients listed in Table 2. In particular, with minimum height gradients of about 5 m/100 km, one is reminded of the importance of accurate site elevations (MSL) for work at these scales. Tests comparing surveyed elevations against estimates from fine scale (1:25,000) topographic charts revealed typical errors of more than 10 meters in the estimates, with 10% of these being in excess of 30 meters (Strong, 1981). The geopotential height field is essential to many analyses; for example, kinetic energy or potential energy budgets. Therefore, the common practice of using elevation estimates from topographic charts for short-term field networks of 100-300 km spacing, where even site location may be in error, appears to be imprudent.

2.2 Gradients for Sub-Synoptic Scale Convective Complexes —

During summer, severe convective weather (large thunderstorms, hail, tornadoes) tends to occur on synoptically active days when strong gradient conditions exist (Strong, 1979). This has made possible studies involving sub-synoptic scale analyses of severe convective weather, using data from upper air networks of this scale (e.g., see Tsui and Kung, 1977; Fuelberg and Scoggins, 1978).

The gradients of Table 2 were derived using only synoptic scale data. It is conceivable that gradients around severe thunderstorm systems may be much greater over shorter distances and time periods. This complicates the problem of network spacing and sounding time interval even further. An example from the 1979 SESAME*3 (Oklahoma) network of 20 sites with 100-km spacing was chosen. Using the AVE-V data set (Sienkiewicz et al., 1980) of 20 May, 1979 (tornado-producing thunderstorm complex), height gradients as large as 60 m/100 km were measured.

*2 National Severe Storms Laboratory, Norman, Oklahoma.

*3 Severe Environmental Storms Area Meteorological Experiment.

3. INTERCOMPARISON TESTS

The foregoing shows the necessity for intercomparison tests of sondes, and the determination of optimum spatial and temporal resolution (de-correlations) of data, whenever a new upper air (or other) data network is being planned. For this reason, the Spatial and Temporal RESolution Study (STRESS) of upper air data over Alberta was commenced in 1980.

The STRESS problem ultimately reduces to the following: for given uncertainties in measured variables, what are the optimum sampling intervals in time and space for an observing network which will resolve the desired scale(s) of motion? It is understood that these intervals may vary depending on:

1. the parameter (temperature, humidity, etc.) being measured,
2. the type of equipment and (for upper air measurements) sondes used,
3. the degree of automation (to reduce observer bias), and
4. varying weather conditions.

3.1 Available STRESS Data —

The object of STRESS then is to provide the best possible network design(s) for Alberta conditions. Initially, this concerns sub-synoptic scale measurements of convective complex environments. STRESS operations and data sources to date, and their purpose are summarized in Table 3. Upper air sites for the operation of 18-20 August, 1981 are shown in Figure 1.

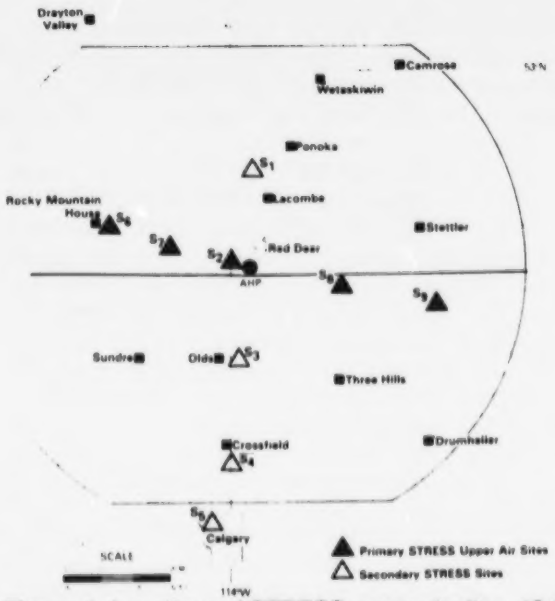

Figure 1. Locations of STRESS upper air sites, 18-20 August, 1981.

Intercomparison tests are necessary not only to verify manufacturers' claims, but also to check consistency between different production runs of sondes. This becomes more important when a network includes two or more different upper air sounding systems. For example, the CCOPE*4 upper air network of seven sites consisted of five GMD-1 and one RD-65M rawinsonde systems (both using VIZ 1680 MHz sondes), and one ADAS system (using 403 MHz Airsondes).

3.2 Recent Intercomparisons —

The Boulder Low-Level Intercomparison Experiment (BLIE, Kaimal et al., 1980) included extensive tests of four sonde systems in flights from 10 meters to 3 kilometers; VIZ 1680 MHz, Vaisala 403 MHz, TDFS 403 MHz, and Airsonde 403.5 MHz. Deviations from mean sensor temperatures were -0.10 to +0.35°C with RMS differences of 0.35 to 0.70. Relative humidity deviations from means were -2 to +3 % RH with RMS differences of 3.2 to 4.6.

McInturff et al. (1979) and Phillips et al. (1981) deter-

TABLE 3. Summary of STRESS operations, other data sources, and analysis purpose, using rawinsondes (R/S) and Airsondes (A/S). CAQF is AHP at Red Deer Airport.

DATE(s)	OPERATION	SYSTEMS USED	ANALYSIS PURPOSE
05 Sep. 80	8 serial releases, CAQF, 2-hr intervals, 1200-0200 UTC	1 R/S	Temporal Resolution weak tendencies
14 Aug. 81	4 releases, CAQF	A/S,R/S	Temporal Resolution weak tendencies
18-20 Aug. 1981	Simultaneous serial releases, 5 sites, straight line, 40-km spacing, 1-1/2 hr intervals (Fig.1)	3 R/S, 2 A/S	Spatial/Temporal Resolution, weak-moderate gradients
14 Oct. 81	2 simultaneous releases, 4 systems, CAQF	3 A/S, 1 A/S	Sensor accuracy repeatability, Temporal Resolution
26-28 May 1982	Simultaneous releases, CAQF	3-5 A/S, 1 R/S	Sensor accuracy, repeatability
24 July 82	Simultaneous separate releases, CAQF	1 R/S, 1 A/S	Sensor accuracy, repeatability
19,26 July 1982	2 simultaneous releases, 4 sites vicinity CAQF	3 A/S (3 frequency), 1 R/S	A/S frequency interference tests
24 Aug. 82	2 simultaneous releases, 3 sites vicinity Limestone Mtn.	3 A/S on 3 frequents	A/S frequency interval tests, mountains
ADDITIONAL DATA:			
20-21 May, 1979	SESAME (Okla.) serial releases 100-km avg. spacing, 1-3 hr. intervals, 1100-1100 UTC	20+ R/S	Spatial/Temporal resolution, moderate-strong gradial, convective
18 June - 08 July 81	CCOPE*4 (Mont.)serial releases 80-km avg. spacing, 1-6 hr intervals	6 R/S 1 A/S	Spatial/Temporal resolution, weak-moderate gradients

mined that radiation effects could cause errors of up to +0.65°C at the surface, and to more than 2°C at normal balloon burst. Many radiosonde manufacturers neglect corrections for radiation effects. Some do provide reflective coatings on thermistors (e.g., VIZ sondes), while other sondes contain substantial radiation shields and additional software corrections (e.g., Vaisala sondes).

3.3 STRESS Intercomparisons —

Using the intercomparison data of 14 October, 1981 (Table 3) data were extracted at 25-mb intervals from two sets of simultaneous releases. Each release consisted of two radiosondes (VIZ 1680 MHz and 403 MHz) and an airsonde (403.5 MHz). For the first flight, all three sondes were tied to the same balloon with an ascent rate of about 5 m/s. For the second launch, the Airsonde was released separately to allow for its optimum ascent rate of 3 m/s. The VIZ 403 MHz sonde was tracked with a single METOX ground station, the VIZ 1680 MHz sonde by two ground stations (an RD-65M and an RD-65A), while the 403 MHz Airsonde was tracked using an optical theodolite. The RD-65A data were used as the reference soundings for these analyses.

Figure 2 depicts differences of the reference sounding dry bulb temperatures (RD-65A) from those of the RD-65M, the METOX, and the Airsonde soundings for the 2200 UTC release. For most of this flight, variations between the two ground stations tracking the 1680 MHz sonde were within +/-0.1°C. However, differences of up to 0.8°C occurred at three levels: the first level above the surface (900mb) and 675 and 650 mb. No explanation for these exceptions is offered at this time. Expected observer error is around +/-0.2°C. Hodge and Harmantas (1965) implied that "the major portion of the scatter originates from sources other than the radiosonde itself."

*4 Cooperative COnvective Precipitation Experiment conducted as part of the HIgh PLains EXperiment (HIPLEX) in eastern Montana during 1981.

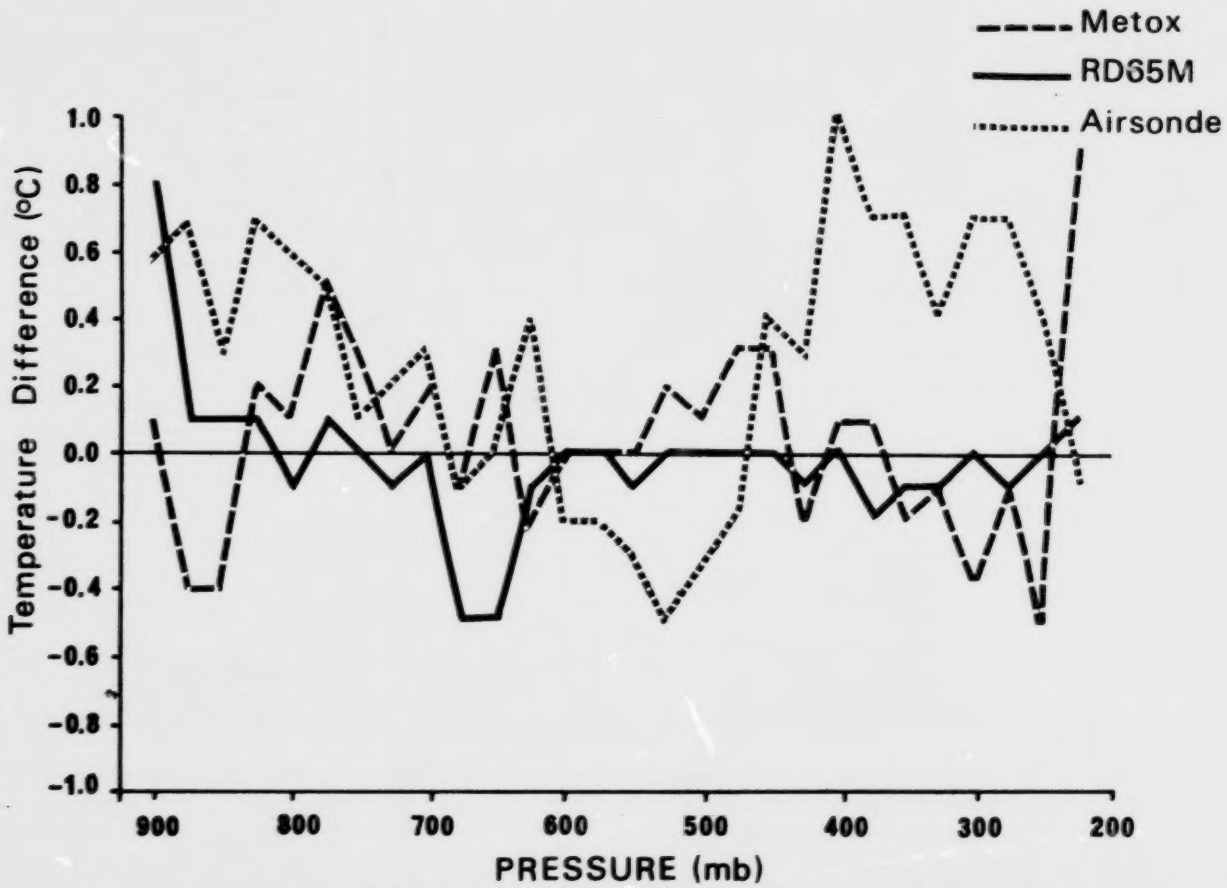

Figure 2. Dry bulb temperature differences between the reference sounding (RD-65A), used as the standard, and the RD-65M, METOX, and Airsonde soundings at 2200 UTC, 14 October, 1981, at CAQF.

The maximum uncertainty of the dry bulb temperature for a single reading was usually within +/-0.5°C for radiosondes, and about double for airsondes. Airsonde data were found to be erratic above 400 mb for the 2000 UTC flight, so that the comparison was made only to 500 mb. Standard deviation of temperature between two radiosondes was 0.26 and 0.28 versus 0.15 and 0.20 for a single sonde and two ground stations; airsonde data shows somewhat higher standard deviations (0.39 and 0.42). This is within both the manufacturer's stated tolerance of 0.4°C RMS and the expected observer error. This error also includes the pressure error, since the data were extracted by pressure levels reported by the sondes. Thus, based on this small sample, it would appear that VIZ sondes may typically be more accurate than the manufacturer's specifications imply.

Dew point temperatures for radiosondes exhibited roughly double the uncertainty of dry bulb temperatures. Of course, larger errors are to be expected since this parameter also includes the error of the moisture sensor (hygristor or wet bulb). The Airsonde had maximum differences of +1.9 and +3.0°C. If this could be construed as a consistent bias, then corrections could be applied. Standard deviation of all sondes including the airsonde ranged from 0.38 to 0.56. Further comparisons between the airsonde and radiosonde systems are required to confirm these initial results.

3.4 Planned STRESS Intercomparisons —

It is important to perform some tests with all instruments on the same balloon train, as time (rather than pressure), can then be used as a basis to extract the data for comparison. This allows direct comparison of pressure, temperature, and moisture sensors. Results presented here were extracted by pressure level rather than time, so that pressure and temperature errors are combined. This is necessary for obtaining a temperature error estimate when using a single sonde, as one must then rely upon transmitted pressure for data extraction at selected levels.

Other sonde tests to be carried out include removal of the wick from the airsonde wet bulb thermistor. By doing this, the variability between the two temperature sensors may be compared. A reverse test is to add a wick to the dry bulb thermistor for comparison of wet bulb readings from the same sonde. This may reveal any inconsistencies between wet bulb thermistors.

4. SPATIAL AND TEMPORAL DE-CORRELATIONS

4.1 STRESS Data Analysis —

A simple analysis routine was adopted as a first approach to the temporal and spatial resolution problems. Profiles of potential temperatures (Theta), wet bulb potential temperatures (Theta-w), and equivalent potential temperatures (Theta-e) at 25-mb increments were used. These were inter-correlated for various time and space intervals, and for varying meteorological conditions (generally for weak, moderate, and strong tendencies and gradients of temperature and pressure height).

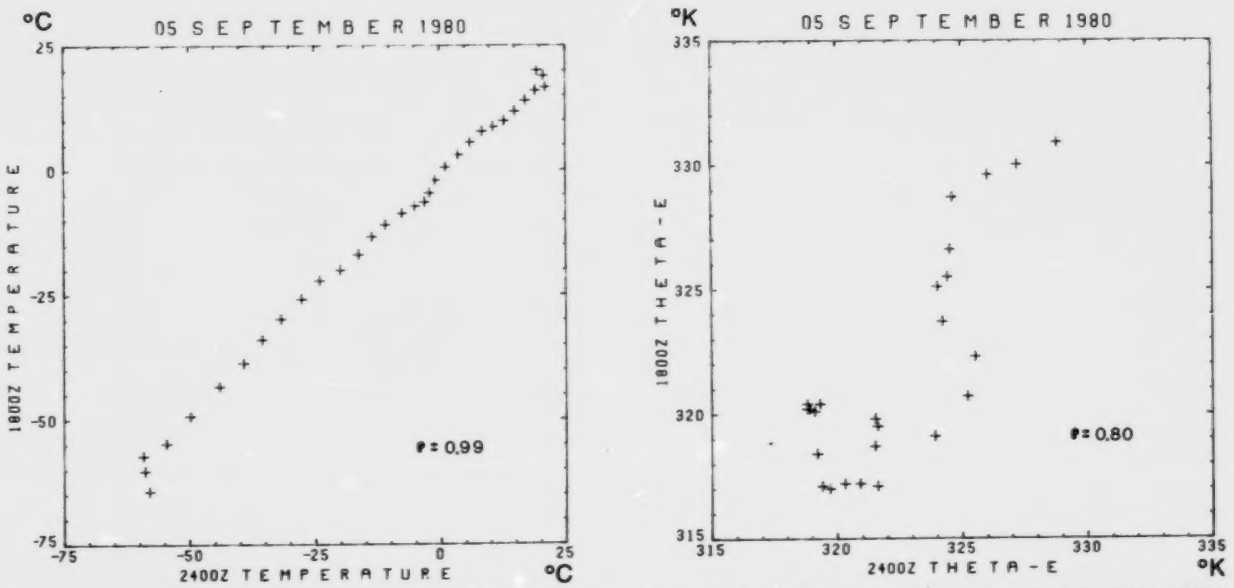

Figure 3. Corresponding plots of (a) dry bulb temperatures (°C), and (b) Theta-e (°K) for 25-mb increments, 1800 and 2400 UTC, 05 Sept. 1980, CAQF.

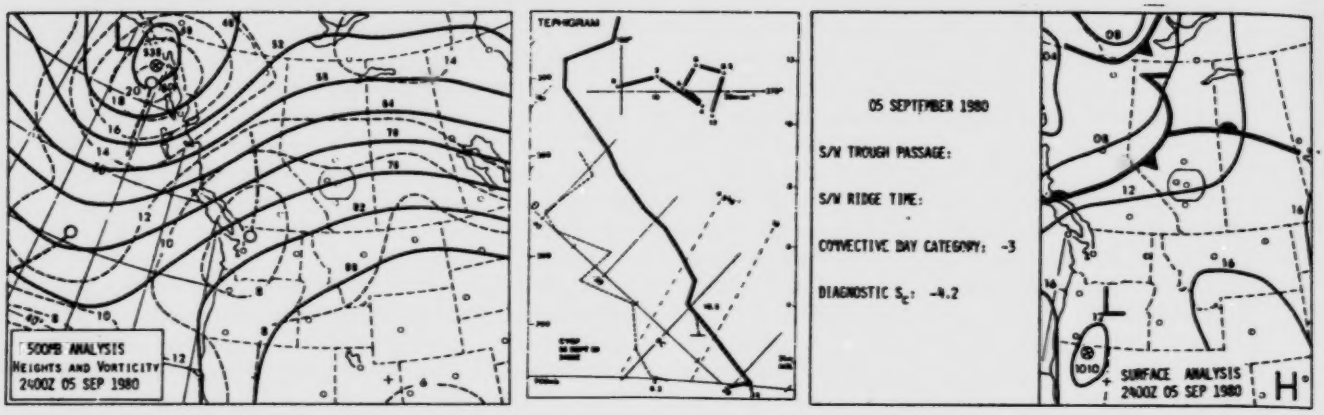

Figure 4. 500 mb and surface analyses, and CAQF sounding for 2400 UTC, 05 September, 1980.

Potential temperatures were used because they are normalized to 1000 mb. This was important for the computation of the linear correlations in this case. Temperature variations from surface to tropopause are much greater than the sounding-to-sounding deviation at a particular level. Relatively little scatter then occurs, and linear correlations are always high. Figure 3 illustrates this problem for soundings 6 hours apart (surface to 200mb) showing a plot of corresponding dry bulb temperatures at 25-mb increments for the two soundings, and a similar plot of equivalent potential temperatures.

4.2 STRESS, Temporal Resolution —

STRESS temporal resolution analyses commence with the set of 8 serial releases at 2-hour intervals from CAQF on 05 September 1980. The 500 mb and surface synoptic patterns over Alberta at 2400 UTC are shown in Figure 4, along with the 2400 UTC sounding for CAQF. While north-south gradients were strong (e.g., pressure height gradient of 30m/100 km at 500 mb), sounding-to-sounding changes in height and temperature at given levels (tendencies) were slight throughout the period, 1200-0200 UTC. Soundings remained very stable and no convective activity occurred over AHP.

The linear correlation coefficients versus time increments for Theta, Theta-w, and Theta-e, are illustrated in Figure 5. The plotted points are average correlation coefficients for each time increment; e.g. average of 7 values for the 2-hour correlations, to only 1 value for 14 hours. This procedure, for example, is made necessary by the natural variability between any two distinct sampling pairs, and has been used by others (e.g. Faller, 1981). The 4-hour correlations of Theta-e ranged from 0.74 to 0.96.

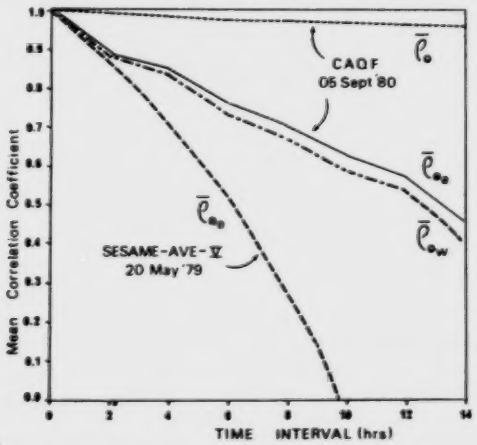

Figure 5. Mean temporal de-correlations for 8 soundings at 2-hour intervals from one location (CAQF), 05 September, 1980.

As might be expected, there is no significant difference between the Theta-w and Theta-e correlations, The correlations for Theta drop off very slowly with time. As in the case of dry bulb temperatures, this occurs because Theta changes faster than Theta-e with height (generally from 285°K to 370°K near the tropopause), making sounding-to-sounding changes at any given level relatively insignificant. Theta-e varied to more than 30 degrees with height, and as much as 20 degrees with time at a given level (see examples in Fig. 3.) Therefore, from this point on, we shall concern ourselves only with Theta-e correlations.

Included in Figure 5 is the mean value (0.94) of 2-hour Theta-e correlations from the 14 October 1981 data set, Also depicted is a plot of comparable mean 3-hour Theta-e correlations from the severe convective storm soundings of the SESAME data set for 20 May 1979. These indicate more scatter, likely due to smaller scale processes and changes associated with severe convection. The weak tendency cases (changes with time) for 05 September 1980 (CAQF) still show moderately high correlation after nine hours (above 0.65), while correlations drop to 0.65 after 4-1/2 hours, and to zero after 9 hours in the Oklahoma severe storm case.

Interestingly, correlations appear to remain above 0.9 for sounding intervals of two hours or less for either weak (no weather) or strong (convective case) tendencies. Further analyses, different statistical tests, and probably more data under varying tendencies are required to ascertain what level of correlation constitutes significance for the temporal resolution problem.

4.3 STRESS, Spatial Resolution —

The logistics of acquiring a good data set for spatial resolution tests is somewhat more complex than for the temporal problem. While it is relatively easy to make serial radiosonde releases from one point under varying conditions, the spatial resolution problem ideally requires data from a line of equi-spaced sites, preferably parallel to the line(s) of maximum gradient.

Figure 6 shows spatial correlations for two lines of sites from the SESAME severe convection data set, one normal to and one parallel to the storm complex direction of motion (west-southwest to east-northeast in this case). Due to the large degree of scatter, especially for the cross-direction line, only polynomial fits to the 'mean' values are shown at this time. Detailed analyses will be necessary to determine the significance, if any, of these fits. At this point, one can only surmise that soundings (of Theta-e) are significantly different even 50 km apart in this case: i.e., correlations drop below 0.8.

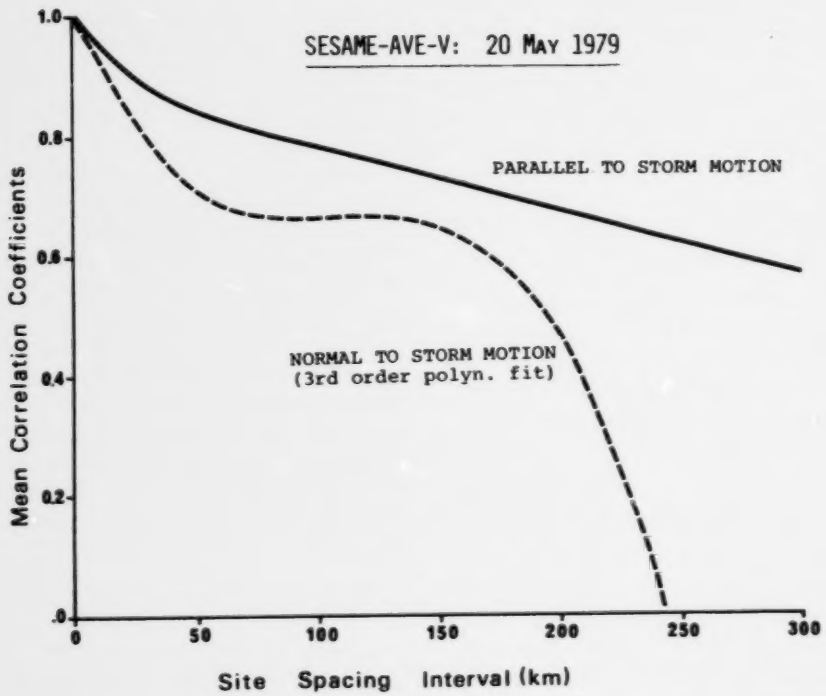

Figure 6. Mean spatial de-correlations for the SESAME-AVE-V data set (20 May, 1979) for lines (a) parallel to and (b) normal to storm complex motion.

For sites parallel to the storm complex motion, mean correlations still drop below 0.8 at 50-80 km spacing, but fall off more slowly with greater separations than for the cross-direction line. Surely, this is as one would anticipate. Still, it helps to provide a basis for deciding how to release soundings on a given day. For instance, changes along the direction of storm motion are spatially less significant (smaller gradient and tendencies) than those normal to this direction. Thus, one might either increase the separation distances along this direction (close down every other site for the day?) or release fewer soundings at every other site. Again, much more detailed analyses and data are required to decide what correlations are significant and, ultimately, what these distances should be.

5. SUMMARY

5.1 Sampling Uncertainty —

The literature supports manufacturers' claims that upper air pressure sensors are accurate to 1-2 mb at the surface, with accuracy increasing at lower pressures (see Table 2). Since surface gradients of 1 mb/25 km occur even during summer conditions, this emphasizes the importance of pre-flight calibration of sondes.

Temperature accuracy of sondes is claimed to be 0.4 +/-0.2°C in most cases. This is supported by the Alberta STRESS tests, except for Airsondes which showed greater temperature deviation from radiosondes above 500 mb. These limited tests could not ascertain whether the Airsonde deviations were due to failure of the pressure sensor, lack of calibration above 300 mb (according to the manufacturer, A.I.R.), or even consistent errors in the radiosonde data, all of which were VIZ sondes. The pressure sensor is the most likely cause here.

5.2 Spatial Resolution of Data —

Maximum summer temperature gradients (from synoptic scale estimates) generally vary between 0.5 and 4.0°C per 100 km. Assuming temperatures are accurate to +/-0.4°C, these values suggest that, for weak gradients, no additional useful information would be obtained from soundings spaced less than 160 km apart. For stronger gradients (more than 1.0°C/100 km), which usually occur with severe convective storms, valuable additional data might be obtained with spacings of 80 km. Alberta and Oklahoma Theta-e STRESS correlations suggest that adjacent soundings on lines normal to storm motion are significantly different for spacings of 50 km or more. Along the motion vector, spacings could be at least doubled without loss of information. Ultimately one should design a flexible network, where spacing and sounding intervals can be varied to suit meteorological conditions. This would provide significant savings in operating costs with no loss of 'usable' data.

5.3 Temporal Resolution of Data —

Under stable Alberta conditions, significant temporal differences (correlations less than 0.8) were noted between soundings five hours or more apart. For the one severe storm case investigated (Oklahoma data) correlations dropped below 0.8 in less than three hours. From this very limited data set, a first guess at optimum sounding intervals for networks with 50-200 km site spacing (sub-synoptic scale studies) might be 6 hours for the most stable cases, and 1-1/2 to 2 hours during severe convective storms. This concurs with earlier recommendations by Fankhauser (1969), and the logistics of the SESAME (1979) and CCOPE (1981) networks.

5.4 Conclusions —

The issue of spatial and temporal data resolution capability is a combined problem of (1) the natural scales of data variability, (2) sampling uncertainty, and (3) data network logistics. Much larger statistical samples will be necessary to arrive at more definitive values and conclusions than presented here. While the user has no control over (1), known information on this natural variability can be used to better control (2) and (3). For instance, more accurate (albeit more expensive) sondes are available where higher accuracy is required. The training of technicians, quality control of data, and surveys of sites could receive more attention, while design flexibility in network spacing and sounding time intervals could take on added importance where necessary.

While most comparisons have involved soundings from surface to tropopause, low-level variations tend to be greatest becasue of diurnal and topographic effects. It may therefore be possible to increase overall data resolution significantly with additional low-level soundings (say, below 700 mb), and by using a denser network of automated surface stations. The Airsonde system is ideally suited for low-level soundings, since it is less expensive, both in initial cost and in operating expenses, yet it provides higher resolution data than radiosondes at low-levels. It will be necessary to repeat all spatial and temporal resolution statistical tests using only low-level data, in order to establish the economic feasibility of these measures.

This paper barely covers the broad aspects of the STRESS problem. The problem of wind variability and resolution, for example, introduces another dimension to the problem since it is dependent on the other measured variables. It is apparent that studies of data representativeness such as this should be considered prior to designing any data network.

6 ACKNOWLEDGEMENTS

The authors thank G. Lamb for much of the raw data processing for this subject, L. Shannon for data key-punching, and H. Sharpe for extracting the synoptic gradient data and drafting.

7. REFERENCES

Faller, A. J., 1981: An average correlation coefficient. J. Appl. Meteor., 20, 203-205.

Fankhauser, J. C., 1969: Convective processers resolved by a mesoscale rawinsonde network. J. Appl. Meteor., 8, 778-798.

Fuelberg, H. E., 1974: Reduction and error analysis of the AVE-11 pilot experiment data. Texas A and M Univ. rep. for Aerospace Environment Division, NASA, 131pp.

Fuelberg, H. E., and R. R. Scoggins, 1978: Kinetic energy budgets during the life cycle of intense convective activity. Mon. Wea. Rev., 106, 637-653.

Gill, G.C., and P. H. Hexter, 1972: Some instrumentation definitions for use by meteorologists and engineers. Bull. Amer. Meteor. Soc., 53, No. 9. 846-851.

Hodge, M. W., and C. Harmantas, 1965: Compatibility of United States radiosondes. Mon. Wea. Rev., 93, No. 4, 253-266.

Huschke, R. E., ed., 1959: Glossary of Meteorology. Amer. Meteor. Soc., Boston, 638 pp.

Kaimal, J. C., H. W. Baynton, and J. E. Gaynor, 1980: The Boulder low-level intercomparison experiment. Preprint of WMO report, 189 pp.

Lenhard, R. W., 1970: Accuracy of radiosonde temperature and pressure-height determination. Bull. Amer. Meteor. Soc., Vol. 51, No. 9. 842-846.

Lenhard, R. W., 1973: A revised assessment of radiosonde accuracy. Bull. Amer. Meteor. Soc., Vol. 54, No. 7. 691-693.

McInturff, R. M., F. G. Finger, K. W. Johnson, and J. D. Laver, 1979: Day-night differences in radiosonde observations of the stratosphere and troposphere. NOAA Techn. Memo NWS NMC 63, Washington D.C.

Oort, A. H., 1978: Adequacy of the rawinsonde network for global circulation studies tested through numerical model output. Mon. Wea. Rev., Vol. 106, 174-195.

Phillips, P.D., H. Richner, J. Joss, and A. Ohmura, 1981: ASOND-78: An intercomparison of Vaisala, VIZ and Swiss radiosondes. PAGEOPH, 119, 259-277.

Richner, H., P. D. Phillips, 1981: Reproducibility of VIZ radiosonde data and some sources of error. J. Appl. Meteor., Vol. 17, 1572-1575.

Sienkiewicz, M. E., L. P. Gilchrist, and R. E. Turner, 1981: AVE-SESAME V: 25-mb sounding data, NASA report TM-82417, 409 pp.

Spiegel, M. R., 1961: Schaum's Outline of Theory and Problems of Statistics, Toronto, McGraw-Hill, 359 pp.

Strong, G. S., 1979: Convective weather prediction based on synoptic parameters. Preprints A.M.S. 11th Conf. Sev. Loc. Storms, Kansas City, Mo., Oct. 79, 608-615.

Strong, G. S., 1981: Establishing field site elevations using the Hypsometric equation. Unpublished report, Alta. Res. Counc., Red Deer, 15 pp.

Tsui, T. L., and E. C. Kung, 1977: Subsynoptic-scale energy transormations in various severe storm situations. J. Atmos. Sci., 34, 98-110.

The SYNOPTIC INDEX of CONVECTION:

Part I.
Evaluation of the
Single-Valued Index, 1978-82

G.S. Strong and W.D. Wilson

Atmospheric Sciences Department
Alberta Research Council
Red Deer, Alberta

Paper prepared for the Mesoscale Workshop, Toronto, Ontario, 24-27 January, 1983, and for the 17th Annual CMOS Congress, Banff, Alberta, 03-05 May, 1983.

THE SYNOPTIC INDEX OF CONVECTION:

Part I

Evaluation of the Single-Valued Index, 1978-82

G. S. Strong and W. D. Wilson

Atmospheric Sciences Department
Alberta Research Council

ABSTRACT

Parcel theory has resulted in a multitude of instability indices and convective cloud models. Most applications of parcel theory employ the same basic thermodynamics in attempting to predict convective clouds and related phenomena, particularly thunderstorms and hail. Normally, these techniques, out of necessity or inability to handle the required data, ignore a rather large portion of the spectrum of atmospheric motions. Forecasters, on the other hand, are forced to use data at one extreme of the scale spectrum (synoptic, generally features greater than 1000 km scale), and attempt to make inferences concerning effects at the cloud scale (about 1-10 km) or smaller.

Part I of this series of papers attempts to show how consideration of the scale spectrum, and judicious use of available data, has led to a useful index of convection, the Synoptic Index. Since 1978, this index has been used to predict the maximum intensity of convection, including maximum hail sizes, for the Alberta Hail Project operations area of southern Alberta. Two versions of the Synoptic Index, the Sc10 and Sc4 employing 10 and 4 predictor variables respectively, have been tested. Forecast verification results are compared against the forecaster's subjective modification of the indices. In general, the forecaster has moderate success in adjusting the forecast intensity, but is unable to better either index in predicting the occurrence of hail. The Synoptic Index also shows success in predicting convective intensity for the following day.

The Sc10 requires data of a more complex nature than the Sc4, making it cumbersome to use. The Sc4 does not require a sounding as input, and yet it is shown to be virtually equivalent to the Sc10 in accuracy. These results justified the implementation of a regional version of the Sc4 during 1982 operations. Evaluation of the latter is discussed in Part II of this series of papers.

The SYNOPTIC INDEX of CONVECTION:

I. Evaluation of the Single-Valued Index, 1978-82

G.S. Strong and W.D. Wilson

ASD, Alberta Research Council
Red Deer, Alberta

1. NUMERICAL CLOUD MODELS and INSTABILITY INDICES

Most instability indices and numerical cloud models incorporate basic thermodynamic parcel theory, with or without other more complex physics. Many efforts here are towards the prediction of various aspects of convective clouds, including showers, thundershowers, and hail. Cloud models, limited by stringent boundary conditions and the sheer volume of computations involved, consider only the cloud scale of atmospheric motion, generally 1-10 km length scale, and 1-60 minutes time scale. One result of this is that contemporary models have been very limited in their use of atmospheric sounding data. For example, the Loaded Moist Adiabatic (LMA) model of Chisholm (1973) provides cloud scale estimates of vertical velocity, and is very responsive to subtle changes to a sounding, thereby providing a very useful diagnostic tool (e.g., English and Wong, 1976). To provide a two-dimensional field of parcel energy, however, soundings at 'cloud scale' intervals in space and time would be necessary. The LMA is therefore confined to one dimension and therefore to a single atmospheric sounding. By the same token, it is rather less useful as a forecasting tool, because of the difficulty in producing an accurate, detailed forecast sounding 6-18 hours in advance. For the more severe convective storms, environmental changes occur too rapidly to consider forecasting with such models using soundings older than an hour or two. Thus, most soundings are obsolete for cloud model forecasts by the time they are received.

More detailed three-dimensional models have been developed (e.g., Schlesinger, 1978) which are useful for demonstrating cloud responses to various environmental and cloud microphysics changes. Unfortunately, because of restrictions such as model initialization and numerical stability, it may be many years before three-dimensional models can accept 'real' data at the model grid boundaries in a nested grid numerical setup. Only then are cloud models likely to see routine application in the forecast situation.

Most instability indices are limited by the number and/or type of variables incorporated, usually two or three thermodynamic variables. The number of levels considered can also restrict the reliability of indices. For instance, an estimate of equivalent potential temperature (Theta-e), or wet bulb potential temperature (Theta-w) can be useful in determining relative instability across a region, but may be confined to surface data only . Most lifted indices incorporate two levels, usually the surface and 500 mb. These may, for instance, under-estimate convective potential when a "capping inversion" is present on the sounding. Such a thermodynamic condition often forms near the top of the planetary boundary layer (about 800 mb in Alberta).

In short, operational use of cloud models for forecasting is limited, because their usefulness is (currently) confined to the time and size characteristics of the 'cloud scale' of motion (1 hour or less, 1-10 km). Instability indices are also limited, since the forecaster must use synoptic scale upper air (sounding) data (12-24 hours, more than 1000 km), and sub-synoptic scale surface data (1-3 hours, 100-1000 km), and then attempt to forecast events at the cloud scale or even smaller; e.g., maximum hail size from a thunderstorm not yet formed.

This wide range of atmospheric scales of motion therefore had to be considered in developing an improved convective index for the Alberta Hail Project (AHP) in 1977. The result was the single-value predictor, the Synoptic Index of Convection (Sc10 - Strong, 1979), which attempts to circumvent the more complex physics and mathematics with statistical relations. This index has now been successfully tested over five seasons, 1978-82. More recently, a simpler form of the Synoptic Index, the Sc4, was implemented as an area predictor of convection. This paper (Part I) re-evaluates these indices as single-valued predictors for the AHP operations area. Part II focuses on operational tests of the Sc4 as a regional predictor of convective activity.

2. DEVELOPMENT of the SYNOPTIC INDEX

Priorities for developing the Synoptic Index were determined by cloud seeding operations for hail suppression. These operations required a forecast of Hail/No Hail for the AHP area, and, if possible, a prediction of the

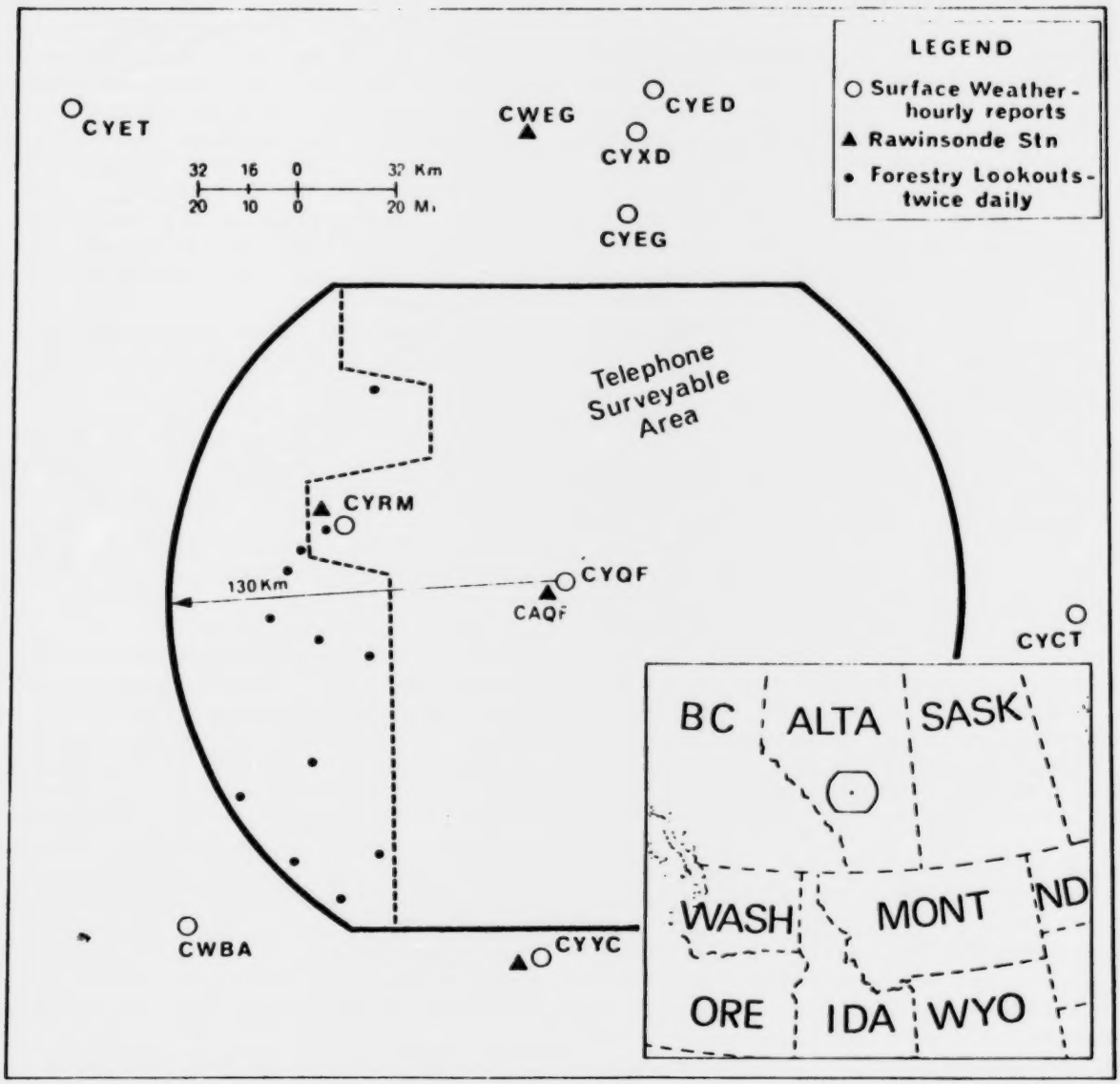

Figure 1. The Alberta Research Council Hail Project (AHP) operations area, showing meteorological data networks, 1978-82.

maximum hail size. At first glance, this appears to fall into the above-mentioned trap of using synoptic scale data to attempt a cloud scale forecast. This is not quite the case, since, at the time, it was only necessary to predict these variables for anywhere over the AHP operations area, a convenient sub-synoptic scale region of 260-km diameter (Figure 1). This scale of area does not allow the forecaster to 'cheat' by using biases in hail day*1 statistics, since hail occurs on about 50% of the operational days (June through August).

It was first necessary to develop a predict and which adequately described maximum convective intensity for a day, and which covered the range of convective weather types in Alberta. The predict and categories were chosen so as to approximate a Poisson type of distribution, similar to the predictor variables to be used. The result was the Convective Day Categories (CDC's), defined in Table 1 (Strong, 1979). Since the CDC for a day is defined as the maximum degree of convective intensity for the climatological day for the entire AHP operations area, any predictor based on the CDC should be interpreted in a similar way; i.e., one number for one 260-km diameter region.

More than 90 instability and synoptic predictor variables were tested, all chosen with some physical, but at the time, unknown mathematical relation with CDC in mind. For example, inspection of the Stability Tendency Equation*2 will suggest several dozen possible predictor variables. These predictor variables were correlated to CDC using an initial three-year (1975-77) data base of 266 operational days. The data base is updated periodically.

*1 A day qualifies as a 'hail day' only if 2 or more hail reports are received during the 'climatological day', 1200-1200 UTC.

TABLE 1. Definitions of Convective Day Categories (CDC's) for the AHP operations area, with qualifying notes (after Strong, 1979).

CDC	DEFINITION
+ 5	LARGER THAN GOLFBALL (52 mm diameter) Maximum size* reported
+ 4	GOLFBALL (33 - 52 mm) Maximum size* reported
+ 3	WALNUT (21 - 32 mm) Maximum size* reported
+ 2	GRAPE (13 - 20 mm) Maximum size* reported
+ 1	PEA (5 - 12 mm) or SHOT (4 mm) Maximum size* reported
0	WIDESPREAD SHOWERS at 3 or more of the synoptic stations BA, YC, QF, RM, CT, and EG, or the occurrence of a THUNDERSHOWER at or near either station after 1700 GMT
- 1	SCATTERED SHOWERS (at 1 or 2 of the 6 synoptic stations after 1700 GMT), with NO HAIL or THUNDERSHOWER
- 2	ACC, TCU, CB reported by 2 or more of the 6 synoptic stations, but no showers after 1700 GMT
- 3	NO DEEP CONVECTION (no ACC, TCU, CB)

QUALIFYING NOTES

1) All HAIL categories are based on a climatological day, 6 A.M. - 6 A.M. MDT (1200-1200 GMT). For forecasting and verification purposes, the day begins at briefing time, 1700 GMT.

*2) At least two hail reports are required to qualify in each HAIL category.

3) Showers must be accompanied by cumulus congestus clouds (TCU) to qualify as CDC = -1 or 0.

4) Three reports of showers from volunteer reports (telephone surveys) or forestry towers are considered the equivalent of one synoptic station reporting showers.

5) The surface synoptic reports used include all 'Specials' and also make use of 'Remarks'

6) Additional restrictions are placed on the use of remarks from those synoptic stations which lie just outside the AHP project area (YC, BA, EG, and CT); e.g., "SHWRS W CT" are counted but "SHWRS E CT" are ignored.

The 10 highest-correlating predictor variables were chosen for the Synoptic Index (Sc10). Each variable was linearly equated to CDC, and also weighted according to the degree of correlation. The 10 correlations and weighting coefficients for the predictor variables for the 1975-79 data base are shown in Table 2, together with similar coefficients used later for the SC4 index.

Statistical problems were encountered in equating the final predictor to CDC because the CDC is discrete-valued with upper (+5) and lower (-3) limits, while the overall Predictor is continuous with no such bounds. This was alleviated by invoking a final linear transformation on the Predictor equation, resulting in the Sc10.

*2 The Stability Tendency Equation is covered in several texts on atmospheric thermodynamics: e.g., Iribarne and Godson (1973).

The EGDEX (Checkwitch, 1971), Tephigram Lifted Index, and Mixing Ratio are initial-time (analytic) variables, reducing subjective input. The remaining seven predictor variables depend on prognostic output from the appropriate synoptic scale models. The "perfect prog" approach was adopted, applying a linear 'prog error trend' to each of the seven prognostic predictors. Diurnal trends (12-2400Z and 00-1200Z) are also applied to the thickness, height, vorticity, and 700 mb temperature predictors for the Sc10.

Detailed information on the development of the Convective Day Category and the Synoptic Index were presented by Strong (1979) and Strong and Wilson (1981) - copies of these conference papers are available. We now turn to evaluation of the Synoptic Index as a single-value predictor (Sc10, Sc4) of maximum convective intensity for the AHP operations area.

TABLE 2. Linear Correlation coefficients between (A) CDC and the 10 predictor variables comprising the Sc10, and (B) CDC and the 4 Sc4 predictor variables, along with weighting coefficients. The data base used here is for 1975-79 (448 days).

PREDICTOR VARIABLE	CORREL. WITH CDC	WEIGHT COEFFS.
(A) Sc10		
1. Max EGDEX over AHP (1500 UTC)	0.577	0.146
2. Representative Tephigram Lifted Index (from morning sounding)	0.456	0.115
3. 12-hr 500mb Height Change (m)	-0.411	0.104
4. 12-hr 1000-500 mb Height Change (m)	-0.386	0.098
5. 12-hr 700 mb Temperature Change (C)	-0.381	0.096
6. LFM Best Lifted Index	-0.381	0.096
7. Trough-Ridge Category (TRC)	0.379	0.096
8. 12-hr 500mb Vorticity Change	0.372	0.094
9. Representative Mixing Ratio over AHP	0.308	0.078
10. 2400Z 500mb Vorticity	0.305	0.077
(B) Sc4		
1. Max EGDEX over AHP (1500 UTC)	0.577	0.288
2. 24-hr 700 mb Temperature Change (C)	-0.492	0.246
3. 24-hr 1000-500mb Thickness Change (m)	-0.479	0.239
4. Representative Tephigram Lifted Index	0.456	0.228

3. EVALUATION of the SINGLE-VALUED SYNOPTIC INDEX

A number of versions of the Synoptic Index have been tested, including several employing more complex stepwise linear regression and Principal Component Analysis (Strong and Wilson, 1981). While the regression equations showed a very slight edge over the simple correlation routine used for the Sc10 and Sc4, there was no easy way of handling missing data, limiting their operational usefulness. With the technique adopted, a simple re-weighting of predictor variables yields little change to the Sc10 (for up to 3 missing variables) or Sc4 (one missing variable allowed).

Tables 3 and 4 summarize operational tests of the Sc10 and subjectively-modified Sc10 (official forecast CDC) for the five years 1978-82, and of the Sc4 for the two years 1981-82. Forecast data are independent of the data base statistics. The latter are updated following each operating season.

TABLE 3. Verification of diagnostic and forecast Convective Day Categories for AHP, centered at Red Deer Airport (CAQF). Evaluations (except correl. coeffs.) are per cent of total forecasts for maximum available periods.

		Sc10	Sc4	Subjectively Modified* Forecast CDC
DIAGNOSTIC (1978-82):				
Correl. with CDC		0.69	0.67	N/A
Correct within 1 CDC Categ.		65	64	N/A
Correct within 2 CDC Categs.		86	87	N/A
DAY-1 FORECAST (1980-82):				
Correl. with CDC		0.68	0.65	0.71
Correct within 1 CDC Categ.		66	64	74
Correct within 2 CDC Categs.		85	83	91
FORECAST DAY 2:	(1979-82)	(1981-82)	(1981-82)	(1981-82)
Correl. with CDC	0.41	0.25	0.24	0.25
Correct within 2 Categs.	76	78	78	76
Correct Hail/No Hail Strat.	63	59	59	61

* Subjective decisions (the 'official' forecasts) are made after viewing the objective indices.

TABLE 4. Forecast Verification of Hail/No Hail stratifications for AHP (1980-82). Note that subjective forecasts are made after viewing the objective indices.

		FORECAST Sc10		FORECAST Sc4		SUBJECTIVE FORECAST CDC	
		Hail	No Hail	Hail	No Hail	Hail	No Hail
OBSERVED	HAIL	109	18	106	19	106	21
	NO HAIL	33	77	30	79	31	81
Correct Hail Days:		86%		85%		83%	
Correct Hail/No Hail:		79%		79%		78%	

It is apparent from Tables 3 and 4 that the Synoptic Index (Sc10 or Sc4) has DAY-1 predictive skill, not only for forecasting the Hail/No Hail stratification (79%), but also in forecasting to within one CDC category (64-66%).

Experienced forecasters are able to subjectively modify the category forecasts with some success (74% within one category to 66% for Sc10). This apparent skill comes in forecasting the median categories (-1 to +2) where, in fact, inaccuracies due to uncertain reports of small hail may be a bias against the forecast. Since the hail (CDC) categories are based on hail size reports from untrained volunteers, there is inherent uncertainty even in the diagnostic CDC categories. Overall, the forecaster has been unable

to better the index in forecasting the Day-1 Hail/No Hail stratifications, scoring 78% compared with 79% for both indices. One factor here appears to be the conservative tendency for forecasters to go with 'initial' conditions during rapidly changing and uncertain meteorological conditions. In such cases, the forecaster can be wrong by 4-6 categories while the Synoptic Index is then almost invariably closer. Certain guidelines, if followed, could improve the human score; e.g., rarely, if ever, forecast No Hail if Sc is greater than +1.5!

The Sc4 has virtually the same potential as the Sc10 in the role of a single-valued predictor, but is also far simpler to compute and to automate. Over the operational test period 1980-82, the Sc4 was within one category of Sc10 89% of the time, and within two categories in 98% of the cases. For the same period, the correlation coefficient between forecast values of the Sc4 and Sc10 was 0.93. In particular, the Sc4, like the Sc10, is most reliable in severe convective situations. It has a slight edge in correctly forecasting the the Hail/No Hail stratifications. These test results suggested that the Sc4 would satisfy major requirements of a state-of-the-art areal predictor of convective intensity; i.e., ease of computation (all 4 predictor variables automated), and known reliability as a forecast index.

Finally, a word about extended convective forecasts. In its current state, the Day-2 Synoptic Index 'outlook' is useful only as a trend. It is correct within two categories more than 75% of the time, but has little useful skill to within one category. This is so primarily because of subjective instability input (often a poor guesstimate) rather than inaccurate prognostic synoptic data. A Day-2 outlook index based only on synoptic data might verify better.

4. CURRENT AND FUTURE IMPROVEMENTS

The Sc4 is almost equivalent to the Sc10 in forecast accuracy. It has now been automated by introducing a surface parcel lifted index (SPLI) to replace the tephigram index. The SPLI is simply the result of subtracting the 2400 UTC 500 mb temperature from the surface wet bulb temperature raised adiabatically to 500 mb. While the SPLI lacks the vertical resolution of a sounding-derived index, it provides additional (horizontal) spatial and time resolution. During the summer, there are only three regular rawinsonde sites in Alberta (the AES one near Edmonton, and two ARC sites at Red Deer and Calgary, all in close proximity - see Figure 1), and none currently in Saskatchewan. Normally, only two daily soundings from each are available (morning and late afternoon). By contrast, the SPLI can be computed for more than 25 surface synoptic stations in Alberta alone, and then updated hourly. There is the conflict that the SPLI is computed similar to the EGDEX and from the same data base. The EGDEX tends to be of coarser resolution, however, because of weighting factors dependent upon wind directions applied to surface wet bulb potential temperatures. In general, the EGDEX is a better predictor than SPLI and is therefore weighted more heavily (see Table 2). In many instances, however, the finer scale features of the SPLI field are valuable in the overall Sc4 computations.

The regional version of the Sc4 was first tested in an analysis of nine case studies for the AES RAINSAT project in 1982. Successful application of the Sc4 in these cases, and consistency between Sc4 and Sc10 forecast values (see Tables 3 and 4) prompted operational implementation of the regional Sc4 index late in the 1982 AHP field operations period. The results of these research and operational tests are discussed in Parts II and III of this series.

Various means to improve on the areal Synoptic Index (Sc4) are being investigated, including the use of new predictor variables such as a wind shear predictor. Significant improvements, however, must now come from three areas:

1) the development of statistical data bases for many new points (synoptic surface stations), instead of the one data base for Red Deer;
2) the development of a completely new 'point' predictand to replace the CDC and obtain higher spatial and temporal resolution;
3) a better understanding of the interactions between physical processes at all scales of atmospheric motion.

There are several problems associated with the current CDC predictand. On the one hand, its discrete values with upper and lower bounds conflict statistically with the continuous-valued Synoptic Index. On the other hand, quantitative hail reports, accounting for five of the nine CDC categories, are available only within the AHP operations area. A combination of surface reports and satellite data to provide statistics on size distributions and types of clouds and cloud clusters, appears to be the best approach to a new predictand. Radar data might also be incorporated, but as with hail data, coverage is not extensive over the Prairies.

AHP work on the first two points can begin in earnest when a planned meteorological data facility is completed. Diagnostic studies on the scale-to-scale interactions between synoptic processes and convective complexes have commenced. Initially this work is investigating synoptic effects on capping inversions which often precede severe convective storms.

5. REFERENCES

Checkwitch, S.M., 1971: A short-range forecast technique for summer precipitation forecasting in the Edmonton area. Unpublished internal AES manuscript by Alberta Weather Centre, Edmonton, Alta., 32 pp.

Chisholm, A., 1973: Alberta hailstorms, Part I: Radar case studies and airflow models. Meteor. Monographs, 14, No.36, Amer. Meteor. Soc., Boston, Mass., 1-36.

English, M. and R.K.W. Wong, 1976: Simple numerical cloud models as potential tools in evaluating hail suppression techniques.

Iribarne, J.V., and W.L. Godson, 1973: Atmospheric Thermodynamics, Geophys. and Astrophys. Monogr., D.Reidel Pub. Co., Holland, 222pp.

Schlesinger, R.E., 1978: A three-dimensional numerical model of an isolated thunderstorm. Part I. Comparative experiments for variable ambient wind shear. J. Atmos. Sci., 35, 690-713.

Strong, G.S., 1979: Convective weather prediction based on synoptic parameters. Preprints A.M.S. 11th Conf. Sev. Loc. Storms, Kansas City, Mo., Oct.79, 608-615.

Strong, G.S., and W.D. Wilson, 1981: The Synoptic (Instability) Index: 1978-80 tests and new versions. Paper presented to 15th Ann. Congr., Can. Meteor. and Oc. Soc., Saskatoon, May 81, 17pp.

APPENDIX

Forecast verification tables, 1980-82, for:

1) Forecast Sc10 index vs. Diagnostic CDC;

2) Forecast Sc4 index vs. Diagnostic CDC;

3) Subjective Forecast CDC (official AHP forecast) vs. Diagnostic CDC;

4) Forecast Sc4 index vs. Forecast Sc10 index.

VERIFICATION TABLES FOR PERIOD 414-2831 FORECASTER: ALL

PREDICTOR: Forecast S_{c10}

PREDICTAND: Diagnostic CDC	-3	-2	-1	0	1	2	3	4	5	TOTALS
-3	8	3	2	4						17
-2	3	3	7	5	1			2		21
-1	4	4	7	3	1	4				23
0	3	3	4	14	9	8	4	3	1	49
1	2	1	3	4	15	10	5	1	1	44
2			1	4	10	9	11	2	5	42
3				1	3	5	8	4	2	23
4						3	3	3	5	14
5						1		1	2	4
TOTALS:	20	14	24	37	39	40	31	16	16	237

	PREDICTAND	PREDICTOR
MEAN:	0.7	1.0
S.D.:	1.9	2.4

PREDICTAND/PREDICTOR CORRELATION COEFFICIENTS

ROUNDED, TRUNCATED: 0.480

PREDICTOR (FORECAST)

PREDICTAND (OBSERVED)	NO HAIL	HAIL
NO HAIL	77	33
HAIL	18	109

NUMBER OF DAYS IN PERIOD: 237 DAYS

HAILDAYS IN PERIOD: 127 DAYS = 53.6%

CORRECT CATEGORY: 69 DAYS = 29.1%

CORRECT WITHIN ONE CATEGORY: 157 DAYS = 66.2%

CORRECT WITHIN TWO CATEGORIES: 202 DAYS = 85.2%

CORRECT HAIL DAYS FORECAST: 109 DAYS = 85.8%

CORRECT HAIL-NO HAIL STRATIFICATION: 186 DAYS = 78.5%

VERIFICATION TABLES FOR PERIOD 414-2831 FORECASTER: ALL

PREDICTOR: Forecast S_{c4}

PREDICTAND: Diagnostic CDC	-3	-2	-1	0	1	2	3	4	5	TOTALS
-3	8	3	4	1						16
-2	3	5	8	2			1		1	20
-1	4	4	6	4	4	1				23
0	4	4	8	11	7	3	8	3	2	50
1		2	3	5	12	11	3	5	2	43
2				8	8	12	4	3	6	41
3			1		1	10	5	5	1	23
4					3	4		3	4	14
5					1			1	2	4
TOTALS:	19	18	30	31	36	41	21	20	18	234

	PREDICTAND	PREDICTOR
MEAN:	0.7	0.9
S.D.:	1.9	2.6

PREDICTAND/PREDICTOR CORRELATION COEFFICIENTS

ROUNDED, TRUNCATED: 0.451

PREDICTOR (FORECAST)

PREDICTAND (OBSERVED)	NO HAIL	HAIL
NO HAIL	79	30
HAIL	19	106

NUMBER OF DAYS IN PERIOD: 234 DAYS

HAILDAYS IN PERIOD: 125 DAYS = 53.4%

CORRECT CATEGORY: 64 DAYS = 27.4%

CORRECT WITHIN ONE CATEGORY: 149 DAYS = 63.7%

CORRECT WITHIN TWO CATEGORIES: 193 DAYS = 82.5%

CORRECT HAIL DAYS FORECAST: 106 DAYS = 84.8%

CORRECT HAIL-NO HAIL STRATIFICATION: 185 DAYS = 79.1%

VERIFICATION TABLES FOR PERIOD 414-2831 FORECASTER: ALL

PREDICTOR: Subj. Forecast CDC

PREDICTAND: Diagnostic CDC	-3	-2	-1	0	1	2	3	4	5	TOTALS
-3	9	2	6							17
-2	6	3	6	3	3	1				21
-1	1	4	10	4	4		1			24
0	1	2	9	16	10	7	3	2		50
1			3	3	7	17	10	3	1	44
2				2	2	10	17	6	3	47
3				1	1	1	11	8	1	23
4					2		4	3	4	1	14
5							1	2	1		4
TOTALS:	17	14	37	34	45	51	28	11	2	239

	PREDICTAND	PREDICTOR
MEAN:	0.7	0.7
S.D.:	1.9	1.9

PREDICTAND/PREDICTOR CORRELATION COEFFICIENTS

RAW: 0.712

PREDICTOR (FORECAST)

OBSERVED PREDICTAND	NO HAIL	HAIL
NO HAIL	81	31
HAIL	21	106

NUMBER OF DAYS IN PERIOD: 239 DAYS

HAILDAYS IN PERIOD: 127 DAYS = 53.1%

CORRECT CATEGORY: 84 DAYS = 35.1%

CORRECT WITHIN ONE CATEGORY: 177 DAYS = 74.1%

CORRECT WITHIN TWO CATEGORIES: 217 DAYS = 90.8%

CORRECT HAIL DAYS FORECAST: 106 DAYS = 83.5%

CORRECT HAIL-NO HAIL STRATIFICATION: 187 DAYS = 78.2%

VERIFICATION TABLES FOR PERIOD 414-2831 FORECASTER: ALL

PREDICTOR: Forecast S_{C4}

PREDICTAND: Forecast S_{C4}	-3	-2	-1	0	1	2	3	4	5	TOTALS
-3	15	3	1							19
-2	2	4	8							14
-1	1	9	5	4	3					24
0	1	1	12	16	5	2				37
1			4	8	14	8	2	1		37
2		1		1	9	20	4	2		39
3					3	10	11	6	1	31
4					1	1	2	6	6	16
5								5	11	16
TOTALS:	19	18	30	31	35	41	21	30	18	233

	PREDICTAND	PREDICTOR
MEAN:	1.0	0.9
S.D.:	2.4	2.4

PREDICTAND/PREDICTOR CORRELATION COEFFICIENTS

RAW: 0.927

PREDICTOR (FORECAST)

OBSERVED PREDICTAND	NO HAIL	HAIL
NO HAIL	84	10
HAIL	14	125

NUMBER OF DAYS IN PERIOD: 233 DAYS

HAILDAYS IN PERIOD: 139 DAYS = 59.7%

CORRECT CATEGORY: 102 DAYS = 43.8%

CORRECT WITHIN ONE CATEGORY: 207 DAYS = 88.8%

CORRECT WITHIN TWO CATEGORIES: 229 DAYS = 98.3%

CORRECT HAIL DAYS FORECAST: 125 DAYS = 89.9%

CORRECT HAIL-NO HAIL STRATIFICATION: 209 DAYS = 89.7%

The SYNOPTIC INDEX of CONVECTION:

Part II.
Applications to
Regional Forecasts of Convective Complexes

G.S. Strong and W.D. Wilson

Atmospheric Sciences Department
Alberta Research Council
Red Deer, Alberta

Paper prepared for the Mesoscale Workshop, Toronto, Ontario, 24-27 January, 1983, and for the 17th Annual CMOS Congress, Banff, Alberta, 03-05 May, 1983.

The SYNOPTIC INDEX of CONVECTION:

Part II.

Applications to Regional Forecasts of Convective Complexes

G.S. Strong and W.D. Wilson

Atmospheric Sciences Department,
Alberta Research Council
Red Deer, Alberta

ABSTRACT

The Synoptic Index of Convection (Sc10) was developed for forecasting maximum convective intensity for a day over the 130-km radius Alberta Hail Project area (AHP) in central Alberta. While it has been a reliable hail predictor for cloud seeding operations for five years (1978-82), data extrapolation and computations for even a single value of Sc10 are time-consuming and too cumbersome for automated use. A new version, the Sc4, is easily computed from two synoptic and two instability predictor variables. Unlike the Sc10, there is no subjective input. The Sc4 showed almost the same predictive skill as the Sc10 during 1980-82 operations over AHP, while the linear correlation between the two indices was 0.93.

An automated regional version of the Sc4 was tested during 192 field operations. It yields a convective forecast for southern Alberta and adjacent regions of Saskatchewan and B.C., also providing hourly updates. This paper evaluates the 1982 performance of this regional forecast index for a wide range of convective weather types, from no convecion to severe hail-producing thunderstorm complexes. Included with the 1982 tests is a hindcast of the most expensive natural disaster in Canadian history, the Calgary hailstorm of 28 July 1981. These tests suggest potential economic benefits from using the Synoptic Index for severe thunderstorm advisories, as well as for field research activities and cloud seeding operations.

The SYNOPTIC INDEX of CONVECTION:

Part II.

Applications to Regional Forecasts of Convective Complexes

G. S Strong and W.D. Wilson
ASD, Alberta Research Council
Red Deer, Alberta

1. INTRODUCTION

Part I of this series reviewed the operational performance of the Synoptic Index of Convection (Sc10) during 1978-82 (Strong and Wilson, 1983). As a predictor of convective intensity for the Alberta Research Council Hail Project (AHP, see Figure 1), the single-valued Sc10 accurately forecast within one CDC (Convective Day Category) category 69% of the 421 operational days during this 5-year period. With subjective modification of the index by the forecaster, this was improved to 75%. However, AHP forecasters have the advantage of 'seeing' the index forecast first. The forecast Sc10 fared better in forecasting the correct Hail/No Hail stratification, and in correctly predicting a hail day!

The potential of the Sc10 as an areal predictor of convective intensity was shown by Strong (1979). Unfortunately, it was not readily amenable to automated forecasts, because the computation was somewhat cumbersome due to the number (10) and type (e.g., the Trough/Ridge Category) of predictor variables. For this reason, a four-predictor version, the Sc4, was developed. Strong and Wilson (1981, and again in Part I of this series) compared both diagnostic and forecast results from the Sc10 and Sc4. As expected, the Sc10 proved slightly better overall, but not significantly so.

To recapitulate 1980-82 operational results for Day-1 forecasts, the forecast indices were correct to within one category 66% of the time, and within two categories 85%. Daily subjective modifications of the objective index by the forecaster improved these category forecasts to 74% within one, and to 91% within two categories. However, subjective modifications provided no additional skill to Hail/No Hail forecasts (78% compared to 79% for both Sc10 and Sc4). These operational results suggested that the Sc4 would satisfy major requirements of a state-of-the-art areal predictor of convective intensity; i.e., ease of computation (all 4 predictor variables automated), and known reliability as a forecast index. Both indices usually result in the same forecast. In fact, the correlation coefficient between forecast values of the Sc4 and Sc10 was 0.93 (1980-82). In particular, the Sc4, like the Sc10, is most reliable in severe convective situations.

1.1 Applications of the Areal Sc4 —

The Sc4 was first applied as an areal predictor for the AES RAINSAT*1 Project of 1982. Nine cases, ranging from severe hailstorms to scattered showers, were investigated (Humphries and Strong, 1982). The diagnostic success of the Sc4 in these cases prompted limited operational tests during the 1982 AHP field program. This paper summarizes results of these tests. They include one severe hail day (July 21), a moderate hail day (July 29), and 13 weak to moderate convective days (September 01-12, and 15). Finally, the Sc4 is tested post facto on the severe Calgary hailstorm of July 28, 1981.

The RAINSAT Study showed that the Sc4 worked best for severe thunderstorm days (Humphries and Strong, 1982). On weak convective days (CDC: -1 to +1), the Sc4 still diagnosed the locations of primary convective versus stable regions quite well, but absolute values tended to be too high for the two or three RAINSAT cases chosen. In general, the latter conditions occurred with cool airmasses and fast-moving synoptic systems, when synoptic influences (700 mb cooling and 1000-500 mb thickness falls) were quite high, but thermodynamic instability was relatively low. The problem is partly statistical, because the predictand (CDC) is discrete-valued and has upper (+5) and lower (-3) limits, while the Sc4 is continuous with no such limits.

In future, these effects may be lessened by fixing limits to individual predictors (e.g., perhaps limit the EGDEX to +/-5). Further experimentation is being carried out on this, but for the current tests, some

*1 The Atmospheric Environment Service (AES) of Environment Canada is examining the uses of real-time satellite, radar, and other data sources to improve short-term forecasting. This project, called RAINSAT, will eventually operate across the country. ARC was contracted to identify important parameters in precipitation processes on the prairies.

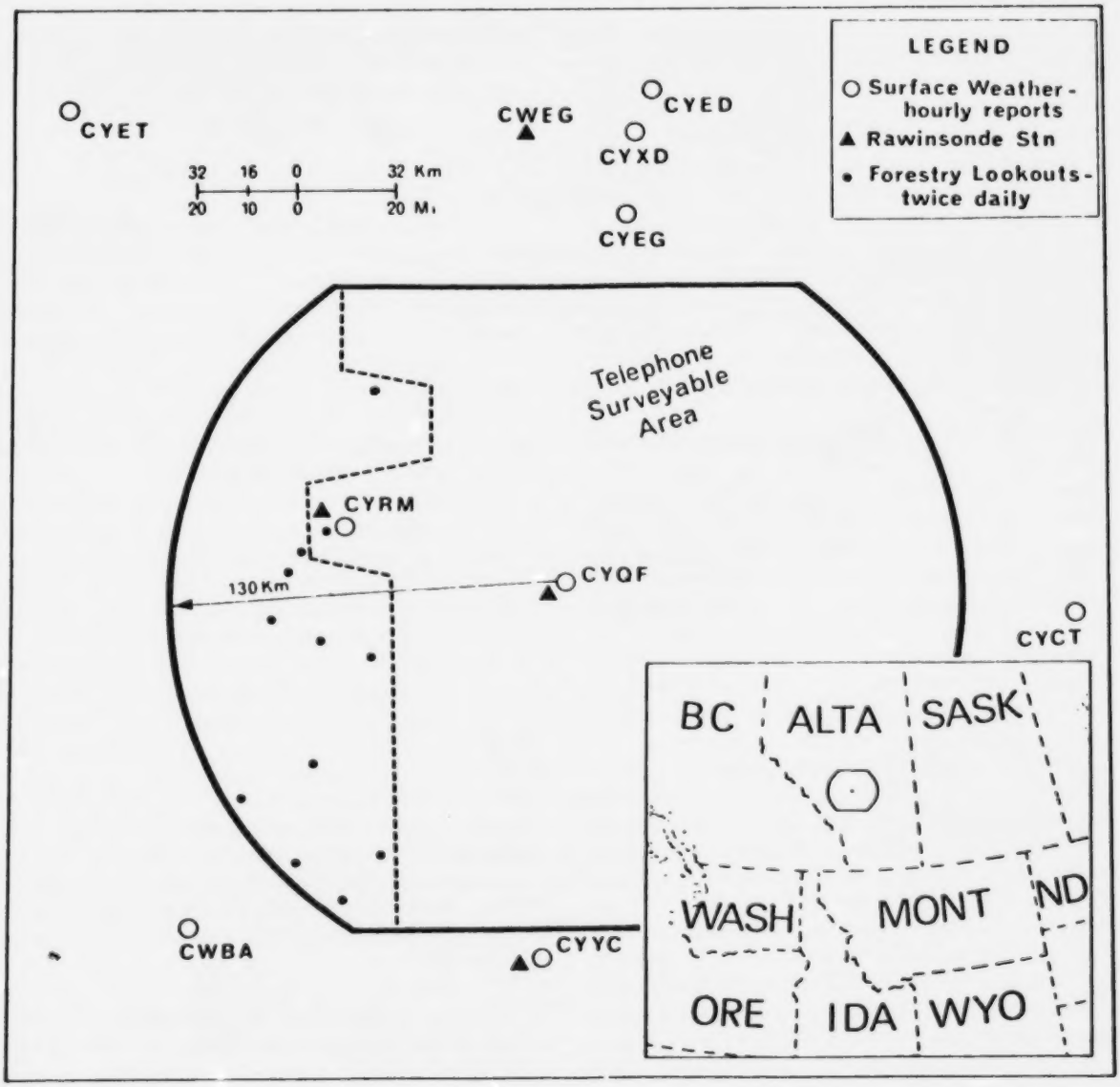

FIGURE 1. The Alberta Research Council Hail Project (AHP) operations area, showing meteorological data networks, 1978-82.

arbitrary adjustment of values appeared to be necessary. Thus, a blanket whole-number adjustment was applied to all Sc4 values on a map. This number was based on a +5 maximum (or -3 minimum) over southern Alberta where the statistics are most valid. For example, if the maximum Sc4 over southern Alberta happened to be +6.4, then +2 was subtracted from all values to force a maximum contour value of +4 (since the maximum possible CDC is +5). This procedure necessitated adjustments to 7 of the 16 cases to be presented here, and in all but one, the original value for Red Deer (centre of AHP) was outside the range -3 to +5. The adjustments are indicated on each Sc4 map.

2. OPERATIONAL TESTS DURING JULY, 1982

2.1 Case Study, July 21, 1982 -

The major hailstorm for this day developed west of Rocky Mountain House (CYRM) and moved east-northeast through AHP, leaving a very well-defined hailswath and widespread crop damage. A small tornado touched down briefly near CYRM. Over 400 hail reports were recorded, of which about 10% included hailstones larger than 50 mm diameter.

At 500 mb (Figure 2a), a closed low had moved off the Gulf of Alaska into southeast B.C., causing surface frontogenesis there. This upper low then turned northeast, crossing the Continental Divide into central Alberta near midnight of the 21st, eventually moving into northern Manitoba. Ahead of it, the surface low split, with one centre moving northeast with the upper feature, crossing AHP during the evening (of the 21st). The second low with frontal wave moved eastward into southern Saskatchewan overnight. These two surface features were directly related to first, the major severe storm complex over central Alberta, evident in the NOAA-7 satellite imagery (Figs.4,5), and second, complex(es) spawned during the evening over southeast Alberta and later (early morning) over southeast Saskatchewan. Figure 3b is a summary composite of all storms for the day.

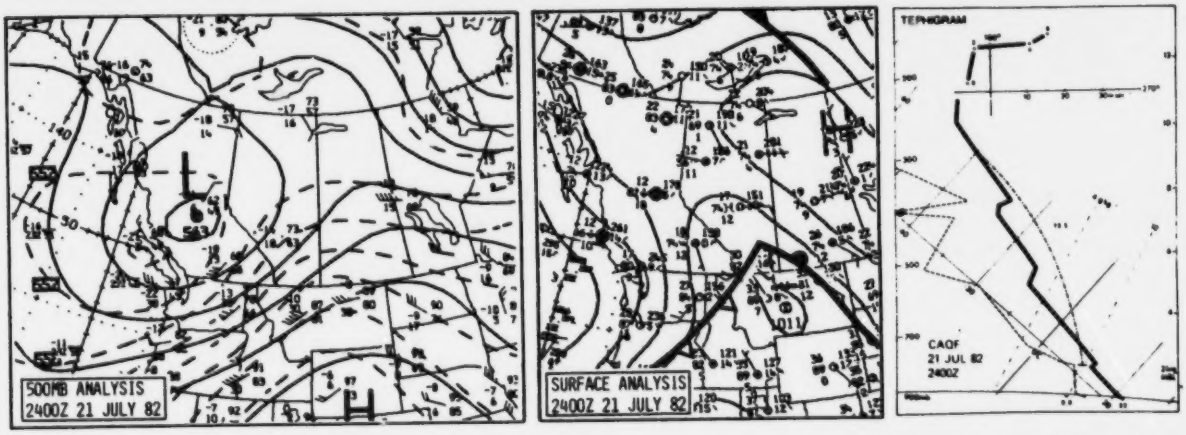

Figure 2. (a) 500 mb and (b) Surface analyses for 2400 UTC, and (c) sounding most representative of maximum convective conditions, 21 July 1982.

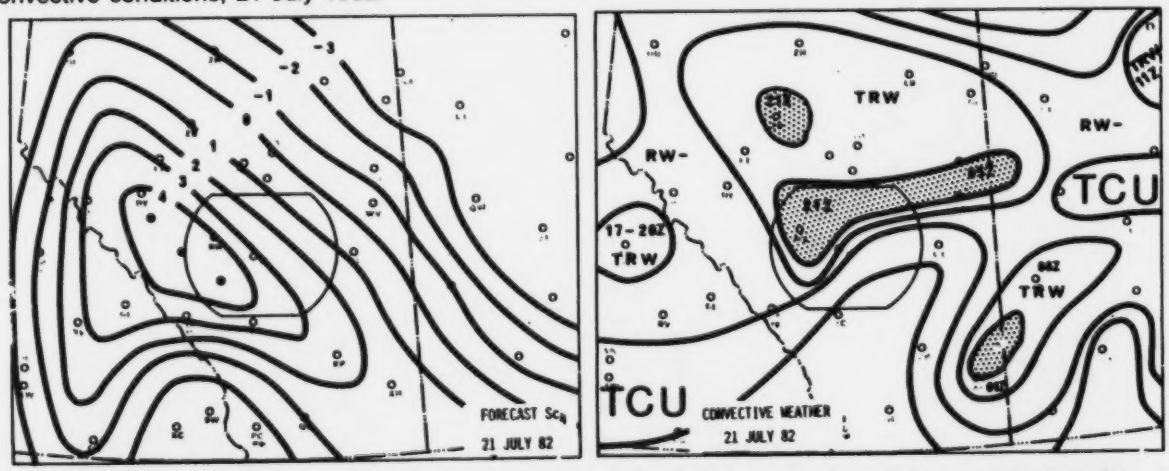

Figure 3. Convective weather, 21 July 1982. (a) Forecast Sc4 map; (b) coarse diagnostic convective weather composite for 1700-1200 UTC, from surface weather observations, AHP hail reports, and satellite imagery. Shading represents approximate hail regions.

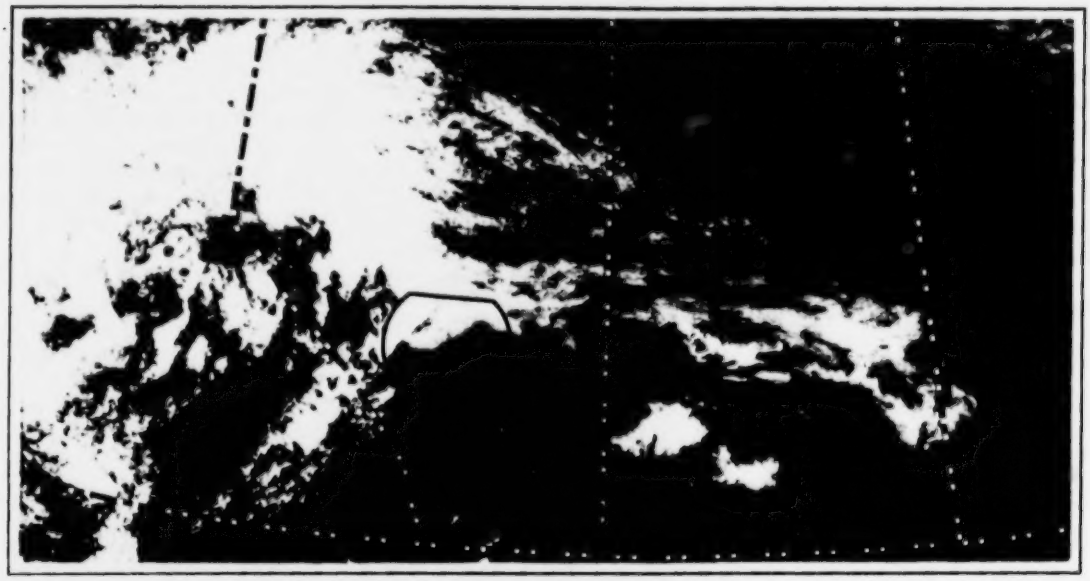

Figure 4. NOAA-7 Visible satellite imagery for 2132 UTC, 21 July 1982.

When a capping inversion (near 800 mb) occurs over AHP prior to a severe storm, normally it is evident on one or more morning (1200-1400 UTC) upper air soundings. In this case, the capping inversion did not show up until an 1830 UTC sounding at Red Deer — it was partially removed again by 2400 UTC (Figure 2c). Soundings used in the AHP forecast briefing at 1700 UTC did not reveal particularly unstable conditions for a mid-July day. As well, broken to overcast cloud conditions had developed over most of AHP by late morning. Consequently, the forecast Sc4 map (Figure 3a), the first ever produced operationally, was downgraded during the briefing and only moderate intensity storms were forecast.

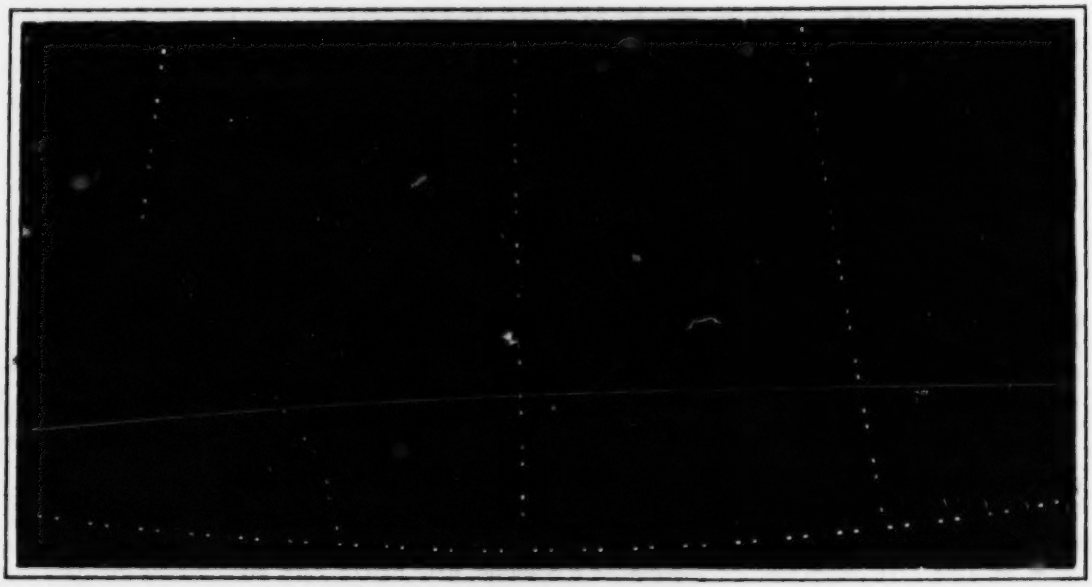

Figure 5. NOAA-7 enhanced infra-red satellite imagery for 2132 UTC, 21 July 1982.

Morning soundings did not support the storm size, intensity, or areal extent suggested by Figure 3b. The Sc4 forecast (Fig.3a), however, proved correct when a major thunderstorm complex developed west of CYRM around 2100 UTC. The surface convective weather composite chart is based on the maximum convective intensity (clouds and precipitation type) reported by each surface synoptic station, from 1700 UTC (forecast time) up to 1200 UTC the following morning (i.e., the climatological day). It is supplemented by the high density hail reporting network over AHP. Times on Figure 3b are approximate reported times of thundershowers and hail.

In evaluating the Sc4 forecast performance in this case, several points can be made in its favour. To summarize, it correctly forecast:

1) the major storm complex development regions, generally a northwest to southeast line just east of the foothills;
2) the location of the most intense storm to within 20-30 km (Sc4 = +5 west of CYRM);
3) the line of weaker convection extending southwestward into southeast B.C. (compare with the satellite imagery of Figure 4);
4) the more stable conditions penetrating into extreme southwest Alberta (negative Sc4 values);
5) hail northwest along the foothills almost to Grande Prairie (QU on map), with convective showers further northwest;
6) thundershowers and hail (Sc4: +1 to +3) over southeast Alberta (e.g., Medicine Hat, XH) and, to some extent, weaker thundershowers (-1 to +1) over southern Saskatchewan*2;
7) essentially no convective weather over northeast Alberta and northern Saskatchewan (Sc4 = -3).

2.2 Case Study, July 29, 1982 -

This storm system, while not approaching the severity of July 21st, nevertheless produced 42 reports of hail within the AHP operations area, including several of 35-55 mm diameter. Synoptic features were weak in this instance. At 500 mb (Figure 6a), a rather diffuse shortwave trough was embedded in a moderate northwest flow over northern Alberta. While the related surface low remained over northern regions (Figure 6b), lee troughing developed east of the Alberta foothills, eventually resulting in a secondary low near the southern Alberta/Saskatchewan border by midnight of July 29th. This drew low-level moisture into southern regions (from dew point temperatures of 6-8C at 12Z to 12-15C 24 hours later) and was probably a major factor in the weak thundershowers reported over southwest Saskatchewan after midnight (Figure 7b).

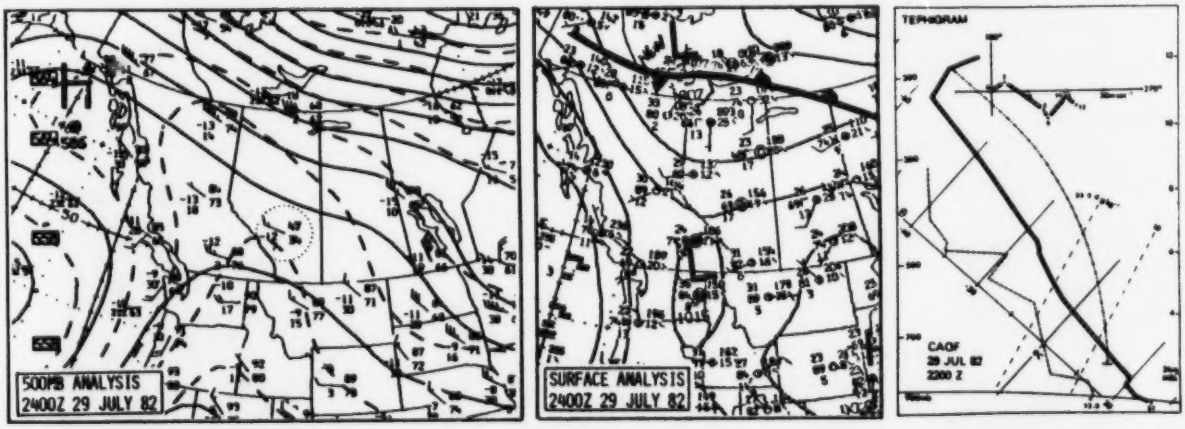

Figure 6. (a) 500 mb and (b) Surface analyses for 2400 UTC, and (c) sounding most representative of maximum convective conditions, 29 July 1982.

*2 Relatively low dew point temperatures over Saskatchewan of 6-8 degs. C at forecast time, resulted in low Sc4 values there (Figure 3a). Updated Sc4 forecasts would have increased this potential, and perhaps forecast a secondary storm maximum as the surface frontal system brought higher dew points into that region (13-16 C 15-20 hours later when storms occurred).

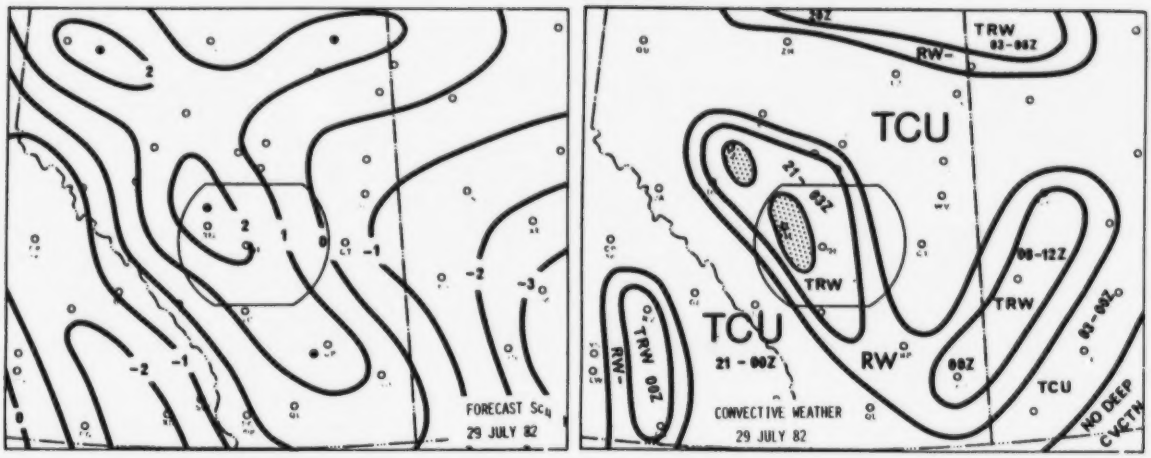

Figure 7. Convective weather, 29 July 1982. (a) Forecast Sc4 map; blanket adjustment to Sc4 values = 0. (b) Coarse diagnostic convective weather composite for 1700-1200 UTC, from surface weather observations, AHP hail reports, and satellite imagery (as Fig.3.).

Figure 8. NOAA-7 Visible satellite imagery for 2137 UTC, 29 July 1982, showing moderate convective complexes corresponding to reported thunderstorm regions of Fig.7(b).

Figure 9. NOAA-7 enhanced infra-red satellite imagery for 2137 UTC, 29 July 1982.

The Sc4 forecast evaluation is again summarized by comparing individual features of the Sc4 map with the surface weather (including AHP hail reports) composite chart and satellite imagery as follows:

1) The main Sc4 maximum near CYRM was confirmed by a cluster of three storms which formed over AHP. The first one developed northeast of Red Deer, and while it is the most obvious storm on the 2137 UTC satellite imagery (Figs.8,9), no hail was reported and it decayed rapidly thereafter. The other two AHP storms intensified during the early evening; the largest hail-producer formed west of CYRM, the other further south near Sundre. Another known hail-producer developed northwest of AHP, and is evident on both the weather composite chart and the satellite imagery.
2) The second Sc4 centre over northern Alberta appears to have a high maximum value in view of weak convective activity there. However, it is known that a complex of moderate intensity initially formed northwest of Lesser Slave Lake (ZH) during early afternoon, and moved east into Saskatchewan (Figure 7b) by midnight. This storm appears just northeast of ZH on the 2137 UTC satellite imagery, after which it intensified somewhat. The apparent ability of the Sc4 to predict this additional detail (mesoscale?, less than 100 km scale resolution) is an unexpected bonus!
3) A thunderstorm complex which formed during the evening over southeast Alberta verifies a secondary Sc4 maximum there as well. This storm appeared to propagate into southwest Saskatchewan overnight (TRW's 08-1200 UTC), as cyclogenesis increased surface convergence and pumped moisture into that region. The lateness of this complex strains the temporal resolution capability of the 1600 UTC Sc4 forecast, but its motion could be inferred from subjective techniques.
4) The line of minimum Sc4 values near the continental divide is somewhat displaced, but forgiveable considering the orographic complexities involved.
5) The small thunderstorm complex over southeast B.C. was not forecast well, although higher values (positive Sc4 values, thundershowers) appear on the southwest boundary of the map. Such storms over the mountains often have a dominant orographic component which is not incorporated into the Sc4. Lack of storm motion, as in this case, is suggestive of a strong orographic influence. This factor is the major weakness in the Sc4, and where caution must be used. The Sc4 bias can be either way, depending on the degree and spatial variability of local subsidence and/or ascent. In this case the Sc4 was low, but more often it is high over the mountains. For a northeast (upslope) low-level flow over the Alberta foothills, however, the bias tends to be low with the Sc4 indicating only weak convection.

2.3 Summary of July Test Cases —

It should be emphasized that the Synoptic Index was developed to forecast the most intense degree of convection for a day, and is naturally biased towards that. Normally, storms tend to reach this stage around maximum temperature time; i.e., mid-afternoon to early evening. The Sc4 forecast therefore will often be most representative for conditions around that period of the day.

All things considered, the Sc4 forecasts proved reliable for these two moderate to severe convective complex days, at least at the sub-synoptic scale. It appears to be capable of correctly predicting even meso scale features in at least some instances. Care should be taken in applying it to cases or regions where orographic influences may be quite significant.

3. OPERATIONAL TESTS DURING SEPTEMBER, 1982

Sc4 computations for the two July cases proved rather time-consuming for an operational setting. But the success achieved during mid-summer prompted further development to automate its use. A useful version was attained in time for an extended AHP field operations period, 01-12 September. This provided an excellent opportunity to test the Sc4 operationally during very weak to moderate convective situations.

Results from these 12 days plus 15 September are summarized in Table 1*3. Interestingly, this period included a small (cold airmass) tornado which touched down in Calgary on 10 September. The Sc4 forecast a secondary maximum of +5 near Calgary in this instance*3.

3.1 Summary of September Tests —

Normally, the Sc4 forecasts regions of maximum/minimum convective intensity accurately. For weak convective cases, absolute values of the forecast Sc4 occasionally prove too high, even after blanket adjustments are applied. For example, for 10 September (Fig.A10), values over southern Alberta were high for the observed precipitation types (only some small hail was reported). On the other hand, the secondary maximum near Calgary verified quite well, considering the thundershowers and confirmed (photographed) sighting of a small tornado over the city.

Several cases also occurred where both synoptic and instability influences were negative (e.g., 01 Sept.). In these cases, some Sc4 values assumed the other extreme and were too low (pre-adjusted values as low as -8 in a few instances). Once again, forecasts of very stable regions were usually confirmed by generally cloud-free skies, while weak maxima showed equally weak convective clouds.

Orographic influences which affect the surface temperature and moisture fields (moisture convergence for example) are accounted for indirectly in the Sc4 (EGDEX and SPLI). However, the Sc4 does not incorporate 'strong' orographic influences which might alter the mid-level dynamics and thermodynamics of the atmosphere. This is particularly true over eastern B.C. where ascent induced by topography helps set off convection. However, the fine-scale structure of mountainous topographic features may, at the same time, inhibit the size and severity of hail-producing cells within convective complexes through local orographic subsidence. Hence, there is often a bias towards high Sc4 values over B.C. during widespread convective weather there — an example is 04 September. Over the Alberta foothills on the other hand, a region of forecast Sc4 minimum may turn out to have a convective maximum if orographic lift with low-level northeast winds contributes to destabilization of the airmass — an example of this occurred on 03 September, 1982.

*3 The accompanying synoptic analyses and summaries, convective weather composite maps, and the Sc4 forecast map appear in an appendix (in the original paper) available from the authors.

TABLE 1. Summary of operational tests of forecast Sc4 values of convective complex intensity during very weak to moderate convective days, 01-12 and 15 September, 1982.

1982 SEPT	FORECAST Sc4 FEATURES	OBSERVED CONVECTIVE WEATHER FEATURES	Sc4 FCST ASSESSMENT		
			General Region	AHP Sc4	AHP CDC*
01	Minimum central Alta., max central Sask. and eastward.	Generally stable over Alta., largest cvctv cells N-S In ern Sask.	Very good	-1	-2
02	Nil sig cvctn except TCU wrn Alta.	Nil sig cvctn isoltd isoltd TCU/CB flwg AM	Excellent	-2	-2

03	General TRW's fcst for Alta.with max(hail)NE, min YC and E,and N ET	Weak to mod TRW's, min YC and E; max near ET due upslope in NE flow	Fair, but poor on main rgns. Orogr.	+2	0*
04	Max SE B.C. (TRW'S), dcrsg to nil sig cvctn central Alta.	RW- AND FEW TRW SE B.C. - nil sig cvctn Alta./Sask.	Very good	0	-1
05	Weak cvctn only alg fthls, psbly SW Sask. RW- E cntrl B.C.	TCU fthls and SRN Sask isoltd RW- ern B.C.	Excellent	-2	-2
06	Max (psbl TRW) cntrl B.C., dcrsg to TCU cntrl Alta.,weak cvctv max NE thru EG	Main cvctv activity B.C.(RW-) - no sig cvctn Alta./Sask. xcp ACC EG area	Excellent	-2	-3
07	Max NRN Alta dcrsg SE weak max SW ptn AHP	TCU/RW- NRN rgns, few TCU AHP, nil sig othrw	Excellent	-2	-2
08	Max SRN B.C., 2ndry max nr YC and vcnty Cold Lake	RW- isoltd TRW SRN B.C., ACC and few TCU NE thru Cold Lake	Very good, xcp AHP over-fcst	+2	-2
09	Maxima SRN B.C. and W of AHP - clear Sask.	TRW SRN B.C., 2nd max displaced sltly E - nil sig cvctn Sask.	Very good	+3	≥ 0*
10	Max ovr Sask.with maj. synop.sys. - 2ndry max SW ptn AHP	TRW's and hail WRN AHP, cold tornado verified ovr YC	Very good, too high over Sask.	+3	≥ +2*
11	No cvctn fcst SRN rgns Alta./Sask. - RW- NRN Sask., ERN B.C.	Nil sig SRN Alta./Sask RW- NRN Sask., few RW- mvd into N cntrl Alta.	Very good, xcp ERN B.C.	-2	-2
12	Rdg max values (TRW,A) along fthls Alta., dcrsg to nil sig Sask.	RW-/TRW/A alg fthls, nil sig cvctn Sask.	Excel.,xcp main max(A) displaced N	+1	≥ 0*
15	TRW and hail fcst QF and N - wk rdg max S along fthls SRN Alta.	TRW and hail as fcst with RW- Southward along foothills	Excellent considering time of year	+1	+1

*No AHP telephone hail surveys during September.

4. THE CALGARY HAILSTORM OF 28 July, 1981

Severe hailstorms such as the one summarized in Section 2.1 for 21 July 1982, often cause tremendous crop damage over large areas. The annual crop loss due to hail in Alberta is now estimated to average around $100 million. However, individual storm days only make national news headlines when large metropolitan areas, sparse on the Prairies, are directly affected. Such was the case on 28 July, 1981, when a thunderstorm cut a hailswath through the eastern half of the city of Calgary. This storm caused two deaths by lightning, and damage claims (from hail, flooding, and wind) exceeding $100 million. This put it into the same damage class as the most devastating hurricanes and tornadoes experienced in the Caribbean and southeast U.S. Yet this storm, yielding 141 hail reports with 5 larger than 50 mm diameter, may not have been as intense (in terms of

reported hail) as the one of 21 July 82.

The aftermath of this Calgary storm brought renewed demands for a Calgary weather radar, and to return forecast staff to the Calgary AES Weather Office. It is questionable whether such moves alone would improve advanced warning of severe convective storms. This case therefore represents an important test for the Sc4 forecast index, depicted in Figure 11a. Forecast values were computed from the (1500 UTC) forecast EGDEX map for 28 July, 1981, 1600 UTC surface observations, and 700 mb temperatures and 1000-500 mb thickness values extrapolated from the AES prognostic charts issued at 1200 UTC.

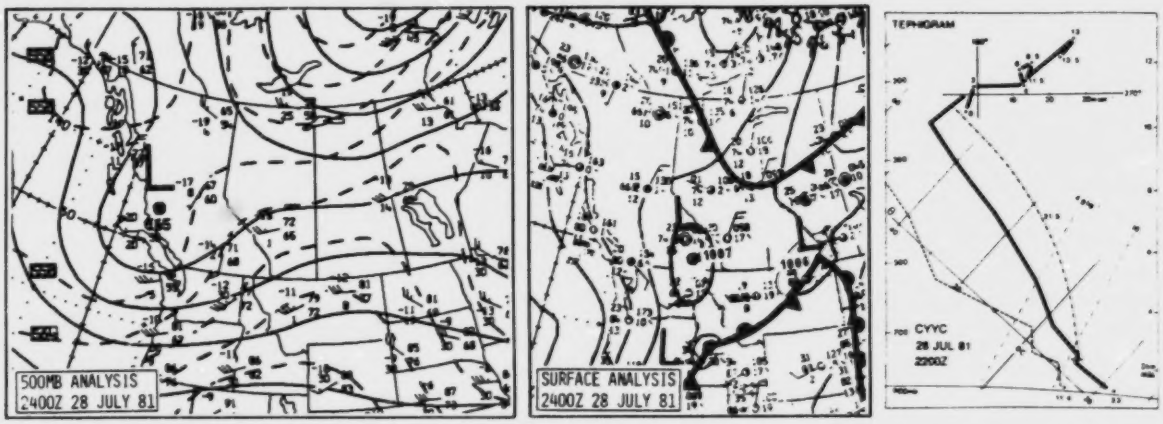

Figure 10. (a) 500 mb and (b) coarse surface analyses for 2400 UTC, and (c) sounding most representative of maximum convective conditions, 28 July 1981.

The synoptic pattern for this day (Figure 10) revealed an upper shortwave ridge pushing east of AHP by mid-afternoon. Behind the ridge, a low from the Gulf of Alaska moved into southern B.C. by 2400 UTC. A diffluent southwest flow aloft over southeast B.C. and southern Alberta preceded this low, resulting in cyclogenesis over B.C., with pressure falls and troughing northeast to near Calgary and into Saskatchewan. North of this surface trough, a light northerly flow of moist, warm air prevailed, with temperatures ranging in the low to mid-twenties, and dewpoints in the low teens.

The major convective storm in this case developed northwest of Calgary, with first radar echoes observed around 1930 UTC. It moved southeast from there, contrary to what the upper flow (Fig.10a) and the hodograph (Fig.10c) would suggest. Upslope conditions (northerly surface flow) and higher humidity southeast may have been factors here. Coarse features of the most intense convective weather for the day, including hail regions, are depicted in the surface weather composite chart of Figure 11b. Figure 12 is an AHP PPI picture of the storm as it moved southeast towards Calgary at 2323 UTC. The infra-red satellite imagery of Figure 13 shows the complex just southeast of Calgary at 0202 UTC. It appears to be closely associated with convergence near the surface low (Fig.10b).

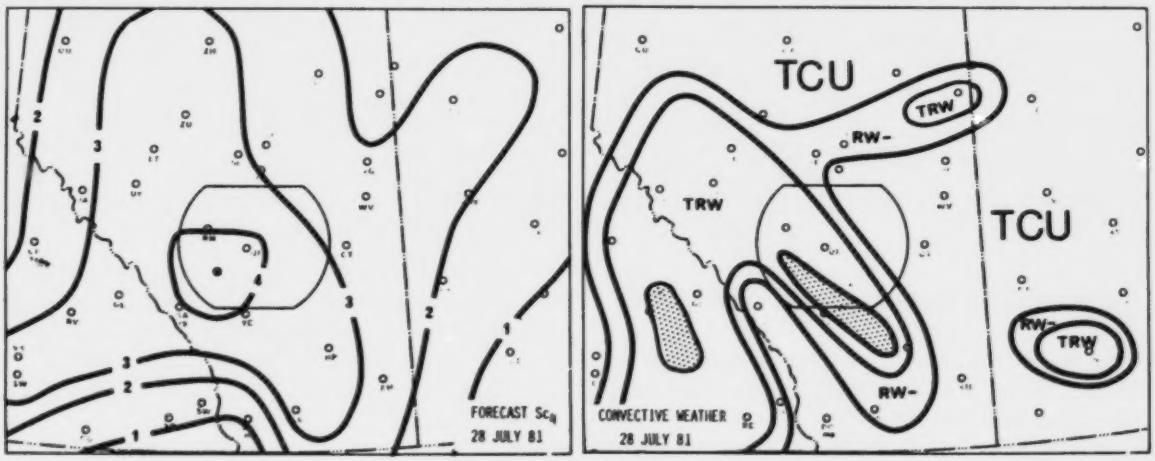

Figure 11. Convective weather, 28 July 1981. (a) Forecast Sc4 map; blanket adjustment to Sc4 values = 0. (b) Diagnostic convective weather composite for 1700-1200 UTC, from surface weather observations, AHP hail reports, and satellite imagery (as Fig.3b).

The evaluation of the Sc4 forecast for this case can be summarized as follows:

1) it pin-pointed the most intense phase of the largest storm; radar reflectivities suggest that this occurred prior to its hitting Calgary;

2) the ridge of high Sc4 values running northwest to southeast parallel to the foothills accurately predicted the composite of maximum convective intensity for the day through that region;

3) weaker thunderstorms were correctly predicted over east-central Alberta;

4) the region of thundershowers and hail in southeast B.C. was as predicted;

5) more stable conditions along the Continental Divide were also predicted on the basis of a trough of lower Sc4 values.

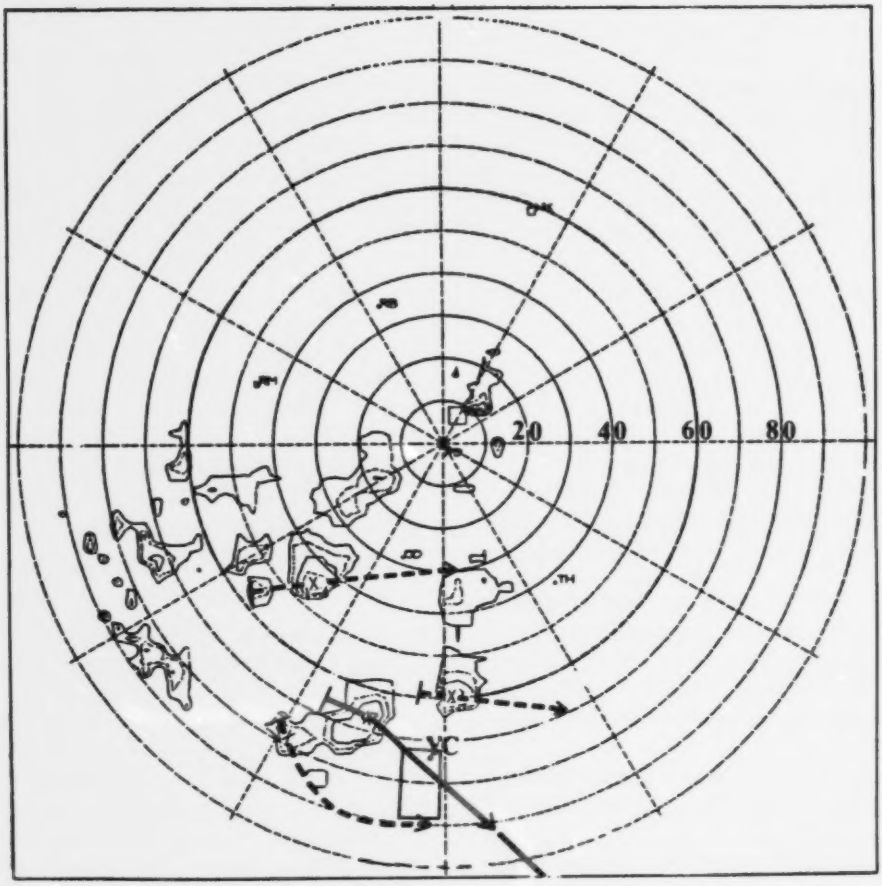

Figure 12. C-Band Radar PPI (centered at Red Deer) at 2323 UTC, 28 July 1981. Range rings are in statute miles, rectangle approximates Calgary boundaries; contours are in 10dBz steps starting at 20. Arrows indicate motion between 2300-0120 UTC of the Calgary storm (solid) and three 2ndry storms (dashed). The latter three all weakened during this period, including the maximum dBz (57 dBz, 223/45) at 2323 UTC.

Absolute Sc4 values for the Calgary storm complex could not have been forecast better, realizing that the Sc4 (and its predictand, Convective Day Category) were originally intended to describe maximum convective intensity within a 130-km radius. Had the Sc4 been in operational use, a confident weather advisory or warning might have been issued several hours in advance in this case. This would have provided forewarning of this financially disasterous storm. Minimal precautions, such as placing cars under cover (a major dollar loss in this case), might have saved millions of dollars.

Figure 13. NOAA-6 enhanced infra-red satellite imagery for 0202 UTC, 28 July 1981. The dark, semi-circular regions are primarily convective complexes.

5. DISCUSSION

5.1 Summary —

The preceding case study summaries illustrate that the areal version of the Sc4, originally developed for the AHP operations area, can be extended to:

1) adjacent regions of Alberta without significant deterioration in reliability; with further testing, this can likely be extended across the prairies and southward*4, while coarser interpretations can be applied to mountainous regions such as eastern B.C.;
2) the spatial resolution of convective intensity at least down to the sub-synoptic scale (100 km resolution or better).
3) Furthermore, with additional operational experience, time-resolved forecasts of convective complexes may be inferred by extrapolating Sc4 maxima backward or forward in time.

These points suggest useful applications of the Sc4 in three areas:

i) daily planning for cloud seeding operations, for more efficient deployment of aircraft and crews;

ii) daily planning for field research activities on severe storms; e.g., deployment of mobile units for collecting precipitation samples, upper air soundings, etc.);

iii) release and updating of severe weather advisories and warnings for public dissemination.

Diagnostic and forecast tests to date have been impressive enough to retire the older Sc10 index in favour of the areal Sc4 predictor for 1983. Not only does the Sc4 provide additional spatial and temporal resolution, but it is relatively simple to automate. The savings in time for the AHP forecaster (and others) will allow time for more productive analysis of satellite imagery, radar data, atmospheric soundings, and the like.

*4 Strong and Wilson (1983) have successfully applied the Sc4 to a rather unusual severe hailstorm over Colorado.

5.2 Future Improvements —

A subsequent paper (Strong and Wilson, 1983) suggests a technique which combines the Sc4 with moisture and upper level wind fields to predict initiation region, scale size, and motion of individual storm complexes for up to 18 hours. Bergwall et al. (1983) further combine radar information to infer mesoscale changes for time periods less than three hours. Adoption of these techniques hopefully will improve forecast accuracy beyond that discussed here, as well as reduce the false alarm ratio.

The next generation(s) of the Synoptic Index will involve an entirely new data base, a new predictand for more efficient regional analyses, and new predictor variables (such as a wind shear parameter). This may lead to finer spatial and temporal resolution and accuracy in convective forecasts. If reliable statistical mesoscale (10-100 km length scale) convective forecasts can be produced for up to six hours, then simple cloud models can be re-introduced to forecast office use for coarse quantitative predictions of precipitation.

Beyond this, a better physical understanding of the interactions between all scales of atmospheric motion will be required. Important questions to be answered include: how does the energy cascade concept help in severe storm initiation, growth, and decay, and what are the feedback mechanisms from the cloud scale back to synoptic scale flow?

6. ACKNOWLEDGEMENTS

The authors thank Mr. H.Sharpe for assisting with final figure drafts, and Mr. J.Gertz for photographic prints. The original satellite images were obtained through the services of the Alberta Weather Centre (AES).

7. REFERENCES

Bergwall, F., R.G. Humphries, and G.S. Strong, 1983: The use of radar and a convective index for 1-6 hour regional forecasts. Preprints A.M.S. 21st Conf. Radar Meteorology, Edmonton, Alta., 19-23 Sept.83.

Humphries, R.G., and G.S. Strong, 1982: Final Rep., Scientific and Tech. support for the RAINSAT Project, Alta. Res. Counc., March, 1982, Vol.1, 400 pp.

Strong, G.S., 1979: Convective weather prediction based on synoptic parameters. Preprints A.M.S. 11th Conf. Sev. Loc. Storms, Kansas City, Mo., Oct.79, 608-615.

Strong, G.S., 1982: Hailstorms — Why Alberta? Chinook Magazine, Winter/Spring, 21-23.

Strong, G.S., and W.D. Wilson, 1981: The Synoptic (Instability) Index: 1978-80 tests and new versions. Paper presented to 15th Ann. Congr., Can. Meteor. and Oc. Soc., Saskatoon, May 81, 17 pp.

Strong, G.S., and W.D. Wilson, 1983: The Synoptic Index of Convection: Application to the Fort Collins hailstorm of 30 July 1979. Preprints A.M.S. 13th Conf. Sev. Loc. Storms, Tulsa, Okla., 17-20 Oct.83.

8. ADDENDUM

In this series of papers, the authors use a number of abbreviations which are standard throughout the meteorological community. It is assumed that the reader is familar with the following abbreviations: UTC — Coordinated Universal Time (formerly Greenwich Mean Time, designated GMT or simply Z); TCU — Cumulus Congestus cloud; RW — rain showers; TRW — thundershower; A — hail.

Large Scale Energetics

and

Small Scale Convection

G.S. Strong

Atmospheric Sciences Department,
Alberta Research Council
Red Deer, Alberta

and

Meteorology Division,
Department of Geography,
University of Alberta
Edmonton, Alberta

Paper presented at the MesoScale Workshop, Toronto, Ontario, 24-27 January, 1983, and at the 17th Annual Congress, CMOS, Banff, Alberta, 03-05 May, 1983.

Large Scale Energetics

and

Small Scale Convection

G.S. Strong

Atmospheric Sciences Department,
Alberta Research Council
Red Deer, Alberta

and

Meteorology Division,
Department of Geography,
University of Alberta
Edmonton, Alberta

ABSTRACT

For many years, forecasters have used the term "trigger mechanism", implying the existence of interacting mechanisms between synoptic scale processes and thunderstorms. Many involved in severe storm research are only recently giving tacit approval to the scale interaction concept. This may be a natural consequence of research being focused primarily on the visible processes and results, namely clouds and precipitation. These scale-to-scale interactions are, in fact, poorly understood. We have little concept as to how the mysterious trigger is pulled, and even less notion of how the projectile(?) is directed to its target. Furthermore, the forecaster can at best, only approximate where the target (in this case, the thunderstorm complex) will be.

This study approaches the subject of scale interactions in terms of atmospheric energetics, focusing first on the larger scales. The goal is to contribute to the development of a total conceptual model of convection, particularly of severe storms. A thorough knowledge of the interactions is imperative if significant gains are to be made in Day-1 forecasting of severe storms and other mesoscale phenomena.

An hypothesis is presented to partially explain the role that large scale energetics may play in the initiation and life cycle of sub-synoptic and mesoscale clusters of convective clouds, and of resulting thunderstorms. It is theorized that an energy cascade and exchange initially takes place at low-levels, with the formation and removal of 'capping inversions' (about 1 km above ground) playing a key role in the more severe storm cases. To test the hypothesis, sub-synoptic scale fields of vertical velocity are computed from sounding data for a severe Oklahoma storm. The fields are shown to have spatial and temporal continuity prior to as well as during the storm. Results are then compared with less extensive data for severe Alberta storms of 1982.

1. INTRODUCTION

Operational meteorologists have long recognized kinematic relationships between synoptic scale processes and severe convective storms. Forecasters speak of thunderstorm "triggers" in reference to cold fronts, shortwave troughs or other synoptic scale features. The research community dealing with severe storms, however, has been more reluctant to accept the concept of "scale interactions". Here, a polarity of ideas has existed mainly because severe storm research has naturally centered on the visible processes and results, namely clouds and precipitation. Indeed, some in this field still argue that larger thunderstorm complexes develop some sort of autonomous mesoscale circulation, moving quite independent of synoptic scale processes, as though existing in a vacuum. Unfortunately, there is no clear understanding of exactly "how" the trigger mechanism assists in the release of instability. Thus far, the evidence for these interactions involving severe convection has been mainly of a kinematic or statistical nature.

Definitions of the atmospheric "scales" of motion being considered are necessary at this point. These scales, shown in Table 1, are not discrete entities, but rather, represent the most common stratifications discussed in the literature (e.g., Orlanski, 1975). Differences of opinion over the names, or space and time scales used are of little consequence, so long as the scales are defined. Visual examples of the synoptic through cloud scales, as defined here, are provided in Figures 1 and 2.

Maddox (1980) defined Mesoscale Convective Complexes (MCC's) as convectively-driven weather systems of quasi-elliptic shape. The total cloud shield of his MCC exceeds 100,000 sq.km (linear dimensions more than 300 km). The life cycle of a MCC is six hours or more. In the context of Table 1, this might more properly be called a Sub-Synoptic Scale Convective Complex (SSCC), such as shown in Figure 1. The smaller scale features of Figures 1 and 2 would then be mesoscale complexes. These still images do not represent proof of the scale interaction concept, but they do provide evidence of some sort of relation between adjacent scales.

While Maddox asserts that his MCC's are convectively driven, experience with somewhat smaller complexes (dimensions of 100-200 km) over Alberta, indicates that the motion of a SSCC usually approximates that of a 500 mb shortwave trough or vorticity maximum slightly upstream (Strong, 1979). Except in rare instances, the SSCC's are accompanied by such shortwaves, leaving little doubt as to the sequence of cause/effect to the operational meteorologist.

SCALE	Range of WAVELENGTH (km)	Time Scale of Asoctd Wx. over area	Scale EXAMPLES	ALBERTA NETWORK (or DATA Source) EXAMPLES	FREQUENCY of Observation	MEAN SPACING or data resolution over Alberta (km)	REMARKS
MACRO	2000-10,000	Several days to several weeks	Long Waves, presistent quasi-stationary highs/ lows	Global Upper Air Network (weekly averages from)	Twice daily; 12Z, 24Z	500	Variable density; e.g., often in-adequate over oceans
SYNOPTIC	1000-2000	1-3 days	Short Waves, migratory lows	AES Rawinsonde (R/S) Network	Twice daily; 12Z, 24Z	500	Irregular design; e.g., no stations directly east of Red Deer
SUB-SYNOPTIC (or Meso-α)	100-1000	3-24 hours	**Sub-synoptic Convective Complexes (SSCC's) or TRW clusters, Hurricanes, 2ndary lows**	(1) AES Surface Obs. Stations	Hourly plus specials	140	Irregular design
				(2) 1980 ASD (+CMEG) summer R/S Network	Twice daily but different hours	120	Irregular design, poor siting, in-adequate no. (3-5) sites
				(3) **Proposed ARC Sub-synoptic U/A Network**	**1½-6 hour intervals**	130	**Uniform design (7-11 sites)**
MESO (or Meso-β)	10-100	1-2 hours	**Cold front zones, squall lines, large thunderstorms or convective complexes (MCC's)**	(1) Alberta Forestry Weather Reports	Twice daily; 14Z, 21Z	30	Irregular design, limited area (mtns), non-repres. obs. (mtn tops)
				(2) **Proposed ARC extended Meso U/A Network**	**1½-3 hour intervals**	**50-80**	**Uniform design (10-16 sites)**
CLOUT (or Meso-γ or Cumulus Scale)	1-10	10-60 minutes	**Single-cell CU TCU, or CB, Tornadoes**	(1) ASD Hailpad/ Raingauge Networks	Once per storm day	2-10	Uniform variations in network density, periodic design changes
				(2) Satellite Imagery	Frequent (~ 1/2 hour)	1-2 (ITOS) 2-5 (GOES)	Continuous (analog) Data, high accuracy
MICRO	Few cm to 1 km	Seconds to minutes	Convective thermals, fine-scale reflectivity patterns, down to wind gusts	(1) Radar Data	Several mins.	0.50	Uniform grid (bins)
				(2) Satellite Imagery	Several days	0.05 (LANDSAT)	Continuous data
				(3) Research Aircraft Data	Irregular, limited cases	0.01	Uniform but 1-D unless several aircraft employed
VISCOUS	Molecular Distances	??	Molecular motions	Electron Microscope (?)	??	??	??

TABLE 1. Definitions and examples of the Scales of Atmospheric Motion discussed in this paper, following closely those of Orlanski (1975).

2. FORECASTING CONVECTION

Typical approaches to the problem of predicting convection have been through kinematic studies, thermodynamic instability theory, cloud physics leading to numerical models, and statistical relations employing various combinations of these. Most research tends to be concentrated in any one of these areas, presumably because of a person's training and personal preference. Because of this, many shortfalls remain in our understanding of scale interactions. Consequently, progress towards successful forecasts of convective clouds and precipitation has been slow. Ideas on how the puzzle might fit together can be gained by reviewing some of the individual efforts.

For example, Beebe and Bates (1955) described how synoptic scale ascent might change an otherwise stable sounding into that observed in the vicinity of severe thunderstorms. Their conceptual model partially explained the role of the "capping inversion", or "lid", a thermodynamic inversion (about 1 km above ground) which often precedes severe thunderstorms in Alberta and elsewhere. The capping inversion initially traps convection, preventing latent heat release. Adiabatic cooling provided by synoptic scale (or other) ascent, eventually removes (or partially removes) the inversion. This allows a sudden release of the trapped energy, and often an explosive and severe thunderstorm. The process is illustrated in Figure 3. Beebe and Bates also related low-level and upper wind maxima to severe storms.

Numerous thermodynamic instability indices have appeared since Showalter (1953) first introduced his lifted index. Based entirely on a single atmospheric sounding, it still receives wide use in forecasting convective weather. More recently, Model Output Statistics from the larger (synoptic) scale models allow statistical combinations of different covariates which give increased skill over the simple lifted index. For example, the Synoptic Index of Convection combined synoptic and instability parameters to provide a forecast of maximum convective intensity over the Alberta Hail Project (AHP) operations area (Strong, 1979). It was shown that for five operational test seasons (1978-82), hail forecast skill was increased by 20-25% from previous years. More recently, a simpler version (Sc4) was implemented. It can provide a reliable sub-synoptic scale 'regional' forecast of maximum convective intensities, storm complex size, and location for most of western Canada. Figure 4 (reproduced from Strong and Wilson, 1983) illustrates its effectiveness in forecasting the severe hail- and tornado-producing storm over central Alberta on 21 July, 1982. The Sc4 values are a forecast of maximum convective intensity for the day within a 130-km radius. Values can range from -3 (no significant convection) to +5 (larger than golfball size hail). A value of 0 represents either widespread showers or a thundershower without hail. In spite of modest forecast success, such statistical techniques contribute little to the understanding of scale interactions.

3. ENERGETICS AND SCALE INTERACTIONS

Following theoretical treatment by Margules (1903) through Lorenz (1955), diagnostic studies using kinetic energy budgets have become popular during the past 20 years. Lorenz showed that while the dominant atmospheric process is kinetic energy production at the expense of baroclinicity (conversion of APE to KE), there are other intermediate sources and sinks of energy. Any of these processes can dominate during given stages of a cyclone's life cycle.

Only a few attempts have been made to compute kinetic energy budgets for scales smaller than synoptic, perhaps because of the added importance of data accuracy and extensive data processing required. The major kinetic energy budget studies of sub-synoptic scale severe convective storm complexes have come primarily from two groups: Kung and associates at the University of Missouri, and Fuelberg and associates at St.Louis University. All of these studies, published between 1972-82*1, employed Oklahoma data from the NSSL*2 and SESAME-AVE-V*3 data sets.

Diagnostic studies of the energetics of sub-synoptic scale convective complexes (SSCC's) should leave no doubt that scale-to-scale interactions exist. Some key observations from studies by the Kung group are:

1) Similar energy processes (generation, dissipation) occur at vastly different scales (McInnis and Kung, 1972).
2) Kinetic energy is input to the sub-synoptic (and other) scale(s) from other (larger and smaller) scales (Kung and Tsui, 1975).
3) Thunderstorm activity actually consumes some energy supplied from the larger scale, in addition to that generated through latent heat release (McInnis and Kung, 1972).
4) The adiabatic conversion of eddy kinetic energy to APE in the middle and upper layers is maximum during periods of maximum convective intensity (Tsui and Kung, 1977).

*1 Further details are included in the original version of this paper. Smith (1980) provides an excellent review of large scale energetics.
*2 NSSL: National Severe Storms Laboratory, Norman, Oklahoma.
*3 SESAME: Severe Environmental Storms Area Meteorlogical Experiment AVE-V: Area Variability Experiment, 20-21 May, 1979.

4. A SCALE INTERACTION HYPOTHESIS

For many years, the Beebe and Bates hypothesis, describing how synoptic scale ascent assisted in the formation of thunderstorms (Figure 3), was not widely accepted by those involved in severe storm research. While perfectly logical to a (synoptic) forecaster, something still appeared to be missing from the chain of atmospheric scales leading to convection. Thus it received little theoretical attention until the work by Kung and his associates. Presumably, the main objection to the Beebe and Bates model was the following: "that if synoptic scale ascent contributes to thunderstorm or thunderstorm complex initiation and growth, why then does one not observe synoptic scale convective complexes, rather than the smaller scale features as noted in Figure 1?" The truth is, that these large convective complexes, while not of synoptic scale dimensions, are usually organized into synoptic scale patterns. This should be obvious in Figure 1 for instance. Since most research was focussed visually at the mesoscale and smaller, this degree of organization was not readily apparent. The advent of satellite imagery in severe storm analysis has since broadened the focus of research.

4.1 Energy Cascade Hypothesis —

Many of Alberta's severe thunderstorms also occur on days with a low-level capping inversion, similar to that of Beebe and Bates (Figure 3). A hypothesis is now presented as an extension to the Beebe and Bates model, as follows:

> It is proposed that the cascade of energy from the larger scales of motion, provides eddy kinetic energy to the sub-synoptic (or even meso) scale; this leads to (horizontally) differential lifting of the air mass, adiabatic cooling (of the 'capping inversion' in particular), and subsequent destabilization of the lower layers within these 'preferred regions' or eddies.

While the air mass cooling effect of synoptic scale ascent presents nothing new by itself, this hypothesis incoporates the cascade concept of the transfer of kinetic energy to smaller scale eddies. If valid, it should be possible to forecast where the preferred regions for convective formations will occur. At the same time, the actual size of a convective complex should be predictable from the relative size and distribution of the eddies. The success of the statistical Synoptic Index (Figure 4 and other cases; Strong and Wilson, 1983) suggests that the cascade process is a deterministic rather than simply stochastic (turbulent) process.

4.2 Testing the Hypothesis —

The hypothesis implies that the eddies help initiate SSCC's by destabilizing preferred (sub-synoptic) regions of an air mass through adiabatic ascent. If this is true, then this ascent and cooling, particularly near the level of capping inversions (generally 800 - 750 mb), must 'precede' significant convective clouds.

With this in mind, the Capping Inversion Study (CIS) was commenced during July, 1982. Three mobile sounding units were deployed on capping inversion days over the AHP operations area. The initial objective of CIS was:

1) to show that significant cooling events occur "prior to" large cumulus congestus formations; otherwise, the capping inversion hypothesis would be wrong. Assuming the hypothesis to be true, subsequent objectives of CIS were:
2) to determine vertical velocity profiles at sites, using a modification of the adiabatic method*4;
3) to show that the spatial/temporal characteristics of the vertical motion is of sub-synoptic scale, as might be caused by the hypothesized eddies;
4) to compare these results with severe storm soundings and vertical velocity profiles from elsewhere. Here, a regional analysis is necessary to determine spatial/temporal characteristics of the vertical motion. CCOPE*5 and SESAME-AVE-V*3 data are being used in this effort.
5) Finally, it is necessary to show that a portion of the measured cooling between soundings is of extra-storm origin; that is, derived from the synoptic scale (through eddies), and not simply caused entirely through a combination of successive bubble penetrations (local adiabatic lift) and later thunderstorm downdraft-outflow.

This latter objective will be tested by examining the temporal continuity of vertical velocity fields prior to and during the severe storm complex.

*4 The adiabatic method is described in many texts on dynamic meteorology (e.g., Holton, 1979). For this study, it was assumed that, for short periods (3 hours or less), significant cooling (warming) was due primarily to adiabatic ascent (descent). This neglects sounding changes due to horizontal transport and radiation. Lower portions of soundings obviously warmed by heating from the ground, were omitted from the computations.

*5 CCOPE: Cooperative Convective Precipitation Experiment conducted in eastern Montana, May - August, 1981.

4.3 Preliminary CIS Results — Oklahoma Data

SESAME data from Oklahoma are used to test the hypothesis because of the availability of a special sub-synoptic scale rawinsonde network (1.5 - 3 hour soundings from 20 sites with 75-km spacing). The AVE-V case (20 May 1979) was chosen because a major severe storm complex passed through this network, with many pre-storm soundings exhibiting capping inversions similar to Figure 3. Composite radar summaries prior to (1735 UTC) and during (1935 UTC) the storm complex are shown in Figure 5.

Vertical velocity profiles were computed for each site, using the simplified adiabatic method*4 on sounding pairs at adjacent times (3 hours or less apart). Figure 6 shows the regional distribution of vertical velocity at 750 mb, just above the capping inversion level, at the median time 1835 UTC. First radar echoes appeared within minutes of this time. Peak values (exceeding 8 cm/s) are rather high to be synoptic scale ascent. The spatial variation is of sub-synoptic scale, since the distance between maxima here is 200-300 km. These maxima also correspond well with later positions of the two major complexes over southwestern and eastern Oklahoma at 1935 UTC (Fig.5). The pattern of 24-hour rainfall amounts in Figure 7 bears a striking resemblance to the vertical velocity pattern of Figure 6.

Figure 8 shows the 750 mb pattern for the sounding pairs, 1405 and 1705 UTC, well before any significant convection formed over this region. Figures 6 and 8 (and others not shown) show good temporal continuity between maxima (and minima), with a general northeast movement of 30-60 km/hr. These patterns should be sufficient evidence to state that sub-synoptic scale regions of ascent (descent) existed well before the thunderstorm complex(es) were initiated. The strong visual correlation between vertical velocity patterns and sub-synoptic scale convective complexes, is thus highly suggestive of an initiating mechanism from the former.

4.4 Preliminary CIS Results — Alberta Data

The CIS experiment conducted in Alberta during July, 1982, provided several successful case study days, including 14, 21 and 29 July. An example vertical velocity profile for a sounding pair of 21 July is shown in Figure 9. A capping inversion appeared on the 1836 UTC sounding at Red Deer (CAQF). This inversion resulted from earlier subsidence over the region. Ascent (and cooling) commenced slowly thereafter, with maxima of 8-11 cm/s near 650 mb. Again, these are not synoptic scale values in this instance, and they are comparable to those of the SESAME data set discussed above. Individual values have an estimated uncertainty of +/-20%. Such errors would still leave spatial patterns generally unchanged.

More detailed analyses of these Alberta data sets are being carried out. Areal analyses comparable to the SESAME case are not possible, since only three mobile and two fixed site sounding systems were available.

5. SUMMARY

5.1 Results —

Additional evidence of scale-to-scale interactions involving SSCC's has been presented. Kinetic energy budget studies at this scale by Kung and associates, and by the Fuelberg and Scoggins groups (1972-82), set precedents for this work. Similar studies of energetics using new data sets are required to verify their results. Fuelberg, currently studying SESAME data sets with at least 20 upper air sites in a sub-synoptic scale network, may provide new insights here.

Concerning the formation and removal of capping inversions prior to severe convective storms, preliminary results suggest that:

1) sub-synoptic scale regions of ascent/descent do exist prior to storm formation;
2) some low-level cooling, particularly of capping inversions, occurs prior to the storm;
3) the region(s) of ascent correspond to subsequent SSCC(s);
4) it is speculated that these regions are associated with eddies of the same spatial scale, resulting from eddy dissipation of synoptic scale kinetic energy. Fixed mesoscale influences, such as might be provided by orographic flow or surface heating, cannot be ruled out entirely. However, both the motion (synoptic scale) and the spatial and temporal continuity of the vertical velocity fields strongly suggest a synoptic scale cause.

Further analysis of the SESAME-AVE-V, CCOPE, and Alberta CIS data may substantiate these suggestions. The eventual goal is to study cloud size populations in conjunction with an energy budget analysis at synoptic and sub-synoptic (and/or smaller) scales.

5.2 Remaining Problems and Recommendations

Many important questions concerning scale interactions remain. For example: What is the nature of the energy cascade concept? What mechanism initiates the cascade? Under what conditions does it initiate? Is the ascent and low-level cooling preceding a convective complex a reflection of the dissipated (eddy) kinetic energy? Does this provide a direct means to measure this energy from soundings using the sounding area/-

energy relation? Do synoptic scale features initiate and control convective features through smaller-scale propagating waves? Without qualitative answers to such questions, we can never really have a thorough understanding of scale interactions and convective processes.

Because of the mean position of the polar westerlies during summer, the effects of large scale energetics on convection might be more important at mid-latitudes than has been found for Oklahoma. The CCOPE (Montana) data set with only 5-7 sites is inadequate for areal analyses. Any future field research efforts must pay more particular attention to data quality, quantity, and continuity. This involves a thorough study of optimum data resolution, network design, operating logistics, and technical training. These efforts are already underway in Alberta. Combined with excellent existing operational support systems, central Alberta, at 51-53N latitude, would provide an ideal setting for a future upper air network for scale interaction studies.

6. ACKNOWLEDGEMENTS

The SESAME data in this study were kindly provided by NASA, Marshall Space Flight Center, Alabama. Satellite imagery were obtained through the services of Alberta Weather Centre (AES), Edmonton, Alberta. Mr. J.Gertz of ARC provided photographic prints.

7. REFERENCES

Beebe, R.G. and F.C. Bates, 1955: A mechanism for assisting in the release of convective instability. Mon. Wea. Rev., 83, 1-10.

Holton, J.R., 1979: An Introduction to Dynamic Meteorology, 2nd ed., Academic Press, New York, 391 pp.

July, M.J., and R.E. Turner, 1981: A preliminary look at AVE-SESAME-V conducted on 20-21 May 1979. NASA Tech. Memo., TM-82416, 56 pp.

Kung, E.C., and T.L. Tsui, 1975: Subsynoptic-scale kinetic energy balance in the storm area. J. Atmos. Sci., 32, 729-740.

Lorenz, E.N., 1955: Available potential energy and the maintenance of the general circulation. Tellus, 7, 157-167.

Maddox, R.A., 1980: Mesoscale Convective Complexes. Bull. Amer. Meteor. Soc., 61, 1374-1387.

Margules, M., 1903: Uber die energie der sturme. Jahrb. kais-kon Zent. fur Met., Vienna. Translation by C. Abbe in Smithson. Misc. Coll., 51, 1910.

McInnis, D.H. and E.C. Kung, 1972: A study of subsynoptic scale energy transformations. Mon. Wea. Rev., 100, 126-132.

Orlanski, I., 1975: A rational subdivision of scales for atmospheric processes. Bull. Amer. Meteor. Soc., 56, 527-530.

Showalter, A.K, 1953: A stability index for thunderstorm forecasting. Bull. Amer. Meteor. Soc., 34, 250-252.

Smith, P.J., 1980: The energetics of extratropical cyclones. Revs. Geophys. and Sp. Phys., 18, 378-386.

Strong, G.S., 1979: Convective weather prediction based on synoptic parameters. Preprints A.M.S. 11th Conf. Sev. Loc. Storms, Kansas City, Mo., 608-615.

Strong, G.S., 1981: Severe Alberta thunderstorms: A post-cold-frontal type. Paper presented at 15th Ann. CMOS Congr., Saskatoon, Sask., 27-29 May 1981, 22 pp.

Strong, G.S., 1982: Hailstorms! - Why Alberta? Chinook Magazine, Winter/Spring, 21-23.

Strong, G.S., and W.D. Wilson, 1983: The Synoptic Index, Part II: Applications to regional forecasts of convective complexes. Paper presented at 17th Ann. CMOS Cong., Banff, Alta., 03-05 May 1983, 32 pp.

Tsui, T.L. and E.C. Kung, 1977: Subsynoptic scale energy transformations in various severe storm situations. J. Atmos. Sci., 34, 98-110.

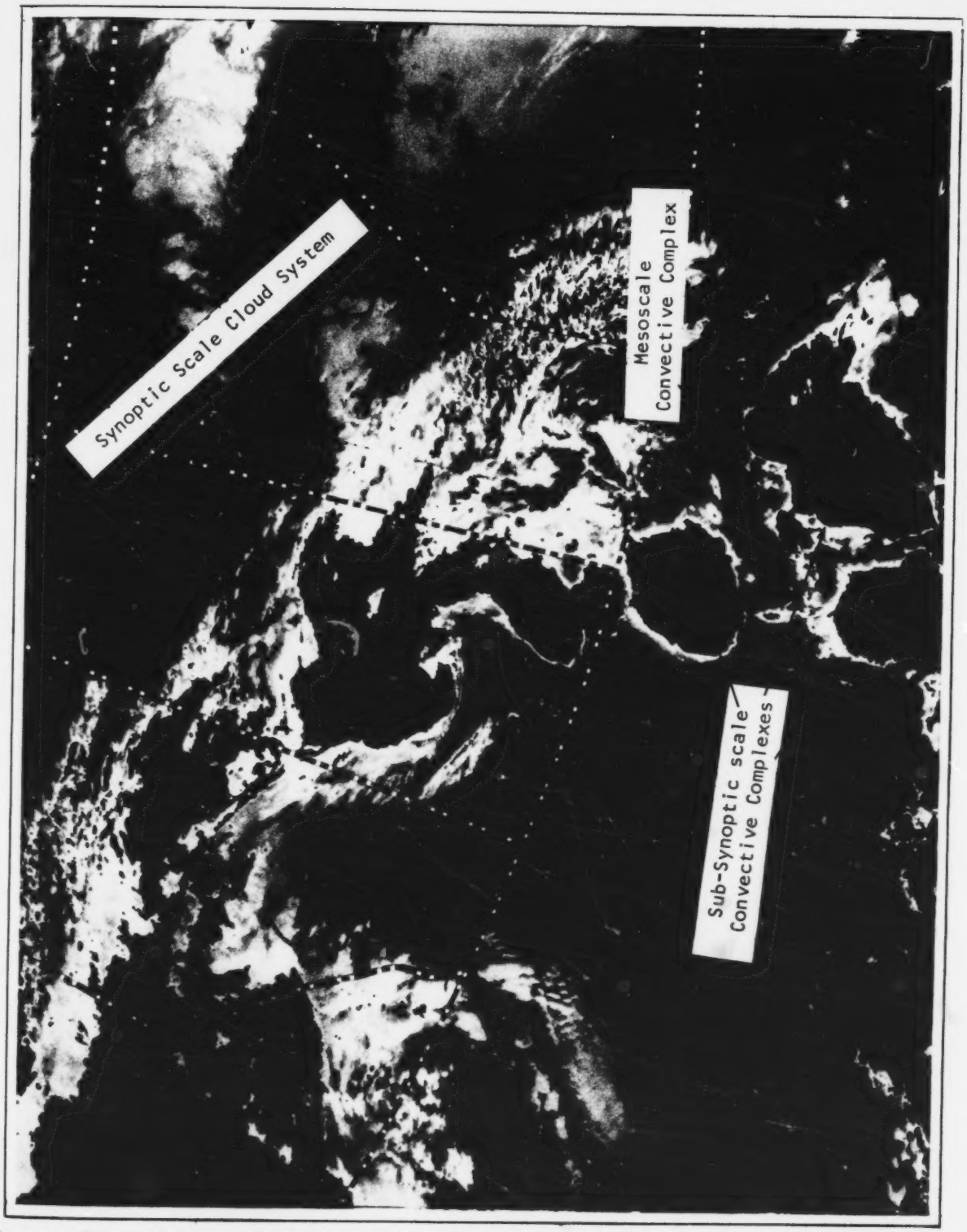

Figure 1. Enhanced infra-red NOAA-6 image for 0136 UTC, 15 July 1982, depicting three of the scales of atmospheric motion indicated in Table 1.

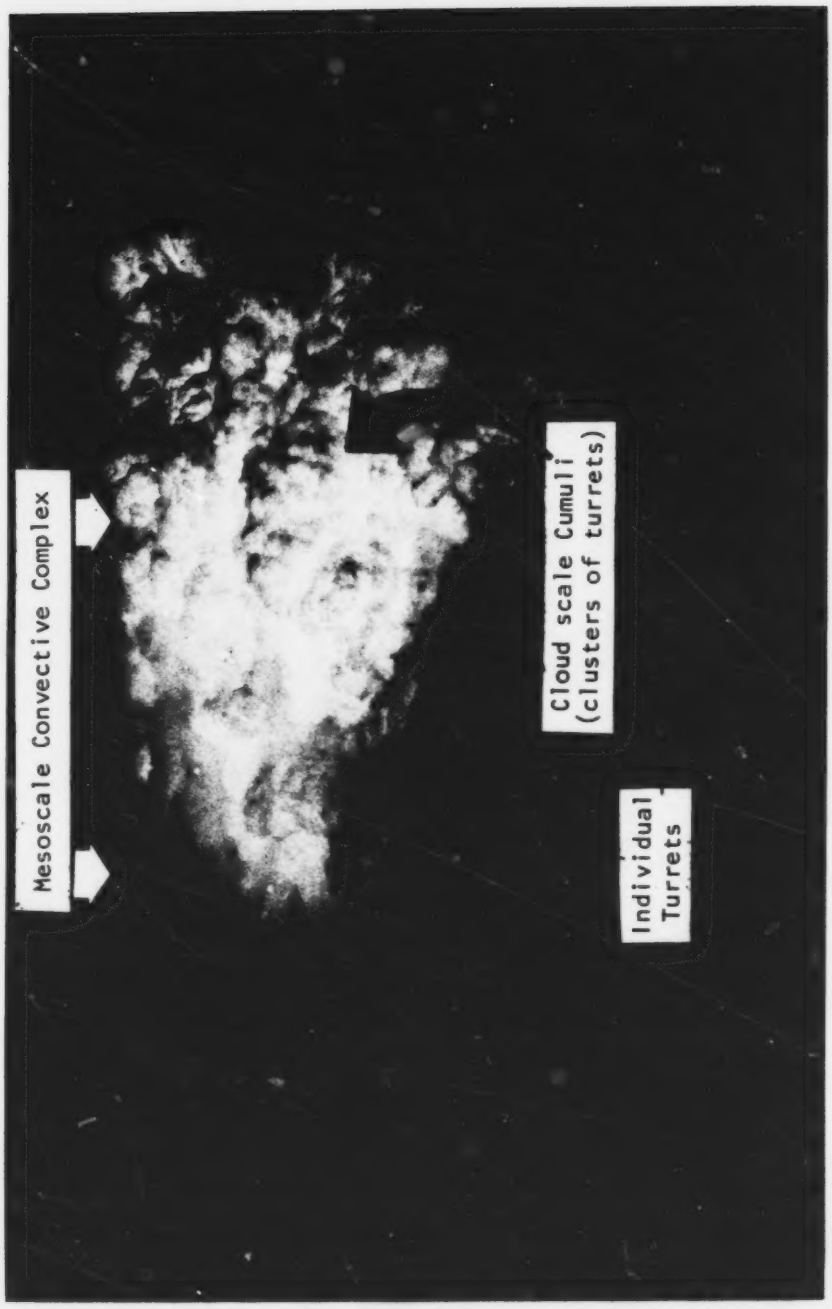

Figure 2. Aerial view of a mesoscale thunderstorm complex (30-50 km across), with cloud scale cumuli (clusters of turrets, 4-8 km across) in the so-called "new growth zone", and individual turrets with horizontal dimensions of 1 km or less - three identifiable interacting scales of motion.

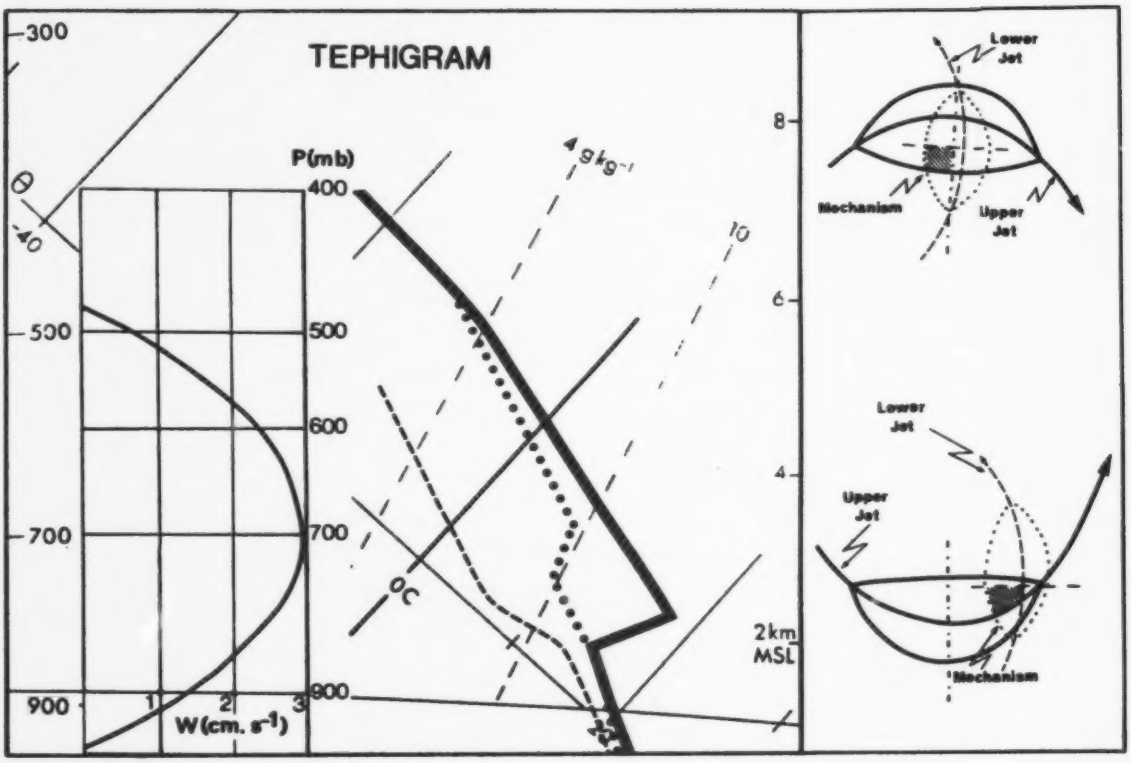

Figure 3. Average pre-tornado sounding showing capping inversion (solid line), and mean tornado-vicinity sounding (dotted line) following typical synoptic scale adiabatic ascent as shown. Typical upper/lower jet couplings for severe storm cases are also indicated. (After Beebe and Bates, 1955.)

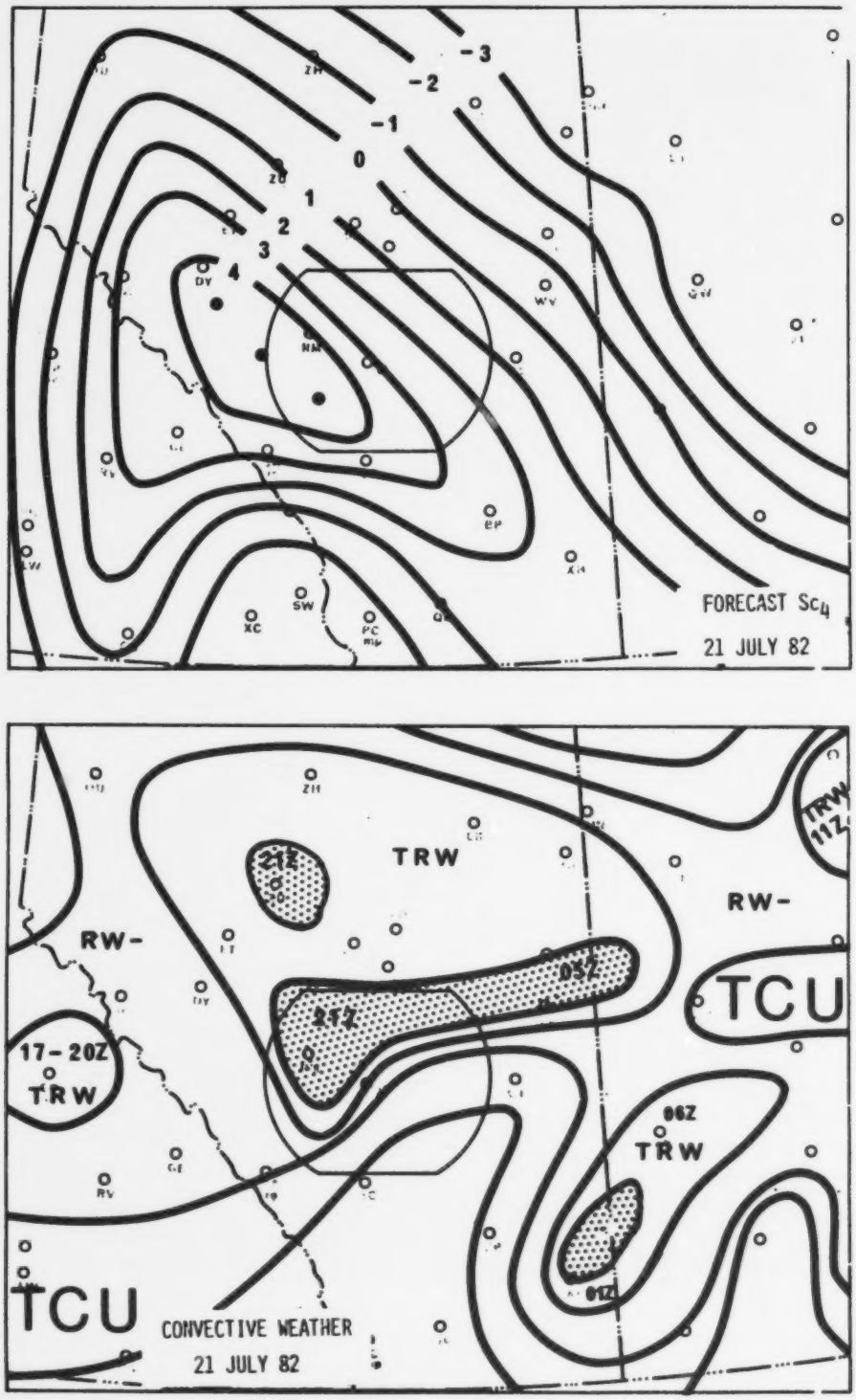

Figure 4. Synoptic Index (1500 UTC) forecast of maximum convective intensity for the day, and observed (composite) maximum convective conditions from 1700-1200 UTC, 21-22 July, 1982. Sc4 values range from -3 (no significant convection) to +5 (larger than golfball hail) within a 130-km radius. (After Strong and Wilson, 1983.)

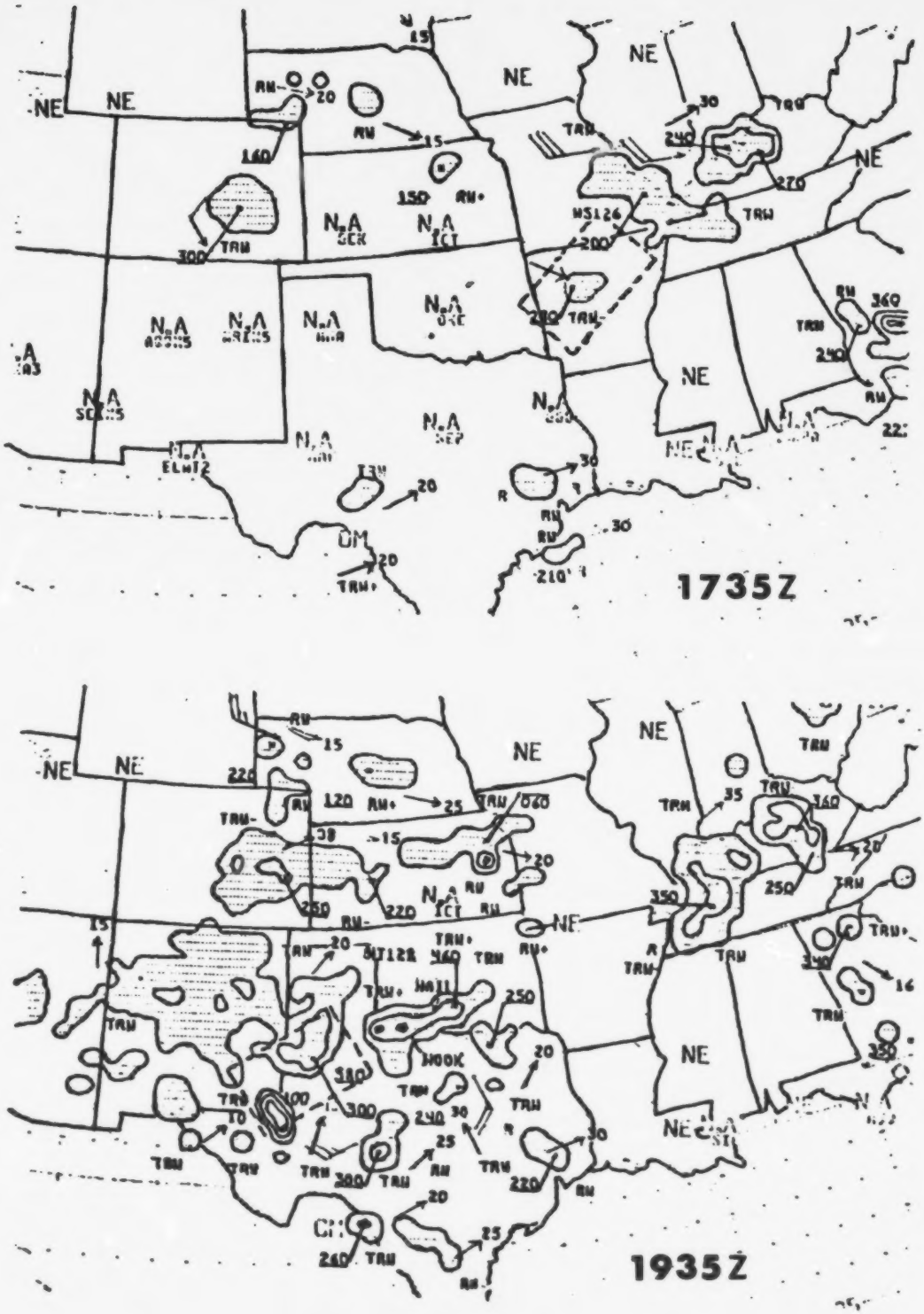

Figure 5. Composite radar summaries for 1735 and 1935 UTC, 20 May 1979. (After July and Turner, 1981.)

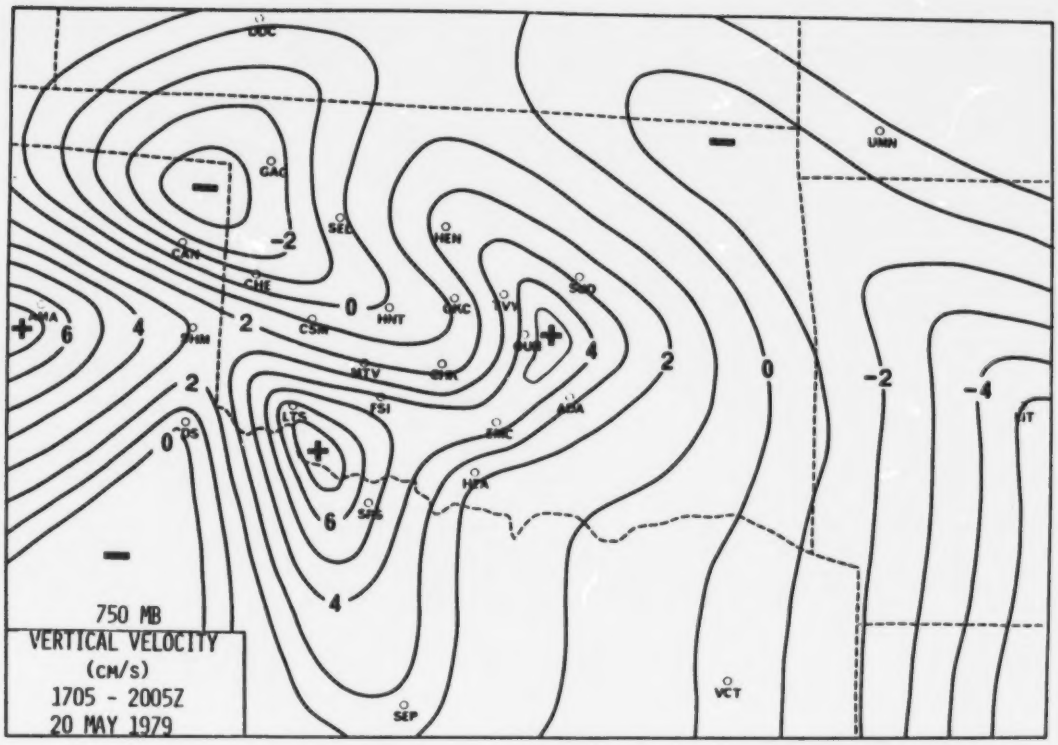

Figure 6. Sub-synoptic scale vertical velocity pattern at 750 mb for SESAME-AVE-V case, median time 1835 UTC, 20 May 1979.

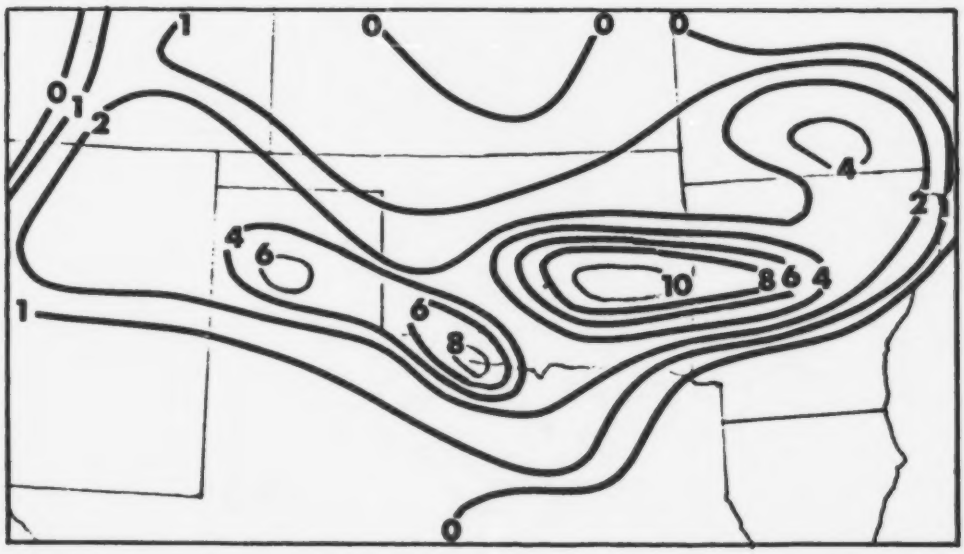

Figure 7. 24-hour rainfall amounts (cm) for the SESAME-AVE-V case, 1200-1200 UTC, 20-21 May 1979. (After July and Turner, 1981.)

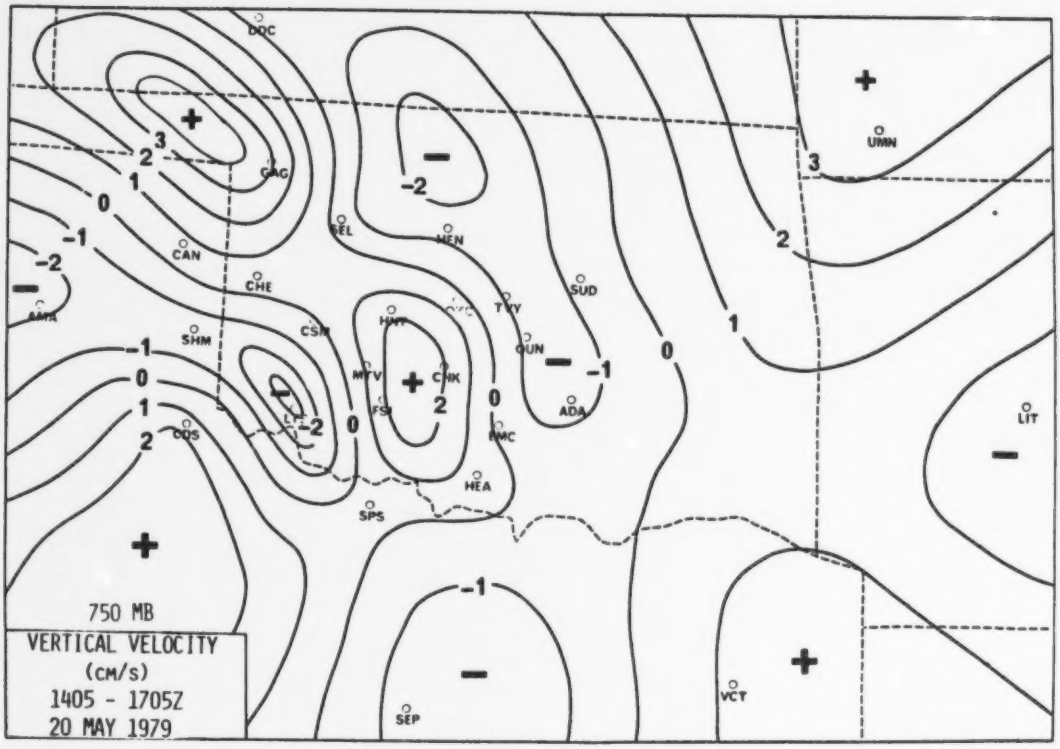

Figure 8. Pre-storm sub-synoptic scale vertical velocity pattern at 750 mb for SESAME-AVE-V case, median time 1535 UTC, 20 May 1979.

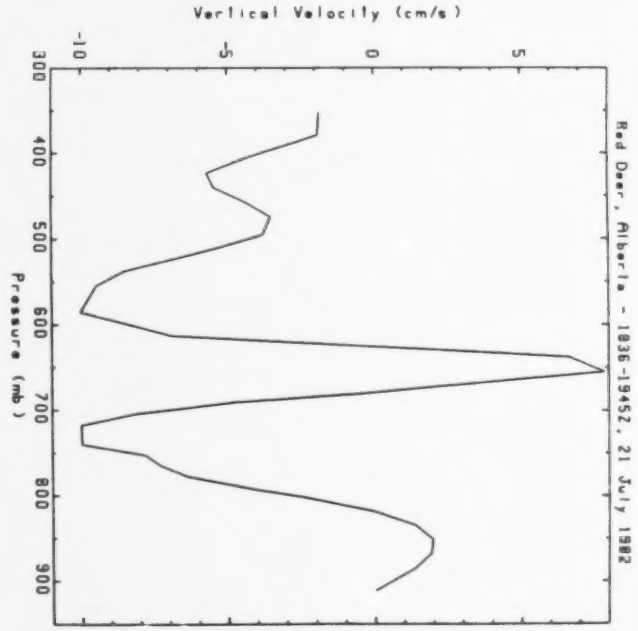

Figure 9. Computed vertical velocity profile, assuming adiabatic cooling (or warming), for Red Deer, Alberta; median release time is 1852 UTC, 21 July 1982.

Cloud Seeding by Ground Generators in Alberta

Field Studies of Generator Targetting

F.E. Robitaille, F.D. Barlow, J.D. Mason, C.M. Sackiw

Atmospheric Sciences Department
Alberta Research Council
Edmonton, Alberta

Cloud Seeding by Ground Generators in Alberta

Field Studies of Generator Targetting

F.E. Robitaille, F.D. Barlow, J.D. Mason, C.M. Sackiw
Atmospheric Sciences Department
Alberta Research Council
Edmonton, Alberta

ABSTRACT

The Alberta Research Council (ARC) is conducting a multi-year program to assess the efficacy of ground-based silver iodide generators for weather modification in the summer months. As part of this program, networks of generators of the coke and arc types were operated by I.P. Krick Associates of Canada, Ltd. in the summers of 1981 and 1982 under contract to ARC. In 1981 66 sites and 86 generators were operated. Slight changes were made to the network for 1982 to include one additional site and two additional generators.

During 1981 and 1982 the principle objective of the program was to measure the concentrations of seeding material delivered by generator networks to target volumes. To do this the INTERA/ARC research aircraft was used to measure ice nuclei concentrations in the target volume using an NCAR ice nuclei counter.

A discussion of the program and results for 1982 are presented. Two case studies are highlighted.

INTRODUCTION

A program to assess the ability of ground-based silver iodide generators of the coke and arc types to seed summer convective clouds for rain enhancement and hail suppression has been underway for two seasons. In the summers of 1981 and 1982, the Ground Generator Assessment Program (GGAP) focused on the detection of generator effluent using an airborne ice nuclei counter. During the 1981 season, problems with the counter precluded quantitative measurements. An improved instrument used in 1982, resulted in quantitative measurements on nine days. This paper discusses the I.P. Krick weather modification technique and reviews of studies relevant to the use of ground-based silver iodide generators. Additionally, results for 1982 are discussed and case studies on 12 July and 2 August, are highlighted.

OBJECTIVES

In 1981 the Advisory Committee on Weather Modification asked the Alberta Research Council (ARC) to evaluate the I.P. Krick weather modification technique. ARC responded to this request by developing the multiphase GGAP. The objective of the first phase, which is discussed here, is to assess the capability of the I.P. Krick technique to deliver effective silver iodide ice nuclei to specified target volumes in the atmosphere.

I.P. KRICK WEATHER MODIFICATION TECHNIQUE

Laboratory tests of silver iodide ground-based generators of the coke type were first carried out in the late 1940's in the I.P. Krick Associates laboratories in Pasedena, California. Field tests followed in 1949 in Arizona. Early models used a chain drive to feed impregnated coke to the furnace. In the middle 1950's the chain drive was replaced by the auger-feed assembly still in use today. Further modifications to the system were designed to increase its operational flexibility by permitting operation using commercial 110 VAC or 6 VDC battery power. Plans to replace the hopper auger-feed motors with a nearly constant RPM motor are underway.

The coke ground generator of I.P. Krick Associates consists of a fuel hopper, feed mechanism, and vaporizing furnace. An on-site storage battery or commercial electrical power is used to actuate the feed mechanism and the fan. The fan forces air into the furnace to assist coke combustion and dispersion of the aerosol.

In preparing fuel for the coke generator, silver iodide is first dissolved with acetone and sodium iodide. Nominally, this solution has a 2 AgI-NaI mole ratio. Quarter-inch foundry coke pellets are immersed in this solution and then placed on drying screens in a thin layer and left in the sun to evaporate the acetone.

The silver iodide output of the coke model generator is variable, dependent upon the concentrations used in the preparation of the coke fuel. Sites using #20 fuel have a nominal output of 15 to 16 grams per hour; sites using #40 fuel have a nominal output of 30 to 32 grams per hour. (I.P. Krick Associates, 1981).

The electric arc generator operates off standard 110 volt power which is boosted by a transformer to a degree sufficient to produce a temperature of approximately 1750°F. Two rods of compressed silver iodide act as electrodes, and the silver iodide is vaporized by the high temperature electric arc. The resulting crystals are expelled from the generator by a small electric blower. These generators have a nominal silver iodide output of approximately two grams per hour (I.P. Krick Associates, 1981).

Tests were conducted in 1981 at the Colorado State University Cloud Simulation and Aerosol Laboratory to determine the effectiveness of ice nuclei production of the Krick coke and arc type generators. The isothermal cloud chamber used in these tests is described in Robitaille et al (1982).

Experiments were conducted to determine aerosol ice crystal production at particular temperatures and liquid water contents (LWC). Tests were conducted at chamber temperatures of -8°C, -12°C, -16°C, and -20°C and at chamber LWC of 0.5 grams per cubic metre and 1.5 grams per cubic metre. Tests were duplicated for each set of conditions. Generators tested were the Krick coke model using types 20 and 40 fuel, the Krick electric arc model 2160, and the North American Weather Consultant's acetone generator using the AgI-NaI fuel mix and an experimental AgI-AgCl fuel mix.

Problems occurred during testing of the arc generator due to its low nominal silver iodide generation rate of 0.033 gm per minute. Standard CSU test procedures require dilution of syringe samples before injection into the chamber cloud. Because of this low nominal output it was necessary to use undiluted arc generator aerosol samples to obtain sufficient ice crystal counts to determine activity and ice crystal formation rates. Since testing was done in the summer, undiluted aerosol samples may have been warm and moist. When they were injected into the cloud chamber local transient supersaturations may have occurred leading to errors in estimates of ice crystal formation

rates. such transient supersaturations should not have changed ice nucleus effectivity data appreciably (Finnégan, 1981).

Aerosols from the arc generator exhibited typical ice nucleus effectivity spectra of relatively pure silver iodide nucleus aerosols. Ice nucleus effectivity ranged from 10 exp 15 per gram at -20°C to 2 x 10 exp 12 per gram at -8°C (for a LWC of 1.5 gm m-3). The mode of nucleation of arc generator aerosol particles was tentatively identified by CSU as contact.

Coke generator aerosol production rate was variable possibly due to the auger feed mechanism adding coke pellets to the furnace in a discontinuous manner. This made effectiveness and rate evaluation of the generated aerosol difficult. At temperatures warmer than -20°C, it was necessary to use undiluted samples to produce quantities of ice crystals detectable on slides exposed in the chamber. Transient supersaturations in the chamber following injection of undiluted samples may have led to errors in ice crystal formation rates. Effectivities were not expected to be appreciably affected by these test conditions.

The coke generator aerosol displayed an effectivity spectra typical of AgI-NaI ice nucleus aerosols. Ice nucleus activity ranged from 10 exp 15 per gram at -20°C to 8 x 10 exp 11 per gram at -10°C. In 1974, effectivities determined for aerosols with natural draft conditions appeared to be greater and values were obtained at temperatures as warm as -8°C. CSU personnel suggest this may be due to variations between fuel samples used in 1974 and 1981. The nucleation mechanism for coke aerosol particles was identified by CSU as "condensation to droplets followed by freezing".

The I.P. Krick weather modification technique considered here, employs a network of ground-based silver iodide generators of the coke and arc types. Usually, residents in or near the Target Area are commissioned to operate and perform routine maintenance of these generators. Detailed maintenance and repairs are the responsibility of Krick field technicians. Instructions to turn on and turn off generators are telephoned to the local operators by the Krick field office. This office is staffed by one or more meteorologists and supervisory staff who base these instructions on an assessment of meteorological conditions. Data for this assessment comes from facsimile and teletype circuits, a nearby upper-air station, pilot balloon reports, and other sources as deemed appropriate.

In 1982 the operational goal of the Krick program was to provide weather modification services in the form of rain enhancement and hail suppression for the specified Target Area south and east of Calgary. To do this for such an area Krick personnel determine the numbers and locations of generator sites by considering size of the Target Area, local relief, prevailing wind direction, and probable motion vectors of convective clouds. Consequently, generators are sited some distance upwind of the Target Area.

Low output (arc type) generators are sometimes co-located with high output (coke type) generators. This permits seeding at night with lower rates of silver iodide generation. According to the Krick rationale, at night the hail threat is lower and clouds can be seeded at a reduced rate.

According to the Krick hypothesis, operating generators produce concentrations of artificial ice nuclei significantly above those found naturally. These artificial ice nuclei are transported by convective currents to the region beneath cloud base. They are eventually carried into convective clouds by updrafts. Once in the clouds they promote the growth of ice crystals at the expense of neighboring water droplets. Such ice crystals later fall through a melting layer and come to the ground as rain (Water Resources Development Corporation, 1977).

REVIEW OF RELEVANT STUDIES

The physical environment may substantially alter the effectiveness of ice nuclei by a variety of mechanisms. This decay is expressed as a rate and implies the loss of effective nuclei over time.

There is general agreement that silver iodide aerosol particles loose ice nucleating ability upon exposure to ultra-violet radiation. The rate of decay of aerosol effectiveness ranges from relatively low values for generator types burning charcoal impregnated with silver iodide (Vonnegut and Neubauer, 1951) to several orders of magnitude greater for hydrogen fired units (Smith et al, 1955). This large variation may be due to the way in which the aerosols were produced. More recent studies suggest that silver iodide particles deactivated by ultra-violet radiation may be rejuvenated upon contact with certain chemical compounds found in the atmosphere (Rosinski and Parungo, 1966).

Tests conducted on the Krick coke generator at CSU in 1974 included estimations of decay of aerosol nucleating properties during exposure to sunlight (Water Resources Development Corporation Generator Tests, Colorado State University, 1974). In these tests decay rates of aerosol samples stored in the dark were compared with those exposed to the sun. It was concluded that sunlight did not significantly affect the

decay rate of the nucleating properties of the silver iodide.

Birstein (1952) related decay rates of aerosol nucleating properties to ambient relative humidities. He found that high relative humidities reduced decay rates appreciably. St. Louis and Steele (1968) also found an increase in aerosol nucleating ability when environmental relative humidities were 50% or higher.

Phase changes of silver iodide-sodium iodide complex aerosols were related to environmental humidities by St.-Amand et al (1971). They showed that the ambient humidity determines when aerosol material goes into solution leaving silver iodide particles immersed in water droplets. At low humidities aerosol particles begin as microcrystalline mixtures of 2 AgI-NaI. Upon acquiring slight amounts of water, AgI and NaI coexist with sodium iodide dihydrate. As more water is picked up the aerosol consists first of silver iodide coexisting with the complex sodium iodide-silver iodide-trihydrate. Later, motes of silver iodide are found in saturated droplets and the complex is dissolved in water. These saturated droplets will later freeze at a temperature determined by the size of the largest particles of silver iodide in them. Ground generator aerosols will function as contact nucleants only if this freezing process proceeds faster than the solution and hydration reactions occur. St.-Amand et al conclude that aerosols composed of silver iodide-sodium iodide complexes will not work well if they spend considerable time in moist air or in clouds too warm to freeze. This conclusion is supported by Blair and Davis (1969), but is contrary to the findings of St.-Louis and Steele (1968).

Blair and Davis (1969) stated that the AgI-NaI aerosol complex is hygroscopic and its ice nucleating effectivity was suppressed by exposure to moist environments with temperatures warmer than -5°C. Bolton and Quershi (1954) in an earlier study concluded that nucleating effectivity of aerosols decayed at warmer temperatures.

Ground generator seeding systems can only be effective if their effluent is transported in sufficient concentrations to the region beneath cloud base. This transport is determined by the prevailing winds and the vertical and horizontal dispersion of the plumes. Dispersion, in turn, increases with increasing instability and distance downwind from the source. Dispersion of aerosols from ground generators is discussed in Robitaille et al (1982).

Mason and Hallette (1956) reported the possibility of lowered aerosol effectivity when generator fuel mix is burned at high temperatures. St.-Amand et al (1971) state that when the flame temperature is too high some of the solid fuel constituents may vaporize and later recondense, producing smaller aerosol particles. Very small aerosol particles produced in this way will dissolve in water droplets more readily and will not be able to function as freezing nuclei at warmer temperatures.

In 1975, the Interim Weather Modification Board (IWMB) of the Alberta Government commissioned I.P. Krick Associates of Canada, Ltd. and INTERA Environmental Consultants Ltd. to conduct a two month summer experiment to determine the feasibility of using ground-based generators for hail suppression. This effort was conducted southeast of Calgary using single and multiple generator sites from 20 June through 20 August. An aircraft equipped with an NCAR acoustical ice nucleus counter was used to seek out the effluent from the generators. Results of this study were published by IWMB in two separate but attached reports (Stone et al, 1976, INTERA, 1975). Methods of analysis and interpretation of experimental data were different in the two reports. As a result, opinions were different on the ability of a network of ground generators to deliver silver iodide ice nuclei to regions below convective cloud base.

PROGRAM METHODOLOGY

At the outset of GGAP, ARC recognized the importance of verification of a sequence of events leading to modification of convective precipitation by ground-based silver iodide generators. Accordingly, a conditional, three-phase strategy was planned. The first phase, discussed in this paper, will attempt to confirm the presence of artificial ice nuclei in concentrations significantly above those occurring naturally in regions beneath the bases of convective clouds. If confirmation occurs, a second phase will assess the effect of these artificial nuclei on ice crystal formation in the updrafts of convective clouds at temperatures between -5 and -15°C. The success of phase one is predicated upon availability of the INTERA-Alberta Research Council Cloud Physics Research Aircraft to GGAP for cloud base mapping flights. This aircraft must be able to measure and record cloud physics parameters, particularly ice nuclei concentrations, together with standard state parameters and aircraft position as a function of time.

A third phase will involve studies of precipitation and will be initiated should results from phases one and two warrant it.

Determining the ability of the Krick technique to deliver artificial ice nuclei to specified target volumes

requires answers to three key questions. If the Krick field office requests operators to run specific generators for prescribed periods of time and prescribed generation rates, what is the likelihood this request is met? If a generator is operating, what is its effective output of aerosol particles and what are the characteristics of these particles? In what concentrations can these particles be expected in the target volume and can their presence be confirmed by measurements? Phase one of GGAP was designed to address these questions by including ground generator operational seeding, site monitoring, laboratory testing, and aircraft mapping.

The ground generator seeding operations program for 1982 was designed for a Target Area defined in the contract with I.P. Krick Associates of Canada, Ltd. To protect this Target Area, the contractor installed a network of 67 generator sites both within and outside of it (Figure 2). Some sites had both coke and arc type generators resulting in a total of 88 generators. The exact number of generators fluctuated slightly as some installations were changed over the project period.

Field headquarters and staff responsible for conduct of the seeding operations program were located in Calgary. Operational support equipment included teletype, facsimile and telecopier installations. Storage of generators, fuel and supplies was also in Calgary at the Krick warehouse.

Local residents were commissioned by the contractor to operate the generators on their property, and Krick technicians provided maintenance support as required. After an examination of meteorological data by contract personnel in Calgary, operational instructions were telephoned to generator operators.

Additional information on the seeding operations program design is contained in contractor's final reports (I.P. Krick Associates, 1981, 1982).

The research program for 1982 was designed to answer the three key questions stated above.

Firstly, a site monitoring subproject was incorporated in which visits were made to generator sites by ARC personnel. Generator operational status was confirmed during such visits and fuel samples were collected for analysis of chemical composition. Results of this subproject are reported elsewhere (Robitaille et al, 1982, 1983).

Secondly, a laboratory testing subproject was included to examine effectivenss of the generator nuclei together with nucleation mechanisms and nucleation rates. The Colorado State University (CSU) Cloud Simulation and Aerosol Laboratory was contracted to perform a series of tests of generator effectiveness. These tests were conducted on the Krick coke and arc type generators and on the North American Weather Consultants (NAWC) acetone type generator. The CSU facility is the only one of its kind in the western world designed for such tests. This facility is described in Robitaille et al (1982). Results are summarized earlier in this paper.

Thirdly, an aircraft measurements subproject was included to measure ice nuclei concentrations in the atmosphere. To do this, an NCAR ice nuclei counter was borrowed from Colorado State University and installed on the INTERA/ARC Research Aircraft. This instrument replaced the Mee counter used in 1981. Dr. James Heimbach of Montana State University, through an agreement with the Alberta Research Council, modified the NCAR counter to meet project requirements for quantitative ice nuclei measurements. Additionally, he spent approximately three weeks in the Red Deer area installing and testing it on the Research Aircraft. Calibration parameters and in-flight test procedures are given in Robitaille et al (1982). Operation of NCAR counters is discussed in Appendix B of Robitaille et al (1982).

The research aircraft was used to map ice nuclei delivered to the Target Area. Pre-planned flight patterns were devised to map spatial distributions of ice nuclei concentrations at three flight levels. An idealized 'diamond' flight pattern was selected. To fly such patterns required forecasts of ground generator artificial ice nuclei locations by contract staff. For the forecast area a characteristic width, W, and length, L, were determined. The centroid of the area, A, was found and the following five points referenced to the pool were plotted:

$$A = (0, 0)$$
$$B = (0, +W/2)$$
$$C = (-L/2, 0)$$
$$D = (0, -W/2)$$
$$E = (+L/2, 0)$$

These points were converted to navigational coordinates and a diamond pattern starting at B planned.

A network of waypoints permitted navigation of the aircraft in the event of failure of the on-board automatic navigation systems. If the automatic data recording capability of the aircraft failed, an analog trace of ice nucleus counts with time was available. Limitations of aircraft availability and instrumentation problems required modifications of these plans.

The aircraft mission scientist (AMS) was responsible

for all flight plan mapping, in-flight procedures and post-flight documentation. Prior to take-off, the AMS examined the morning forecast provided by the Krick Calgary field headquarters. If the mission was in the afternoon, a forecast update was requested from Krick. The AMS plotted a diamond pattern in the pool area using the waypoint locations as vertices. Photographic records of weather conditions and surface wind indicators (e.g. smoke, dust) were kept by the AMS when possible.

GENERATOR OPERATIONS SUMMARY

A network of 67 sites and 88 generators was operated from 21 June through 20 August inclusive to seed convective clouds for rain enhancement and hail suppression within a 14,000 sq. km Target Area in southern Alberta (Figure 1). A summary of generator operations is given in Table 1 showing a total of 3,606 hours of generator operation releasing a nominal 29.5 kilograms of silver iodide during the 40 day period. Temporal and spatial characteristics of generator operations in 1981 and 1982 are discussed and compared in Robitaille et al (1983). Additional information on 1982 generator operations may be found in the contractor's final report for 1982 (I.P. Krick Associates, 1982).

Table 1. Summary of generator operations in 1982.

	Coke operations (hours)	Arc operations (hours)	AgI output (kilograms)
June	238	706	6.96
July	520	1092	12.71
August	393	657	9.86
Totals	1151	2455	29.53

NCAR ICE NUCLEI DATA ANALYSIS

Two basic approaches were used to analyse the aircraft NCAR ice nuclei (IN) measurements within the Target Area. The first focused on the identification and analysis of "encounters" with discrete ice nuclei plumes. The purpose was to document the characteristics of these encounters, specifically their ice nuclei concentration and frequency of occurrence. These were used as the basis for the detailed case studies cited in a subsequent section of this report.

The second approach was to examine all of the NCAR data measurements made in the project area. It's goal was to provide an overall profile of the occurrence of atmospheric ice nuclei. Included are analyses of data sets recorded during various generator operation configurations. "Background" measurements made during non-operational days are also included as a benchmark for comparison. This section examines the wide area or "broadcast" seeding effect of the generator system.

A quality assessment was made of all NCAR data and erroneous data was excluded from any data analysis.

Ice nuclei plume segments are defined as those portions of the measurement flight track in the Target Area having positive ice nuclei counts. These segments represent regions of discrete ice nuclei plumes which are readily distinguishable from "background" or disperse IN conditions.

Aircraft measurements of ice nuclei concentrations provide only a discrete slice of the generator plumes. These slices, or "plume segments", may have concentrations representative of those in the plume if the generator source strength, environmental winds and stability remain relatively constant during the measurements. Plume segments can be of varying lengths depending on aircraft altitude, flight direction and distance from the source.

There are limits on the ability of the airborne system measurements to resolve such segments. The minimum segment length resolvable by the NCAR counter is defined by the data acquisition system characteristics and aircraft speed. For the 2-second sampling total interval and an average aircraft speed this is about 200 metres.

Segments were defined using objective criteria based on the characteristics of the NCAR counter data. A segment was identified as a region of continuous positive ice nuclei counts registered for a sample volume of one litre or more. this corresponds to a minimum sampling flight track distance of six (6) seconds duration, or approximately 600 m in length. Segment start (stop) points were defined as the last non-zero data value preceded (succeeded) by one litre of a nuclei-free sample volume.

Examination of the data supported this criteria. Continuous positive counts were generally found to occur in sequences longer that six (6) seconds. Scattered counts were almost exclusively of shorter durations.

Ice nuclei segments identified during the 1982 field measurement program are summarized in Table 2. A total of 28 segments were identified on eight of the ten mapping flights. Table 2 lists various physical characteristics of these segments including: segment length, duration, mean ice nuclei concentration and standard deviation. Also included are environmental parameters including average height and air temperature during segment encounter. These segments

were identified for approximately 230 km of the total aircraft flight track for all mapping flights. The average segment length was approximately 8.2 km.

For purposes of assessing segment frequency, intersegments were also identified for the mapping flights. Intersegments were defined as those portions of the flight track within the Target Area where distinct segments could not identified. They generally occur between plume encounters and may include those portions of the flight where positive IN counts were noted but discrete plumes could not be defined. Approximately 4500 km of the total flight tracks within the Target Area were identified as intersegment regions. The average ice nuclei concentration for all of the intersegment regions was 1.8 IN per litre.

Table 3 summarizes mean ice nuclei concentrations for segments, intersegments, and total measurement distance for 10 mapping and 2 background missions. For each flight day, generator seeding amounts were estimated by converting nominal production of silver iodide by all operating generators to nuclei effective at -20°C and 0.5 grams liquid water per cubic metre. Under natural draft conditions and with coke fuel silver iodide content of 9% and arc rod silver iodide content of 99%, one gram of silver iodide burned in a coke generator yields about 4 x 10 exp 13 nuclei and one gram of silver iodide burned in an arc generator yields about 5 x 10 exp 14 nuclei (Robitaille et al, 1982, Appendix F). Any departures of coke fuel silver iodide content from nominal values were likely on the positive side (see Robitaille et al, 1983 pp. 10-11).

Background concentrations were on the order of 0.1 nuclei per litre, a value similar to that in found in Alberta by others (Stone et al, 1976). No segments were detected during two mapping missions when only arc generators were in operation. On 28 July the aircraft was upwind of arc generators at flight level. However, on the morning of 2 August the aircraft was downwind of sources and the lack of flight segments during this mission remains unexplained. Segments for two mapping missions when only coke generators were operating constituted 4% and 11% of total mapping lengths. Six missions during simultaneous coke and arc generator operations had segments constituting from 0.4% to 15% of total mapping lengths.

The ratio of total segment length to total flight track length within the Target Area gives an indication of the frequency of distinct ice nuclei plume encounters within the Target Area. This ratio for the 10 mapping flights was 0.049. This indicates that positive IN plume encounters accounted for approximately 5% of the total flight track measurements.

Table 2. 1982 ice nuclei segment summary. Average IN values and selected parameters for segment period.

Flight #	Date	Segment #	Length m	Duration sec	IN/litre	σ°	ZMSL m	T°C
5	27 June	1	24250	268	39	69	1255	13.0
14	12 July	1	1902	42	31	33	1173	19.6
		2	712	8	120	123	1127	20.4
		3	6086	68	123	126	1078	21.3
		4	8935	102	39	69	1160	17.6
		5	28397	318	119	204	1143	19.9
		6	2864	32	13	15	1107	20.5
15	21 July	1	6755	82	11	16	1201	23.3
		2	1381	16	30	28	1978	15.3
16	25 July	1	2715	28	17	15	2150	8.3
18	31 July	1	5798	64	8	15	1176	22.9
		2	9574	108	6	12	1151	21.7
20	2 August	1	23162	258	20	24	1228	18.2
		2	9922	112	18	24	1313	16.4
		3	6391	70	15	23	1190	17.1
		4	2065	24	15	20	1150	17.6
		5	3655	42	11	15	1151	18.1
		6	5149	56	13	19	1875	10.4
		7	8703	94	12	20	1873	10.1
21	3 August	1	11145	146	10	16	1248	12.1
		2	8982	112	91	89	1093	12.7
		3	6888	78	13	17	1503	12.2
22	3 August	1	9176	108	19	26	1187	13.5
		2	5316	60	45	35	1189	12.9
		3	8320	96	23	22	1236	14.2
		4	6483	74	9	20	1267	13.9
		5	7653	86	9	17	1194	15.1
		6	6339	70	9	16	1845	8.1

Table 3. Summary of 1982 aircraft missions showing mean number of ice nuclei per litre effective at -20°C for intersegments (INIS), segments (INS), and total measurement distance (INFLT). The ratio of total segment length to total mapping length (R) is shown in percent. Nominal generator seeding amount prior to aircraft entry into Target Area in numbers of ice nuclei effective at -20°C is shown in the last column.

Date	Objective	Number of Segments	INIS	INS	INFLT	R	Nominal IN Production (10 exp 16)
26 June	background	0	0.1	—	0.1	0.	0.
27 June	coke & arc mapping	1	0.3	39.	2.4	6.	7.35
3 July	background	0	—	—	—	0.	0.
12 July	coke & arc mapping	6	1.6	93.	15.1	15.	6.70
21 July	coke & arc mapping	2	0.6	14.	10.8	4.	1.78
25 July	coke & arc mapping	1	0.3	17.	0.4	0.4	2.61
28 July	arc mapping	0	0.9	—	0.9	0.	1.34
31 July	coke & arc mapping	2	0.3	6.	0.5	4.	0.78
2 Aug am	arc mapping	0	0.6	—	0.6	0.	9.18
2 Aug pm	coke mapping	7	3.1	17.	4.6	11.	12.4
3 Aug am	coke mapping	3	2.3	38.	3.8	4.	2.4
3 Aug pm	coke & arc mapping	6	2.2	18.2	3.7	9.	9.6

The segment data analysis indicates that while significant ice nuclei concentrations were occasionally encountered, the average concentrations were on the order of 30 per litre. These segment encounters occurred for only a few percent of the measurement program.

Extensive analyses of all the mapping flight NCAR data within the Target Area were also completed. Periods of erroneous data or instrument malfunction were excluded. This data set included both plume segment and intersegment periods, encompassing all "good" data. A ten-second averaging period was selected as the smallest interval where the instrument effects on data characteristics would be at a minimum (J.H. Heimbach, personal communication, 1983).

Ten-second average IN concentrations were calculated for the following categories of flight missions and are summarized in Table 4:

1. All mapping flights (except background) (10)
2. Mapping flights for arc-type generator operations only (2)
3. Mapping missions for coke-type generator operations only (2)
4. Mapping missions for both arc and coke generator operations (6)
5. Background mapping missions (2)

Table 4. Data summary — 1982 GGAP mapping flights IN concentrations (10-second averaging period).

Type	Flights	Samples (10 sec)	Max IN (#/1)	IN (#/1)	Sigma IN (#/1)	Coefficient of variation*
All (no back)	10	5863	504	3.1	15.8	5.1
Arc only	2	1226	30	1.2	3.4	2.8
Coke only	2	1530	204	4.4	11.7	2.6
Coke/arc	6	3107	504	3.2	20.0	6.3
Background	2	554	12	0.1	0.9	7.5

*Coefficient of variation is a dimensionless index with variability increasing with increased value.

The table suggests generally low values throughout the flight areas, with the average concentration for all flights combined (excluding "background") equal to about three (3) ice nuclei per litre. The coke-only and combination coke/arc mission data show a marginal increased concentration, while the arc-only cases show a marked decrease. The background data, although a smaller sample set, shows an average concentration of about 0.1, an order-of-magnitude less than that of days when generators were operated.

Frequency distributions for these flight types are also examined. The majority of values indicate no (zero) ice nuclei. Excluding these zero values, a rapid decrease

is indicated with most values being less than 10 per litre. A probability plot (not shown) of these values based on their cumulative probability shows that 92% of the data values are less than a 10 per litre concentration and less than 0.5% of the cases exceed the 100 per litre value.

CASE STUDIES

Coke and Arc Mapping Mission on 12 July 1982: A small surface disturbance associated with a weak upper-level trough moved over the Target Area during this day. Several heavy thunderstorms developed along the foothills by midafternoon, then drifted eastward across the northern half of the Target Area.

Six arc generators were started at noon along the foothills. Mostly coke units were operated thereafter concentrated over the northern and central regions. A total of 124 hours of generator operations occurred producing a nominal 1.52 kilograms of silver iodide. This was the fourth most heavily seeded day of the operational period.

The aircraft departed Red Deer at 1645 M.D.T. and flew a mapping mission over the western portions of the Target Area. All measurements were made near 160 meters above ground. Six segments representing 15% the total mapping length were found. Their characteristics are given in Table 5. Mean number of nuclei per litre, IN, and standard deviation, , are for NCAR counter chamber temperature of -20°C. Mean temperature, T, should be interpreted as representative of ambient conditions in the segments.

Table 5. Segment characteristics for 12 July flight.

Segment Number	Length (meters)	Mean Altitude (meters MSL or approx 160 m above ground)	T (°C)	IN (per litre)	s.d. (per litre)
1	3,902	1,173	19.6	31	33
2	712	1,127	20.4	120	123
3	6,086	1,078	21.3	123	126
4	8,935	1,160	17.6	39	69
5	28,397	1,149	19.9	119	204
6	2,864	1,107	20.5	13	15

Segment locations, nominal generator plumes and the 1800 M.D.T. Lethbridge hodograph are shown in Figure 2. Winds at Lethbridge indicate flight segments are downwind from operational generators.

Of particular interest is segment 5, the longest of the field season. Ten-second average ice nuclei concentrations and plotted two-second relative concentrations are shown in Figure 3. Average values fit reasonably well within generator plume boundaries along the western portion of the flight. However, nuclei concentrations further east are much lower than expected using the Gaussian plume model for a continuous point source on flat terrain with light to moderate winds and a slightly unstable lapse rate (Robitaille et al, 1982, Appendix A).

Relative frequencies of occurrence of various ranges of ten-second average ice nuclei concentrations were computed for the entire flight, for intersegments, for segments, and for segment 5. Table 6 stratifies these results as to frequency of ice nuclei concentration.

Table 6. Relative frequencies of occurrence for particular 10-second mean ice nuclei concentrations on 12 July 1982 mission.

	Ice nuclei concentration frequencies			
Portion greater than:	100/litre	60/litre	40/litre	20/litre
Entire mapping length	3.2%	4.6%	6.2%	9.4%
All intersegments	0. %	0. %	0. %	0.6%
All segments	27.9%	33.5%	42.8%	61.3%
Segment 5	34.4%	34.4%	40.7%	53.2%

For the overall flight it is apparent that concentrations exceeding 100 nuclei per litre were experienced infrequently. In fact, concentrations exceeding 40 per litre, were measured only marginally more often (6.2% versus 3.2%).

Coke Mapping Mission on Afternoon of 2 August 1982: A broad 500 mb trough covered western Canada. In the morning, a short wave was embedded in a line from Jasper to Medicine Hat. At the surface a trough extended from central Alberta to eastern Montana. Systems moved to the east northeast during the day. General instability produced scattered light showers and thunderstorms during the early morning. Conditions stabilized during the afternoon as dry westerly winds prevailed.

By special request, ten coke generators were operated from mid afternoon till evening over the northern portions of the project. A total of 44 hours of operations produced a nominal 1.06 kilograms of silver iodide.

The aircraft took off from the Red Deer airport at 1630 M.D.T. and flew two mapping circuits in the north-central part of the Target Area. Circuit one was flown near 160 meters above ground and circuit two near 750 meters above ground. Seven segments representing 11% of the total mapping length were found. Their characteristics are given in Table 7.

Table 7. Segment characteristics for 2 August afternoon flight.

Segment Number	Length (meters)	Mean altitude (meters MSL)	T (°C)	IN (per litre)	s.d. (per litre)
1	23,162	1,228	18.2	20	24
2	9,922	1,313	16.4	18	24
3	6,391	1,190	17.1	15	23
4	2,065	1,150	17.6	15	20
5	3,656	1,151	18.1	11	15
6	5,149	1,875	10.4	13	19
7	8,703	1,873	10.1	12	20

Mean concentrations for all segments are similar and are well-below 100 per litre.

Figures 4 and 5 show segment locations, nominal generator plumes, and Calgary and Lethbrige evening hodographs. Flight segments appear approximately 15 to 50 km downwind of operating generators. A comparison of observed mean concentrations and theoretical Gaussian plume concentrations is given in Table 8. Theoretical values are estimated (Robitaille et al., 1982, Appendix A).

Table 8. Theoretical (INT) and observed (INO) mean concentrations for segments of 2 August 1982 afternoon flight. Distances given are for segment centers.

Segment Number	Altitude (metres AGL)	Distance downwind from source (km)	Distance from centerline (km)	INT (per litre)	INO
1	ca. 160	15	3	25	20
2	160	25	6	20	18
3	160	10	10	1	15
4	160	40	4	20	15
5	160	45	10	1	11
6	750	22	2	25	13
7	750	25	6	1	12

Theoretical concentrations agree well with the observed segment average values provided the segments are within a few kilometres of the plume centerline. Considering the plumes in the figures are only estimated and considering the uncertainty in the local wind profiles, the aircraft observations appear reasonable. The lack of consistent ice nuclei concentrations across all nominal plumes may be explained by one or more of the following:

1. Nominal plumes may not be representative of actual plumes at flight level due to wind shear
2. Temperature lapse rates may differ from the slightly unstable criteria assumed (Robitaille, et al, 1982)
3. Aircraft measurement patterns may not adequately transect plume geometry
4. The gaussian plume model assumption may not be valid for these cases

SUMMARY

The mapping of ice nuclei concentrations using an airborne NCAR acoustical counter revealed an average of three (3) nuclei per litre in the Target Area. Some 28 encounters with ice nuclei segments were defined and comprised about five percent (5%) of total mapping length. Average concentrations of ice nuclei within these segments ranged six (6) to 123 per litre. Only one-half of one percent (0.5%) of all NCAR data exceeded 100 nuclei per litre.

In weighing the results of the analysis of the NCAR data, it must be kept in mind that most mapping flights were well-below the level at which convective clouds formed. Aircraft deployment must consider variations of the environmental winds with height so that measurements downwind of generators are obtained.

One of the important elements of the GGAP aircraft program is the mapping of ice nuclei concentrations near convective cloud base. Simultaneous measurements of ice nuclei concentrations and atmospheric vertical velocities are necessary since ground-based seeding devices must be able to produce ice nuclei concentrations near 50 per litre in convective cloud updrafts. Consequently, the occurrence of updrafts must correlate with the occurrence of ice nuclei segments before in-cloud microphysical measurements are priorized.

Chemical analyses of coke fuel samples indicated percentages of silver and silver iodide above nominal values (Robitaille et al., 1983). Similar analyses is planned for 1983 to corroborate these percentages.

Site monitoring operations showed network operations to be reliable in 1982.

ACKNOWLEDGMENTS

The authors acknowledge with thanks the assistance of I.P. Krick Associates of Canada, Ltd., the Department of Atmospheric Science of Colorado State University, and INTERA Environmental Consultants of Calgary. Dr. J. Heimbach of Montana State University provided assistance and advice that was essential to the successful operation of the CSU NCAR counter. Dr. T.W. Krauss of the Atmospheric Sciences Department provided valuable assistance as an Aircraft Mission Scientist. Drafting assistance was provided by R.H. Myrick. Computer programming assistance was provided by N. Chidambaram. Chemical analyses of fuel samples were carried out by the ARC Chemistry Analytical Services Laboratory under the direction of Dr. J.M.L. Gray and care of E. Zacharuk.

This project was supported by the Advisory Committee on Weather Modification of the Alberta Government and was funded by the Alberta Department of Agriculture.

REFERENCES

Birstein, S.J. 1952: The effect of Relative Humidity on the Nucleating Properties of Photolyzed Silver Iodide. Bull. Am. Met. Soc., 33, pp. 431-434.

Blair, D.N., and B.L. Davis, 1969: Aging of Silver Iodide-Sodium Iodide Generator Effluent in Moist and Dry Air. J. Appl. Met., 8 (4), pp. 551-555.

Bolton, J.G., and N.A. Quershi, 1954: The Effects of Air Temperature and Pressure on the Decay of Silver iodide. Bull. Am. Met. Soc., 35, pp. 395-399.

Colorado State University, 1974: Water Resources Development Corporation Generator, .47 gram AgI/min. Cloud Simulation and Aerosol Laboratory, C.S.U., Ft. Collins, Colo. 20 pp.

Finnegan, W.G., 1981: A Report to the Alberta Research Council on the Characterizations of the I.P. Krick Associates of Canada, Ltd., Electric Arc AgI Generator, and Coke Burning AgI Generator and the North American Weather Cosultants Acetone Burning AgI and AgI-AgCl Generator. C.S.U., Colo. 18 pp. plus Appendices.

INTERA Environmental Consultants Ltd., 1975: Published as Part II of Final Report, 1975 Ground Generator Study. Alberta Weather Modification Board, Report No. 3. 223 pp. plus Appendices.

I.P. Krick Associates of Canada Ltd., 1981: Final Opera- tions Report, 1981 Ground Generator Study and Weather Modification Project (Project AL-3). Published by I.P. Krick Associates of Canada, Ltd., Palm Springs, Ca. 83 pp.

I.P. Krick Associates of Canada, Ltd., 1982: Final Operations Report, 1982 Ground Generator Assessment and Weather Modification Program (Project AL-3). Published by I.P. krick Associates of Canada, Ltd., Palm Springs, Ca. 72 pp.

Mason, B.J., and J. Hallette, 1956: Artificial Ice-Forming Nuclei. Nature, 177 (4511), pp. 681-683.

Robitaille, F.E., F.D. Barlow, T.W. Krauss, J.W. Mason, and C.M. Sackiw, 1982: Ground Generator Assessment Project 1981 Project Report. Alberta Research Council, Atmospheric Sciences Department, Edmonton, April. 59 pp. plus six Appendices.

Robitaille, F.E., F.D. Barlow, J.W. Mason, and C.M. Sackiw, 1983: Ground Generator Assessment Project 1982 Project Report. Alberta Research Council, Atmospheric Sciences Department, Edmonton, June. 41 pp. plus two Appendices.

Rosinski, J., and F. Parungo, 1966: Terpene and Iodide Compounds as Ice Nuclei. J. Appl. Met., 5 (1), pp. 119-123.

Smith, E.J., K.J. Heffernan, and B.K. Seely, 1955: The Decay of Ice-nucleating Properties of Silver Iodide in the Atmosphere. J. Met., 12 (4), pp. 379-385.

St.-Amand, P., W. Finnegan, and L. Burkhardt, 1971: Understanding of the Use of Simple and Complex Ice Nuclei Generated from Pyrotechnics and Acetone Burners. J. Wea. Mod., 3, pp. 31-48.

St. Louis, P.T., and R.L. Steele, 1968: Certain Environmental Effects on Silver Iodide Ice Nuclei. Proceedings of the International Conference on Cloud Physics. (Toronto, Canada, 26-30 August 1968), pp. 178-182.

Stone, N.C., et al., 1976: Published as Part I of Final Report 1975 Ground Generator Study. Alberta Weather Modification Board. Report No. 3. 228 pp.

Vonnegut, B., and R. Neubauer, 1951: Recent Experiments on the Effect of Ultraviolet Light on Silver Iodide Nuclei. Bull. Am. Met. Soc., 32, pp. 356.

Water Resources Development Corporation, 1977: Why and How the Krick System of Cloud Seeding Works. 12 pages. Palm Springs, Ca. 12 pp.

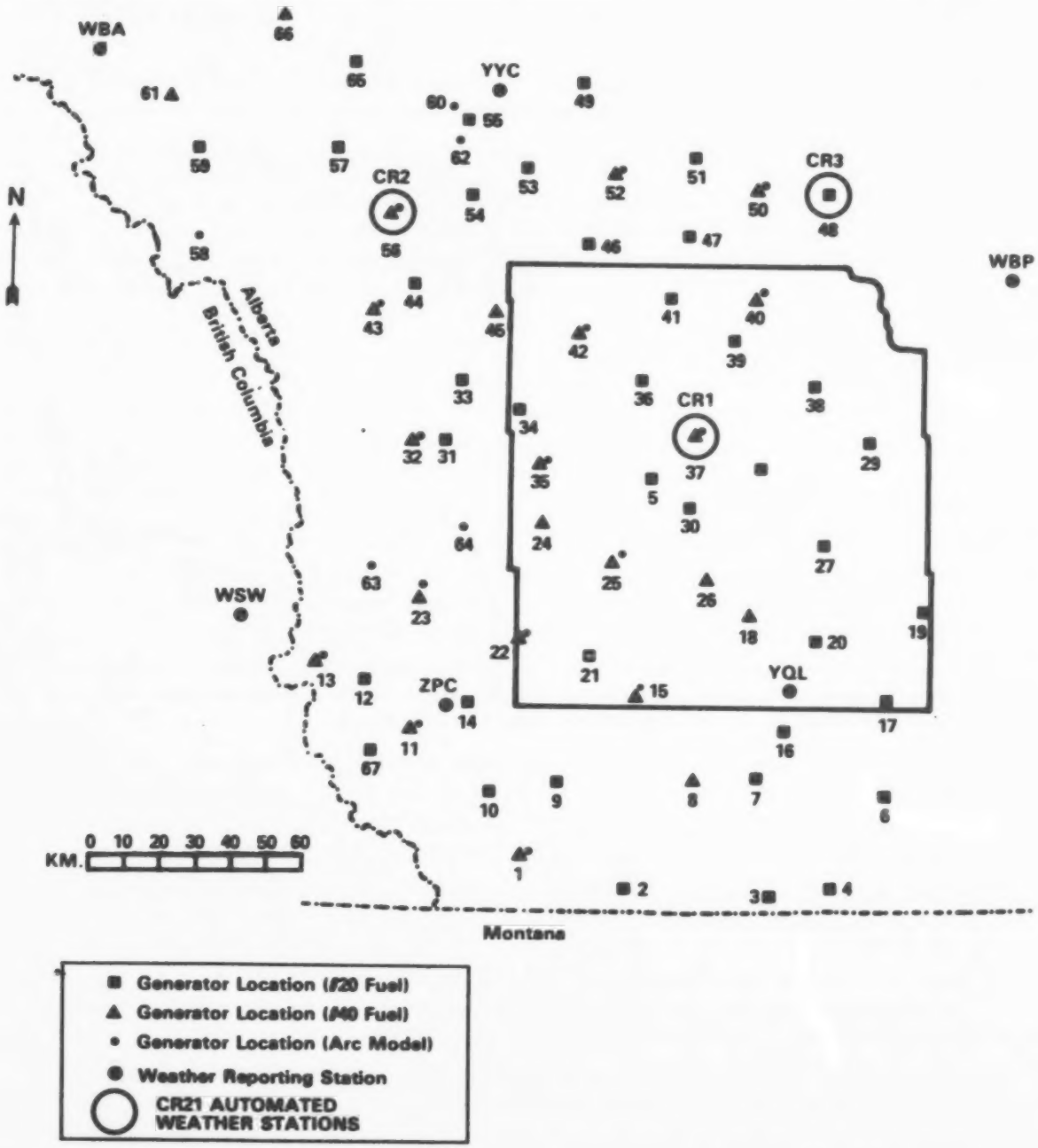

Figure 1. 1982 GGAP area showing I.P. Krick Target Area bounded by solid line and generator and automated weather station locations.

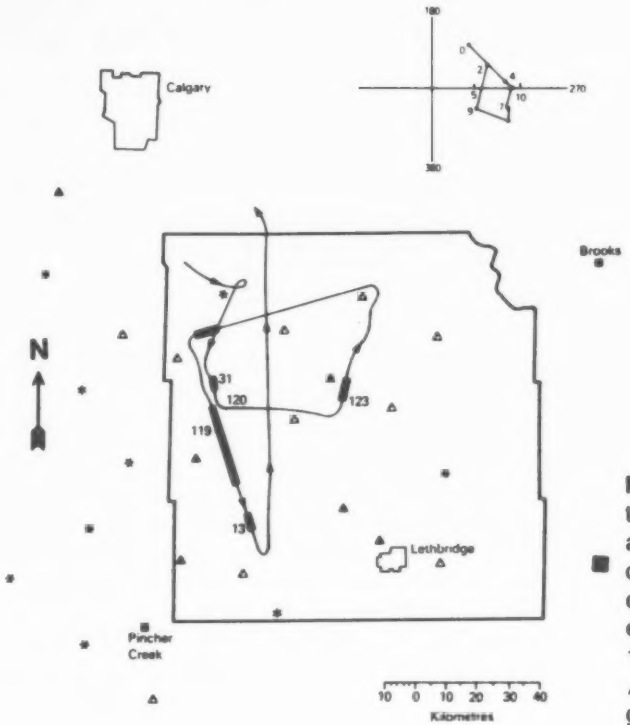

Figure 2. Segment locations and mean IN concentrations for 12 July 1982 mission flown at approximately 160 m above ground. Generator sites operating during aircraft flight are shown. Plume centerlines were estimated by contractor to be aligned southwest to northeast. Hodograph from Lethbridge 1800 M.D.T. pibal ascent is shown. (° = arc generator; △ = 15 g hr^{-1} coke generator; ▲ = 30 g hr^{-1} coke generator). Reference times indicated.

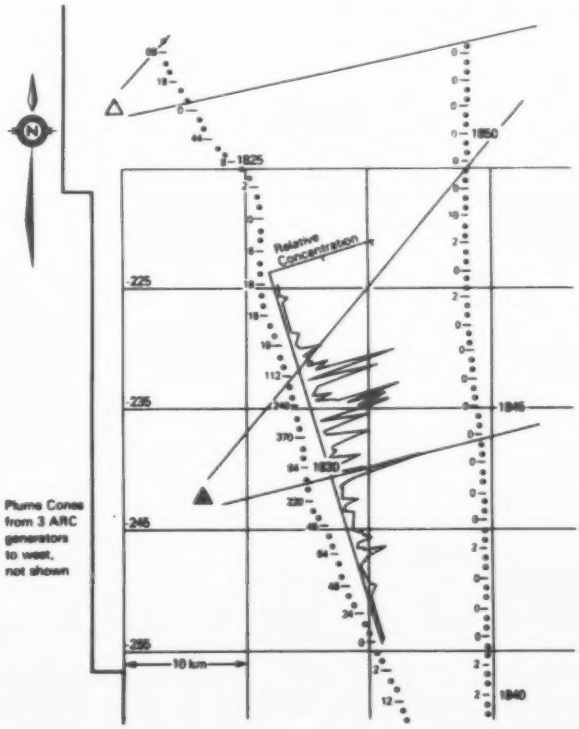

Figure 3. Ten-second average ice nuclei concentrations for a portion of the flight track for 12 July 1982 mission flown at approximately 160 m above ground. Plot of two-second concentrations also shown. Estimated generator plumes provided by I.P. Krick Associates. (△ = 15 g hr^{-1} coke generator; ▲ = 30 g hr^{-1} coke generator).

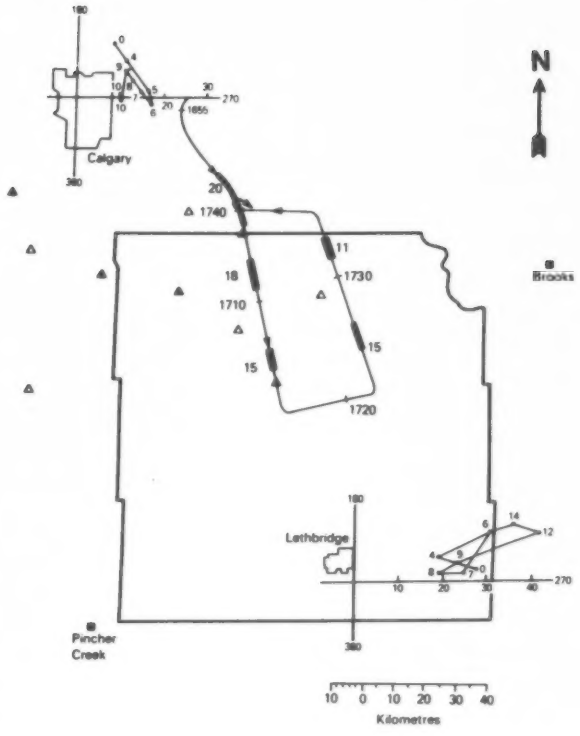

Figure 4. Segment locations and mean IN concentrations for circuit 1 for 2 August 1982 mission flown at approximately 160 m above ground. Generator sites operating during aircraft flight are shown. Plume centerlines were estimated by contractor to be aligned from just south of west to just north of east. Hodographs from Lethbridge 1800 M.D.T. and Calgary 1700 M.D.T. pibal ascents are shown. (Δ = 15 g hr^{-1} coke generator; ▲ = 30 g hr^{-1} coke generator). Reference times indicated.

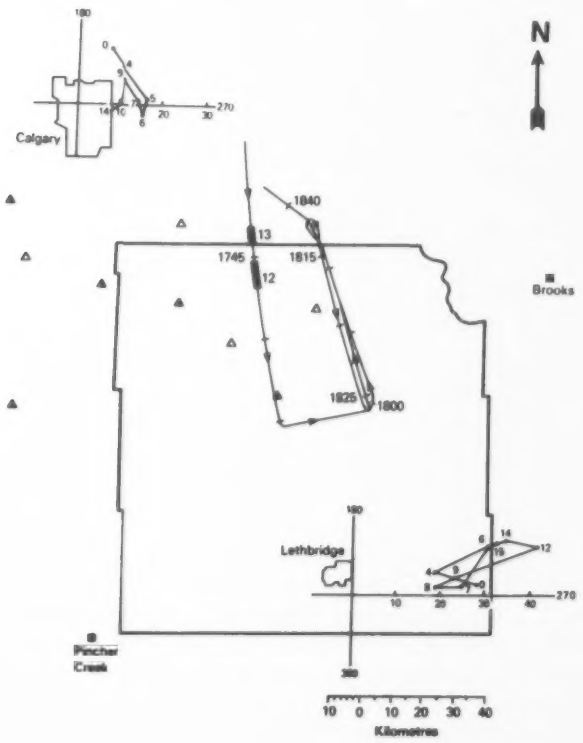

Figure 5. Same as Figure 4 but for circuit 2 flown at approximately 750 m above ground.

Modification Potential of Orographic Cloud Systems in the Southern Canadian Rockies: Preliminary Aircraft Observations

by

T.W. Krauss, F.E. Robitaille, F.D. Barlow, J.W. Mason

Atmospheric Sciences Department
Alberta Research Council
Edmonton, Alberta

Paper presented at the 17th Annual CMOS Congress, Banff, Alberta,May 1983.

Modification Potential of Orographic Cloud Systems in the Southern Canadian Rockies: Preliminary Aircraft Observations

by

T.W. Krauss, F.E. Robitaille, F.D. Barlow, J.W. Mason

Atmospheric Sciences Department
Alberta Research Council
Edmonton, Alberta

ABSTRACT

A preliminary experiment was performed from 16 to 26 March 1982 as a prelude to a proposed multi-year program to assess the modification potential of winter-time orographic clouds in the southern Canadian Rockies.

The INTERA Environmental Consultants Ltd. - Alberta Research Council research aircraft flew five missions during the experimental period. Case study analysis for a mission on 23 March is presented. The orographic cloud that day contained regions with supercooled liquid water concentrations as high as 0.6 grams per cubic metre. Regions of supercooled liquid water existed where the concentration of precipitation size particles (diameter greater than 200 microns) was less than 1 per litre. The computed precipitation conversion efficiency for a major portion of the cloud was less than 50 percent. The possibility exists that the liquid water was not being efficiently converted to precipitation and that the precipitation process could have been made more efficient if artificial ice nuclei had been added.

The 23 March 1982 case study differed greatly from a classic mountain orographic cloud because saturated upslope conditions at the lower levels existed east of the mountains. The saturated upslope conditions acted to enhance the growth of precipitation east of the mountains.

1.0 INTRODUCTION

The orographic clouds which frequently occur over Alberta's higher mountain peaks during winter may be a potential source of significant amounts of additional water. Weather modification involving the 'seeding' of these orographic clouds may offer a way of augmenting Alberta surface water resources by making greater utilization of our atmospheric water resources.

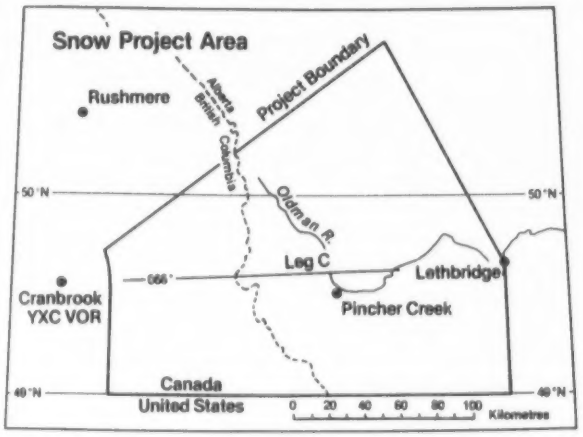

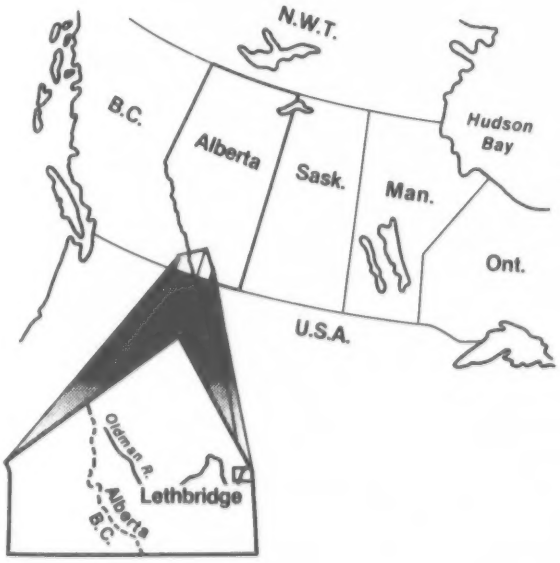

Figure 1: A map showing the location of the Snow Project study area. The line labelled Leg C is the research aircraft flight leg (066 deg radial from the Cranbrook VOR) flown during the experiment. The Continental Divide is the border between Alberta and British Columbia.

Climatological data for the Rocky Mountain region between 49 deg and 52 deg north latitude during the winter season suggests that the temperature in a substantial layer above the mountain barrier is, on the average, between -10 to -20 deg C. At such temperatures precipitation formation may be inefficient due to a lack of natural ice nuclei necessary for ice crystal formation. Often, only a small fraction of the water vapour that is condensed to form orographic clouds actually falls to the ground as snow. The rest is evaporated on the leeward slopes. The addition of artificial ice-nuclei may make the natural precipitation processes more efficient and consequently provide additional precipitation. A considerable effort will be necessary to assess the technical, economical, and social feasibility of increasing the snow in southwestern Alberta by cloud seeding. These problems have not been addressed in this phase of the study.

A map of the project area is shown in Figure 1. The target area was selected mainly because the area contains the drainage basins of the Oldman and Bow Rivers, the principal sources of irrigation water for southern Alberta and because of the favourable temperature regimes. In attempting to predict potential cloud seeding effects, it is important to have knowledge of the cloud hydrometeor phase and size distributions in the natural clouds. This project was designed to obtain in-situ observations of the cloud composition and thermodynamic structure. The primary research tools employed were the INTERA Environmental Consultants Ltd. - Alberta Research Council Research Aircraft and the Alberta Research Council's mobile rawinsonde system.

This paper presents an analysis of data collected during a successful research flight on 23 March 1982.

2.0 23 MARCH 1982 CASE STUDY

The weather over the project area on March 23, 1982 was dominated by brisk northwesterly flow above 2 km MSL and shallow upslope conditions east of the divide (see Fig. 2 for a vertical cross-section). An environmental sounding was recorded by the aircraft during an ascent from the Cranbrook airport immediately upwind of the mountain barrier. The atmosphere was convectively unstable above 2.3 km MSL. The barrier height is approximately 2.5 to 3 km MSL. Surface winds at Cranbrook at the time of the sounding were from 290 deg at 9 m/s with wind gusts to 15 m/s. Air was being forced to ascend over the mountains becoming unstable and producing strato cumulus, alto cumulus, and embedded towering cumulus clouds with associated snow showers. Cloud tops were near 6 km. Cloud bases ranged from 3 km in the west to less than 1.5 km in the east.

A 150 km long flight track between Cranbrook and Lethbridge was flown 6 times at altitudes of 3.61, 3.77, 3.94, 4.10, 4.27, and 4.59 km MSL. A summary of the conditions observed during each flight leg is given in Table 1.

Table 1: Summary of the average In-Cloud Measurements on 23 March 1982. The pressure and temperature values are averages for the cloud pass. The liquid water concentration is the maximum 2s (200m) value.

No.	Time (MST)	P (mb)	T (C)	LWC (gm^{-3})
1.	1247 - 1313	670	-12.8	.2
2.	1315 - 1348	654	-14.2	.5
3.	1351 - 1415	643	-16.0	.3
4.	1418 - 1449	631	-17.2	.6
5.	1451 - 1514	620	-19.0	.4
6.	1517 - 1544	600	-21.2	.6

The liquid water content measurements are summarized in Figure 2, a schematic vertical cross section of the cloud system. The vertical axis includes the wind and temperature profile measured with the Alberta Research Council's mobile rawinsonde unit located at Rushmere. The horizontal axis includes the terrain height along the flight track and the reported weather conditions at Cranbrook, Sparwood, Pincher Creek, and Lethbridge. The liquid water contents were measured with a Johnson-Williams hot-wire probe and averaged over 10 s (approximately 1 km distance). The observations were verified by the integrated values of the cloud droplet distribution measured with a Forward Scattering Spectrometer Probe. Maximum cloud droplet concentrations were in the range 600 to 800 per cubic centimetre. Maximum liquid water contents were observed within the embedded convective cloud turrets east of the Continental Divide. Moderate riming on the aircraft wings was noted within the convective elements. Isolated regions with liquid water contents in the range 0.2 to 0.3 g per cubic metre and light aircraft riming were observed within the cloud over the mountains. The cloud system persisted throughout the afternoon and appeared to be quasi-steady. Although the individual legs of the flight each took approximately 30 min to complete, the observations have been contoured, assuming a steady state system. The convective clouds shown in the schematic figure are meant to imply that at any one time, towering cumulus did exist, however, as expected individual embedded towering cumulus clouds did not persist throughout the three hour study period.

In this study, a precipitation size particle is defined to be any hydrometeor greater than 200 microns in diameter since this is the minimum detectable size of the 2D-P optical array spectrometer probe. The next several figures summarize the 2D-P measurements. All of the 2D-P measurements have been averaged over 5 min (approximately 30 km distance) intervals. The precipitation concentrations are shown in Figure 3. Most of the cloud over the mountains had a precipitation particle concentration less than 1 per litre. The highest concentration (greater than 10 per litre) was in the upper regions of the embedded convective elements east of the mountains. The observations are consistent with the surface observations. Pincher Creek reported snow showers while stations in the mountains did not.

The mean precipitation sizes are shown in Figure 4. The size of particles increased from west to east. The largest particles (greater than 1 mm) were observed in the lower cloud regions east of the divide. These observations are consistent with a primarily horizontal particle trajectory through the cloud. Ice crystals probably formed along the western edge of the cloud and grew as they were transported by the westerly winds across the mountains and then descended on the eastern slopes, falling as snow.

The 2D-P probe measures particle sizes and concentrations. By assuming a diameter to mass relation, and particle density, the radar reflectivity can be computed. The radar reflectivity of the precipitation, assuming that all the particles are thick plate crystals, is shown in Figure 5. The diameter D (cm) to volume V (cm^3) empirical relation is taken from Pruppacher and Klett (1978, page 40):

$$V = .0897\ D^{2.778}$$

If we assume that the average particle density is 0.81 g per cubic centimetre, the diameter to mass (M g per crystal) relation is:

$$M = .0725\ D^{2.778}$$

The equivalent drop diameter is then computed from the mass:

$$D^6 = 36\ M^2/\pi^2$$

The radar reflectivity Z ($mm^6\ m^{-3}$) is then computed by summation over the volume (m^3) of the particle Diameters (mm) where:

$$Z = 0.212\ D^6$$

The factor 0.212 is the ratio of the complex indices of refraction for ice and water(Battan, 1973). The reflec-

tivity is then converted to decibels by:

$$dBZ = 10 \log_{10} Z$$

The assumption that all particles are thick plate crystals is appropriate for the major portion of the cloud over the mountains but not appropriate for the larger snow flakes east of the mountains. The largest particles within the convective turrets appeared to be moderately rimed particles with some aggregates. Undoubtedly these particles would have a lower density than that assumed. However, the relative differences in the numbers are useful, even if the absolute magnitude is not. The error involved is estimated to be approximately 5 dBZ. The main point displayed in Figure 5 is that the highest reflectivity corresponded to the larger particles in the lower regions of the embedded convective turrets. The computed reflectivity is in qualitative agreement with the observations from the aircraft radar system.

Using the same assumptions, the mass of the precipitation is shown in Figure 6. Once again, the absolute accuracy of the amounts is only within a factor of 2 to 5. Most of the cloud system contained precipitation mass amounts less than 1 g per cubic metre. The mass amounts greater than 4 g per cubic metre within the embedded convective turrets appears rather excessive and is likely due to the overestimated density of the rimed snow flakes which were encountered. The main point is that the greatest precipitation mass was located downwind of the mountains.

The total available condensate available to the cloud can be estimated using parcel theory and the upwind environmental sounding. The total amount of vapour condensed is approximately 2 g per cubic metre. Since the mass of precipitation within the cloud has been estimated the precipitation conversions efficiency can be determined. Although the efficiency ratios greater than 100% are questionable considering the assumptions involved, the relative differences are the important feature. The precipitation conversion efficiencies for the cloud over the mountains are thought to be quite accurate since the particle assumptions are reasonable there. As the previous figures indicated, the orographic cloud system was quite inefficient. Regions of supercooled water greater than 0.2 g per cubic metre over the mountains were less than 50 per cent efficient in their conversion to precipitation size particles. The high conversion efficinencies were associated with the embedded convective clouds and the upslope conditions east of the mountains. This conclusion is consistent with the surface observations. Stations east of the mountains received snow while stations in the mountains did not. The high efficiency of the clouds east of the mountains deserves some explanation or rather speculation. The convective elements contained the strongest updrafts and the greatest supercooled liquid water contents. This region appeared to be an accumulation region for the ice crystals which were transported from the cloud over the mountains from the west. The ice crystals had already grown to an appreciable size and were very efficient rime collectors when they encountered the higher liquid water regions and consequently grew very rapidly. The classic mountain orographic scenario differs substantially from the 23 March 1982 case study because of the saturated upslope conditions at the lower levels east of the mountains. Rather than dry downslope conditions east of the mountains, where ice crystals would normally evaporate, the saturated upslope conditions acted to enhance the growth of precipitation.

3.0 CONCLUSIONS

The experiment performed from 16 to 26 March 1982 gathered physical evidence concerning the modification potential of wintertime orographic clouds over the Rocky Mountains of southern Alberta. These measurements were the first of their kind in Alberta. The case study analysis of the 23 March 1982 cloud data suggests that the mountain orographic clouds do on occasion contain rather appreciable amounts of supercooled liquid water which may not be effectively converted to precipitation.

A substantial portion of the cloud layer on 23 March 1982 was warmer than -20 C, and the precipitation conversion efficiencies were less than 50 per cent, therefore, it is possible that the precipitation process could have been made more efficient if artificial ice nuclei had been added.

These results are sufficiently encouraging to propose a multi-year program to continue the investigations. During March 1983 another eight research flights with a total of 32 hours of flight time were accumulated. It now appears that the synoptic condition giving upslope east of the divide with convective instablility west of the divide occurs quite frequently. Analyses will continue to assess the weather modification potential of the various weather conditions and cloud systems which have been encountered.

ACKNOWLEDGEMENTS

The authors would like to specifically thank A. Lisonbee and D. Healey of INTERA for their efforts in the research aircraft on the day of this experiment. Grateful acknowledgement is made to all staff of the Atmospheric Sciences Department of the Alberta Research Council involved in the collection of the upper air data. This project was funded by Alberta Agriculture and the Alberta Research Council.

REFERENCES

Battan, L.J., 1973: Radar Observations of the Atmosphere. University of Chicago Press. Chicago, 324pp.

Pruppacher,H.R., and J.D. Klett: 1978: Microphysics of Clouds and Precipitation. Reidel Publishing Co. Boston, 714pp.

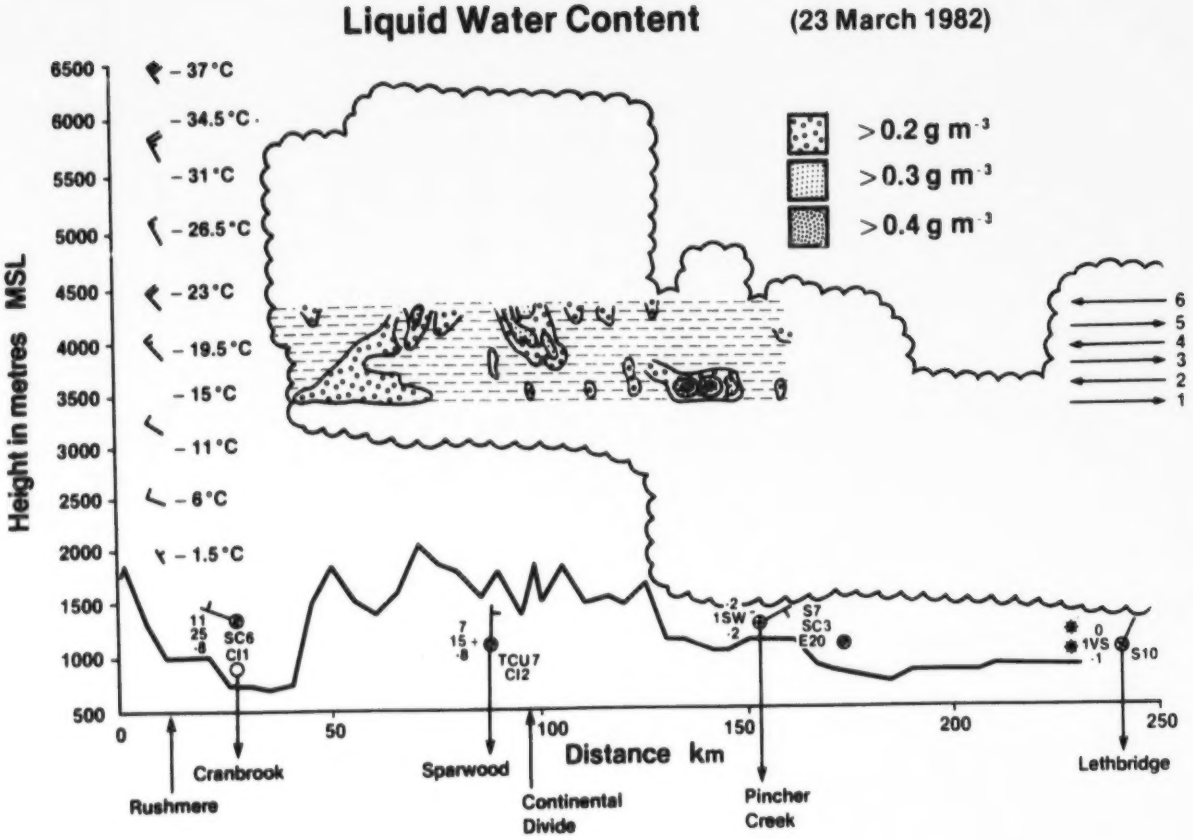

Figure 2: A schematic vertical cross section along Leg C of the cloud system and the measured liquid water contents on 23 March 1982. The liquid water contents represent 10 s averages (approximately 1 km distance) from the Johnson- Williams hot-wire probe. The vertical profile of wind (full barb equals 10 m/s) and temperature from the mobile rawinsonde at Rushmere is located along the vertical axis. The terrain height and surface weather observations at Cranbrook, Sparwood, Pincher Creek, and Lethbridge are shown along the horizontal axis. The locations and directions of the six research aircraft cloud penetrations are indicated.

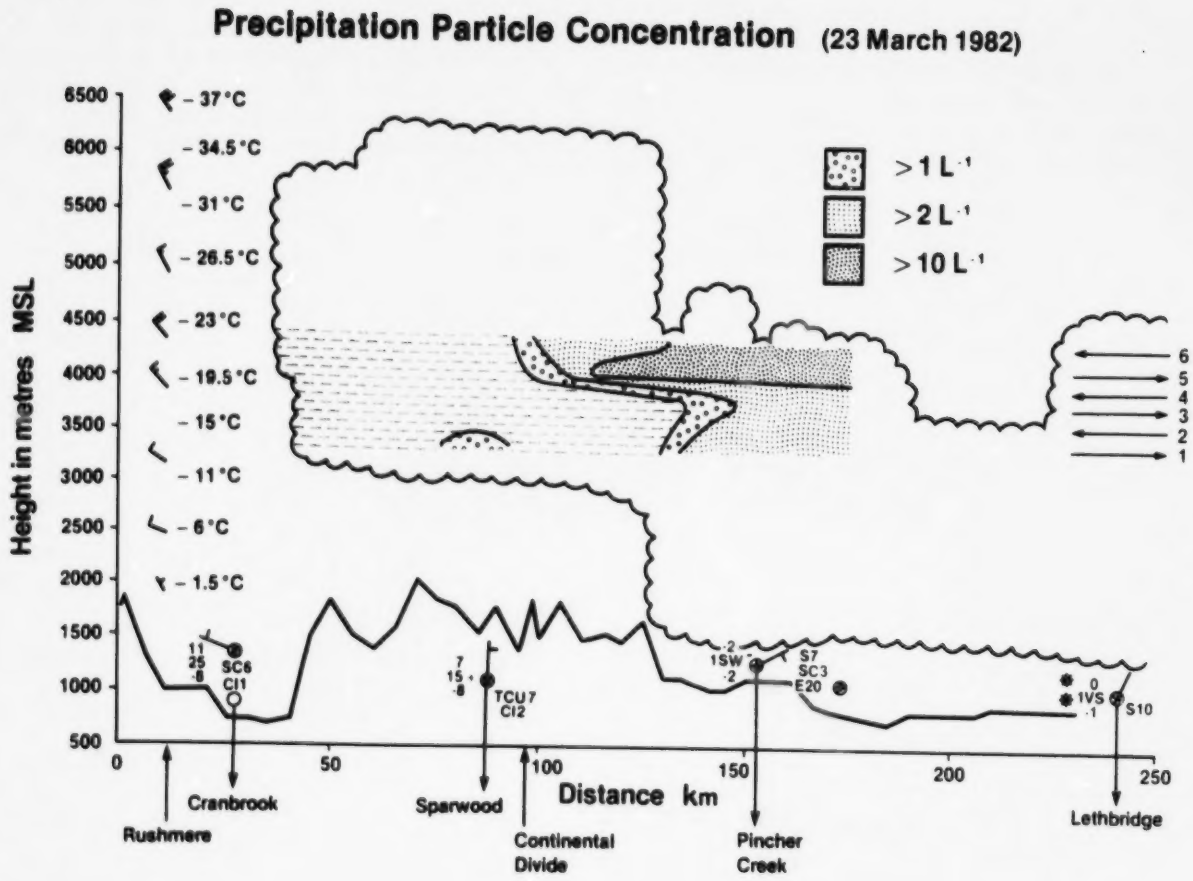

Figure 3: The precipitation particle concentration on 23 March 1982.

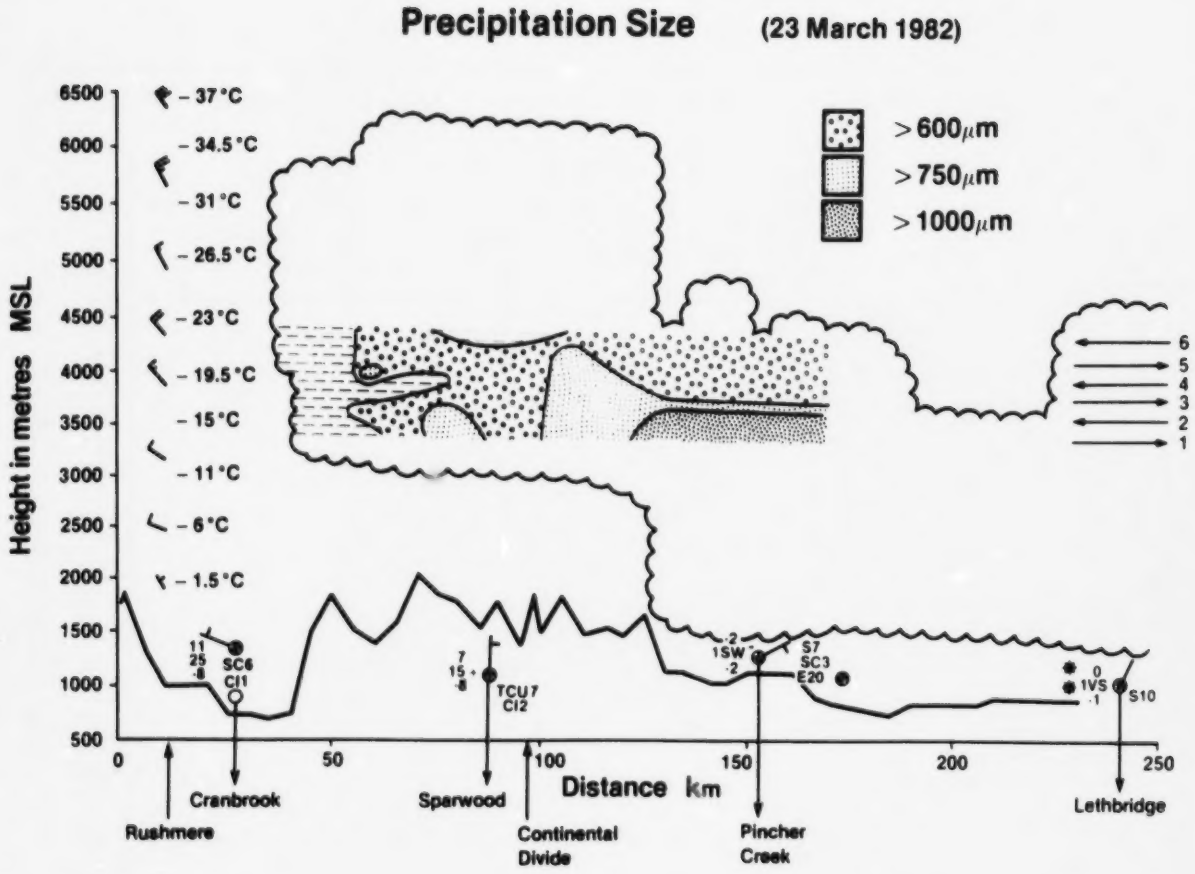

Figure 4: The average sizes of precipitation particles on 23 March 1982.

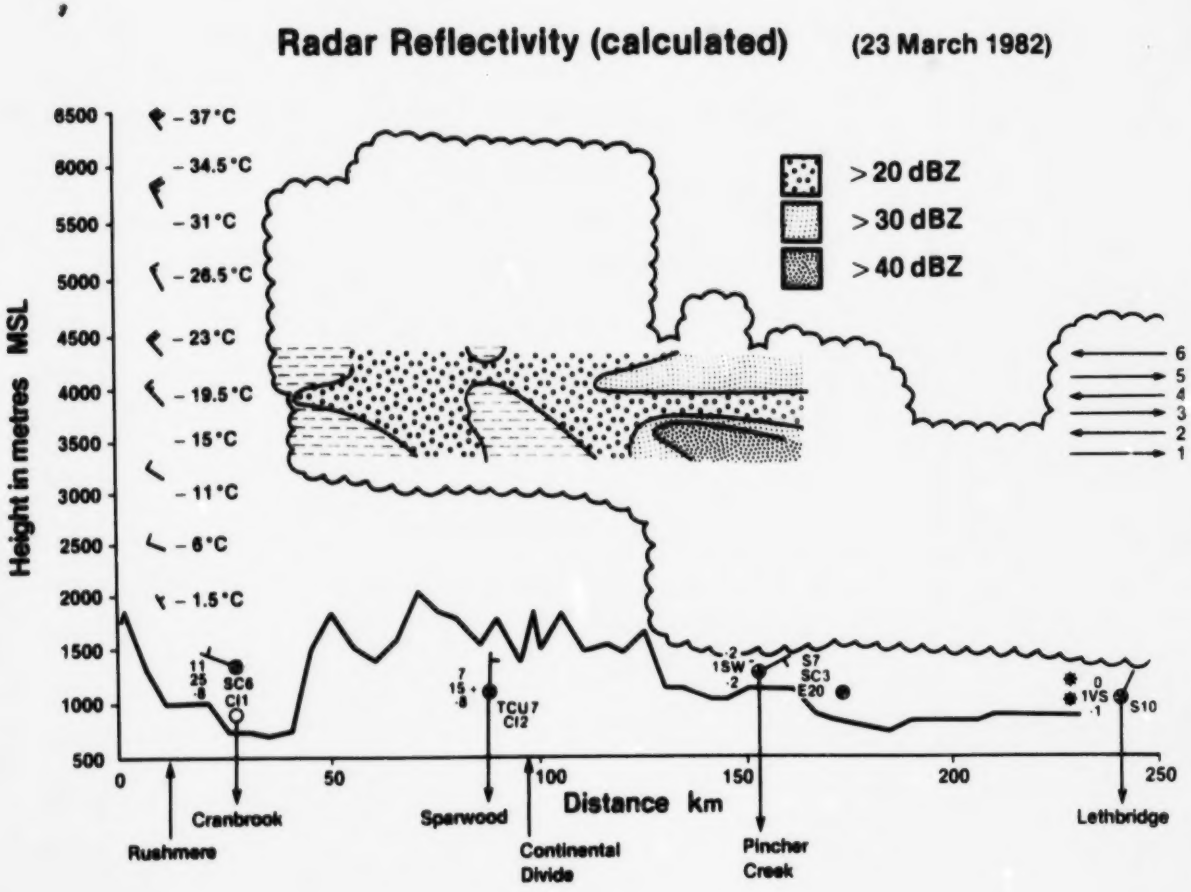

Figure 5: The calculated radar reflectivity of the precipitation particles observed on 23 March 1982. See the text for an explanation of the assumptions used in the calculation.

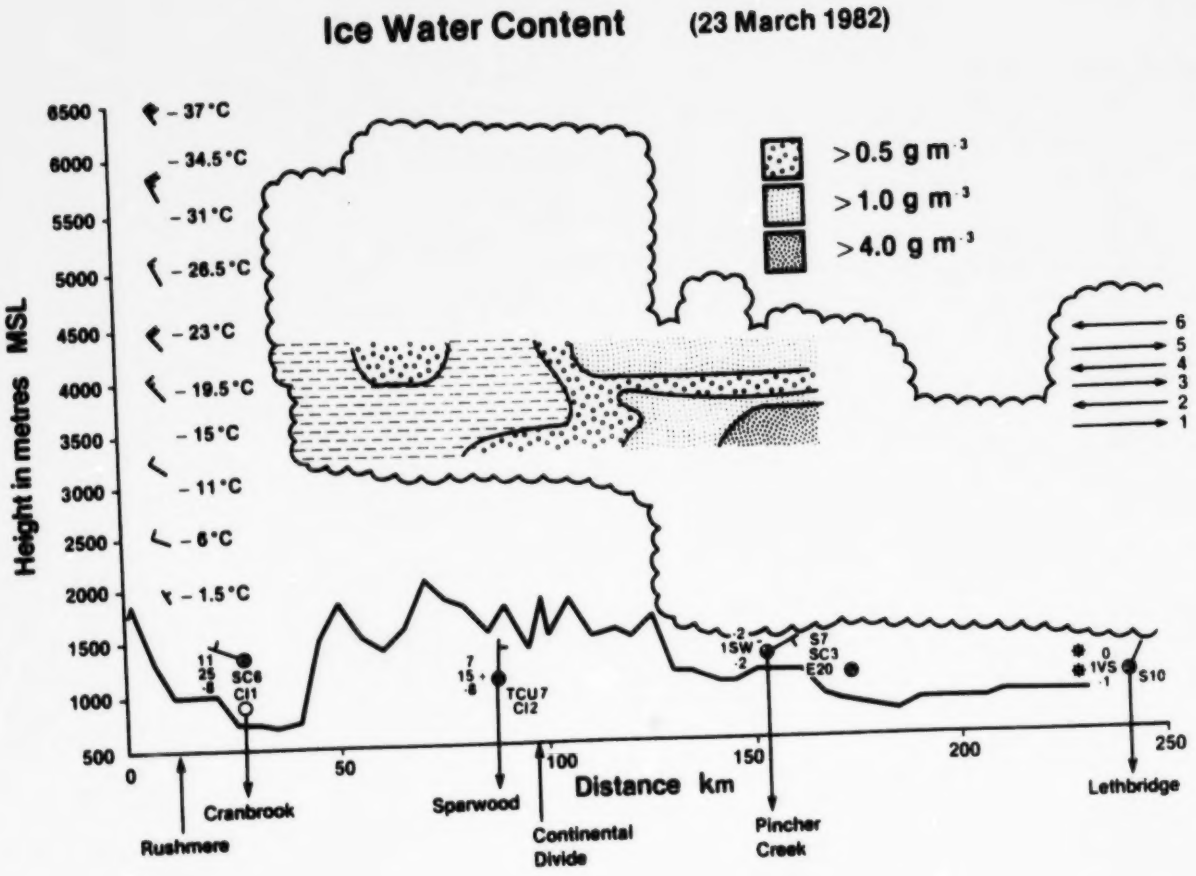

Figure 6: The ice water content (melted ice mass) of precipitation particles on 23 March 1982.

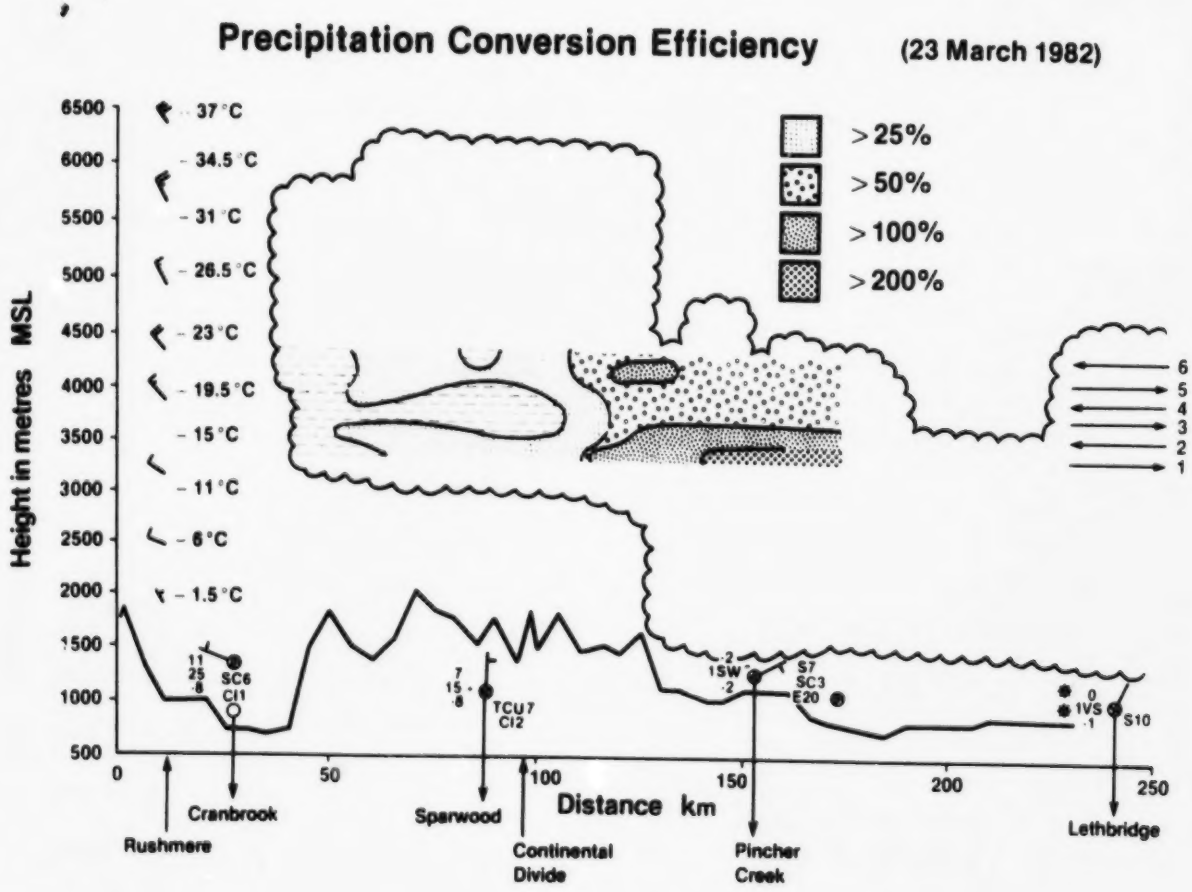

Figure 7: The precipitation conversion efficiency of the cloud system on 23 March 1982. The precipitation conversion efficiency is defined as the ratio of Ice Water Content to Total Vapour Condensed as determined from the environmental sounding at Rushmere.

Results of a Cumulus Seeding Experiment

B. Kochtubajda

Atmospheric Sciences Department
Alberta Research Council
Edmonton, Alberta

Paper prepared for the 17th Annual Congress, Canadian Meteorological and Oceanographic Society, Banff, Alberta, May 3-5, 1983

Results of a Cumulus Seeding Experiment

B. Kochtubajda

Atmospheric Sciences Department
Alberta Research Council
Edmonton, Alberta

ABSTRACT

Seeding experiments, to assess the potential for increasing or decreasing rainfall in towering cumulus clouds, using silver iodide flares or dry ice pellets, have been conducted in Alberta since 1978. The results of a cumulus seeding experiment performed on June 15, 1982 are presented.

A test cloud meeting the liquid water and ice content criteria was seeded at the -10°C level with silver iodide flares. Microphysical measurements were made with the INTERA/ARC Research Aircraft Facility. The ice crystal concentration increased by two orders of magnitude, within the in-cloud seeding plume, 6 minutes after seeding. A radar detectable echo, oriented parallel to the seeding track and displaced downwind, was observed about 10 minutes after seeding. These observations are consistent with previously defined weather modification hypotheses.

1. INTRODUCTION

Seeding experiments on towering cumulus clouds conducted in Alberta (English and Marwitz, 1981), suggested that cloud seeding can initiate the precipitation process and that droppable silver iodide (AgI) flares may be more effective in enhancing precipitation than dry ice (CO_2) pellets. The hypothesis is that the ice process can be initiated earlier by introducing seeding material in the cloud which is low in natural ice crystals. Further experiments are required to support these results and to determine the range of conditions for which they apply.

Additional cumulus cloud seeding experiments were conducted, as part of the Alberta Hail Project during the summer of 1982, to document the effects of applying various treatments to these clouds. The results from a seeding experiment conducted on June 15,1982 are presented here.

2. EXPERIMENTAL PROCEDURE

The experiments involved the INTERA/Alberta Research Council instrumented cloud physics research aircraft (a Cessna 441 CONQUEST) and a seeding aircraft, flying in formation with the seeding aircraft about 5 km behind and 300m above the research aircraft. A towering cumulus cloud was accepted for experimentation if the research aircraft measured liquid water contents in excess of 0.5 gm^{-3} , and ice crystal concentrations less than 1 l^{-1} , for five consecutive seconds, on their initial penetration. The supercooled water was measured using the Johnson-Williams (JW) liquid water probe, and the ice crystal concentration was measured with the Particle Measuring Systems OAP-2D-C probe.

The crew of the seeding aircraft was then instructed to open an envelope specifying which of three possible treatments was to be applied. The seeding treatments include: droppable AgI flares (one flare every 250 m), a low rate of dry ice pellets (ten gm CO_2 every 100 m), and a placebo. After applying the specified treatment, the seeding aircraft would stand off to photograph the cloud while the research aircraft would penetrate the test cloud repeatedly, making its measurements.

3. DESCRIPTION OF JUNE 15,1982 CUMULUS SEEDING EXPERIMENT

A cumulus cloud experiment was conducted on June 15, 1982. The cloud was located approximately 137 km west-north-west of the radar site. The initial penetration by the research aircraft indicated that the cloud had met the criteria for a seeding experiment. The cloud was then seeded with 27 AgI pencil flares (NEI TB-1 20g) at the -10°C level.

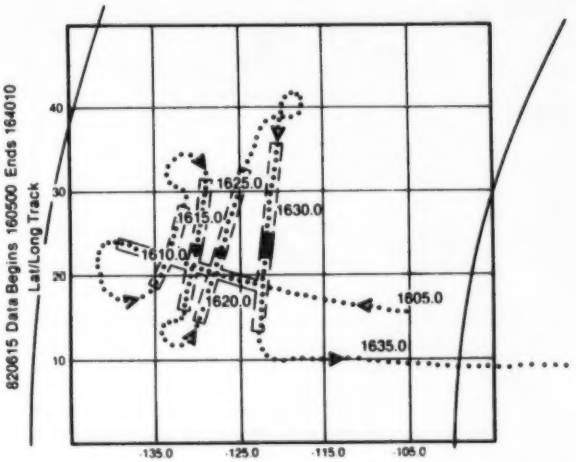

Figure 1. The research aircraft flight track on June 15, 1982. The outlined regions represent the time that the aircraft was in cloud. The stipled regions represent the locations where the aircraft encountered the seeding plume, defined by 2D-C ice particle concentrations >10 : l^{-1}.

The flight track of the research aircraft is shown in Figure 1. Five penetrations were made on this test cloud. Some of the microphysical properties measured during each penetration are summarized in Table 1. The outlined region in Figure 1 represents the time that the aircraft was in cloud. The stipled areas represent the locations where the aircraft encountered the seeding plume. Ice crystal distributions were measured with a PMS OAP-2D-C probe. The seeding plume was defined by 2D-C ice particle concentrations >10 l^{-1} .

The ice crystal size distributions encountered in this flight are presented in Figure 2. The minimum detectable crystal diameter is 25 microns. The ice crystal size distributions for the first two penetrations represent averages over the entire cloud width, while the distributions for the next three penetrations represent averages over the seeding plume.

There were few ice crystals encountered during the first two penetrations, and the maximum 1 sec (90 m) concentrations were less than 1 l^{-1} . During the third penetration, a seeding plume approximately 500 m wide was detected. An increase in the concentration of small ice crystals was observed. The average concentration in the plume was 15 l^{-1} , and the maximum 1 sec concentration was 17 l^{-1} . During the fourth

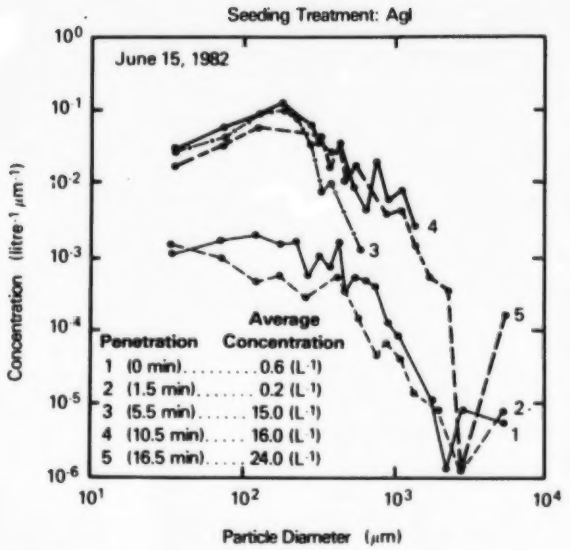

Figure 2. The ice crystal size distributions for each penetration. The size distribution for the first two penetrations represent averages over the entire cloud width. The remaining three ice crystal size distributions represent averages over the seeding plume.

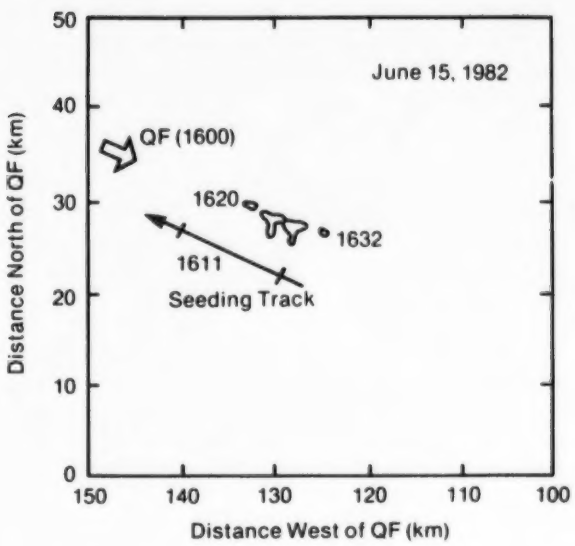

Figure 3. The track of the seeding aircraft, and the resulting radar echoes. The arrow represents the wind direction at the seeding level as reported from the afternoon sounding at Penhold. The radar echo contours represent the 20 dBZ boundary. The times on either side of the echoes indicate when the cloud first became radar detectable and when it disipated.

penetration, the seeding plume (approximately 250 m wide) was detected again. The average concentration in the plume was then 16 l^{-1}, and the maximum 1 sec concentration was 23 l^{-1}. On the last penetration, 16.5 min after seeding, the seeding plume was approximately 1.7 km wide and had an average concentration of 24 l^{-1}, with a maximum 1 sec concentration of 64 l^{-1}. The high concentrations of small ice crystals during the last three penetrations indicate a strong seeding effect. The results are consistent with observations of AgI seeded cumulus clouds in Yellowknife (Strapp et al., 1979).

4. RADAR DATA

The flight track of the seeding aircraft and the radar echoes resulting from the seeding experiment are presented in Figure 3. The apparent north-east displacement between the seeding track, the seeding plume and the radar echoes may be attributed to errors in data processing and/or winds in the vicinity of the experiment. The winds at the seeding level were from the west-north-west.

The seeded cloud became radar detectable 10 minutes after the seeding treatment was applied (Minimum Detectable Signal at this range was 19.5 dBZ), and its echo lasted for about 12 minutes before dissipating. It was oriented parallel to the seeding track and displaced downwind. Over the time that the seeded cloud was radar observable, there were no natural echoes within 60 km. The echo developed at the -8.0°C level and reached a maximum of 24 dBZ approximately 8 minutes after it was initially detected by radar. This distinctive radar signature agrees with the findings reported by English and Marwitz (1981,1982).

5. SUMMARY

A cumulus seeding experiment was conducted on June 15, 1982. The findings corroborate the results reported on the experiments conducted in Alberta in 1978 and 1979.

This case study revealed that cloud seeding can be effective in producing ice crystal concentrations higher than natural concentrations. A distinctive radar signature, elongated in shape, oriented parallel to the seeding track and displaced downwind was observed.

More seeding experiments are planned to confirm these results.

6. ACKNOWLEDGEMENTS

The author gratefully acknowledges the efforts of the crews in the research and seeding aircrafts, and of the staff of the Atmospheric Sciences Department of the Alberta Research Council on the day of this experiment.

This project was funded by Alberta Agriculture and the Alberta Research Council.

7. BIBLIOGRAPHY

English, M., and J.D. Marwitz, 1981: A Comparison of AgI and CO_2 Seeding Effects in Alberta Cumulus Clouds. Journal of Applied Meteorology, Vol. 20, 483-495.

English, M., and J.D. Marwitz, 1982: The Evolution of Radar Echo in a Seeded Cloud. Atmosphere-Ocean, Vol. 20, 28-38.

Isaac, G.A., J.W. Strapp, R.S. Schemenaur and J.I. MacPherson, 1982: Summer Cumulus Cloud Seeding Experiments near Yellowknife and Thunder Bay, Canada. Journal of Applied Meteorology, Vol. 21, 1266-1285.

Strapp, J.W., H.G. Leighton, and G.A. Isaac, 1979: A Comparison of Model Calculations of Ice Crystal Growth with Observations Following Silver Iodide Seeding. Atmosphere-Ocean, Vol.17, 234-264.

Table 1

Cloud Penetration Data Summary

Time (MDT)	Altitude (m)	Temperature (°C)	Max. JWLWC (gm^{-3})	Max. One Sec Ice Conc. (l^{-1})
1. t-3 min	4515	-7.9	0.78	<1
Seeding at 1611				
2. t+2 min	4602	-8.6	1.32	<1
3. t+6 min	4533	-8.1	0.80	17
4. t+11 min	4507	-7.7	—	23
5. t+16 min	4506	-7.7	—	64

There are no values of liquid water content after the third cloud penetration because the probe malfunctioned.

Ice Crystal Evolution in a Hailstorm Feeder Cloud Following AgI Seeding

by

Terrence W. Krauss

Atmospheric Sciences Department
Alberta Research Council
Edmonton, Alberta

(Version: July 17, 1983)

Paper presented at the 17th Annual CMOS Congress, Banff, Alberta, May 1983.

Ice Crystal Evolution in a Hailstorm Feeder Cloud Following AgI Seeding

by

Terrence W. Krauss

Atmospheric Sciences Department
Alberta Research Council
Edmonton, Alberta

ABSTRACT

Three cloud turrets (feeder clouds) within the convective new growth zone of a severe Alberta hailstorm on 30 June 1982 were seeded with AgI flares as part of a controlled seeding experiment. One of the seeded feeder clouds was penetrated six times by the INTERA Environmental Consultants Ltd. — Alberta Research Council instrumented cloud physics aircraft within a 20 min period before the feeder cloud merged with the main storm complex. The natural ice particle concentration, during an initial aircraft penetration near the -8 deg C level, was less than 1 per litre. Six minutes following seeding the maximum ice concentration was greater than 100 per litre. The seeded feeder cloud developed millimeter size graupel and produced a distinct radar echo within 20 minutes after seeding. This case study demonstrates our ability to artificially increase the ice particle concentration within a hail embryo source region.

1.0 INTRODUCTION

The basic physical hypothesis underlying the present Alberta technique for hail suppression is that large, damaging hailstones occur because of a natural deficiency of freezing nuclei. It is suggested that the injection of suitable numbers of artificial nuclei promotes the formation of a large number of smaller, less damaging hailstones. The seeding hypothesis assumes that a chain of physical processes leads to more and earlier hail embryo (graupel) production, starting with an increased concentration of ice crystals. Controlled seeding experiments on hailstorm feeder clouds were conducted as part of the Alberta Hail Project during the summer of 1982 to document the microphysical and radar echo evolution of the precipitation processes within the feeder clouds. This paper presents in-cloud measurements documenting the sequence of events leading to a 'seeding signature' within a feeder cloud of a typical severe hailstorm on 30 June 1982.

2.0 EXPERIMENTAL PROCEDURE

The cloud selection, seeding, and evaluation procedures were centered around the coordinated efforts of a seeding aircraft and the INTERA Environmental Consultants Ltd.- Alberta Research Council Cessna Conquest cloud physics research aircraft. The aircraft flew in stacked formation near the -10 deg C level, with the seeder about 300 m above and 5 km behind the Conquest. The crew of the Conquest selected the test clouds and made a SEED decision during their initial penetration if several criteria were met (supercooled liquid water content exceeded 0.5 g m^{-3} and ice concentration was less than 1 L^{-1} over a 500 m interval). After cloud treatment, the Conquest then conducted systematic penetrations of the test cloud to document the effects of treatment. After treatment, the seeder aircraft would stand by and photograph the cloud.

3.0 CASE STUDY - 30 JUNE 1982.

Three cloud turrets (feeder clouds) within the convective new growth zone of the severe Alberta hailstorm on 30 June 1982 were seeded with AgI flares (NEI-TB1 with 55 g AgI each). The term 'feeder cloud' (Vickers and Goyer, 1966; Dennis et al., 1970) is used for a convective cloud turret located upwind with respect to the low-level inflow air or the mid-level flow of the main storm (same definition as that used most recently by Heymsfield et al., 1980). The successive positions of three experimental clouds (A, B, and C) are shown relative to the low level radar echo and hailswath in Figure 1.

Cloud A (seeded with 7 flares) dissipated quickly and an ice crystal plume was not detected. Feeder clouds may decay rapidly (evaporate) due to entrainment. While rapid decay prevents precipitation development, it also represents an effective method of reducing hail embryo production. Future experiments will continue to investigate entrainment and cloud lifetimes. Cloud B (seeded with 39 flares) was very close to the main storm and merged quickly. An ice crystal plume was again not detected, probably because the seeding material was transported into the main storm which was not penetrated. Cloud C (seeded with 13 flares), however, was long-lived and was penetrated 6 times by the Conquest within a 20 min period before it merged with the main storm complex. Two photographs of the storm are shown in Figure 2. The first photograph shows feeder cloud C and the southern end of the new growth zone at 1554, looking towards the southeast. The second photograph shows feeder cloud C at 1613 looking towards the northwest. By 1613, feeder cloud C had grown substantially and had merged with the main storm cloud mass.

The evolution of the ice crystal size distribution within cloud C after seeding is summarized in Table 1 and shown in Figure 3. The distributions were measured with an OAP-2D-C probe from Particle Measuring Systems, Inc. (PMS) and represent averages over the entire cloud width. The minimum detectable crystal size is 25 microns. The probe's maximum optical aperture is 800 microns; however, larger particles can be viewed and are sized according to their maximum dimension viewed along the direction of flight. Although the absolute accuracy of the particle concentration is approximately within a factor of 5, most of the uncertainty is due to systematic errors which result reproducibly from faulty calibration and bias associated with the instrument. The precision of the PMS probes is very good, therefore, the size distributions are shown without error bars and a high degree of confidence is placed on the relative differences in the distributions.

For the first two cloud penetrations, very few ice crystals were encountered and the concentration was less than 1 L^{-1} . The size distribution of the natural ice, shown in Figure 3a, peaks near 100 μm for the first two penetrations. During the third penetration (6 min after seeding) a dramatic increase in small ice crystals was detected. The maximum 1 s (100 m) ice concentration was 146 L^{-1} and the average ice concentration for the penetration was 3 L^{-1} . Ice crystals cannot be clearly distinguished from water drops at sizes less than 100 μm using the 2D-C probe. The small images are assumed to be ice crystals because water droplets of this size are not generally seen within these young continental cumulus clouds. An ice phase precipitation mechanism dominates within Alberta summer cumulus clouds

rather than a liquid droplet coalescence precipitation mechanism (Krauss, 1981).

Ten min after seeding (Figure 3b) the maximum ice concentration was 73 L^{-1} and the average concentration was 4 L^{-1} . Thirteen min after seeding the maximum concentration was 32 L^{-1} and the average concentration was 6 L^{-1} . Twenty min after seeding the maximum concentration was 94 L^{-1} and the average concentration was 5 L^{-1} . Graupel particles 1 to 2 mm diameter were also observed on the final pass. The increased concentration of large particles with time was verified by the measurements of the OAP-2D-P probe which has a minimum detectable size of 200 microns and a maximum optical aperture of 6.4 mm. It recorded concentrations less than 0.1 L^{-1} during the first four penetrations and then measured maximum concentrations of 2 L^{-1} and 6 L^{-1} for the penetrations at 13 and 20 min after seeding. The persistently high concentration of small ice crystals is consistent with the observations of Strapp et al. (1979) in their case study analysis of AgI seeded clouds near Yellowknife. The continued production of small ice crystals appears to be a characteristic of AgI rather than the result of a secondary ice production mechanism such as drop shattering, rime splintering, crystal fragmentation, or cirrus seeding.

The concentration of particles larger than 100 μm increased by an order of magnitude 10 min after seeding. This dramatic increase in the concentration of large ice crystals is a primary indicator in the identification of a seeding signature. These observations are similar to those of Isaac et al. (1982) for their cloud seeding experiments near Yellowknife and Thunder Bay.

It might be expected that ice crystals due to the AgI should have been observed during the second penetration. However, typical diffusion rates would only have dispersed the plume to approximately one tenth the horizontal size of the cloud in four minutes, so the likelihood of missing the plume was 90%. Secondly, the crystals may not have reached minimum detectable size even if the edge of the plume had been penetrated. The observed ice crystal size distributions are not thought to have been contaminated by the main storm because the environmental winds at the penetration levels were from the southwest at 12 to 18 m s^{-1} , thereby carrying any ice crystal blow-off from the anvil towards the northeast, away from the new growth zone.

A quantitative ice-water budget could not be determined for this case study due to limitations in the liquid water instrumentation. Qualitative observations indicate that the supercooled water which existed initially was reduced substantially. However, the cloud is not thought to have been overseeded because the 2D images indicated that the riming of ice particles led to the formation of millimeter size graupel rather than ice crystal aggregates.

4.0 RADAR ECHO DEVELOPMENT

The Alberta Hail Project C-band radar indicated that feeder cloud C produced an echo with reflectivity greater than 20 dBZ at 1610 MDT. The first echo appeared rather fragmented with a portion near the 0 deg C isotherm and an upper portion between the -10 to -20 deg C levels. The radar reflectivity calculated from the aircraft measurements during penetration 6 was 5 dBZ. The echo near the 0 deg C level may have been associated with the melting of ice crystals and graupel. A PPI representation of the storm at 1610 is shown in Figure 4. The first panel shows the radar echo near 1.5 km MSL (+ 20 deg C) corresponding to the precipitation below cloud base. Reflectivities of 45 dBZ and greater are indicative of heavy rain and/or small hail. The second panel shows the radar echo near 6 km MSL (-15 deg C). Reflectivities greater than 50 dBZ existed within the main storm cell, and feeder cloud C contained an isolated echo greater than 25 dBZ. The visual cloud outline and the aircraft flight track are also indicated. The third panel shows the digital radar data corresponding to the second panel. The minimum detectable signal this close (30 km) to the radar is approximately 8 dBZ.

A history of the radar vertical cross section of feeder cloud C along line AB in Figure 4 is shown in Figure 5. The line AB is oriented along the mid-level wind direction and the sequence depicts the motion of feeder cloud C with respect to the ground. For clarification, the vertical cross section at 1613 can be compared to the cloud photograph at the same time which appears in Figure 2b. At 1613 feeder cloud C contained reflectivity near 40 dBZ in the upper levels. The reflectivity increased to 45 dBZ between 4 and 8 km MSL about 3 minutes later. The main reflectivity core within feeder cloud C then descended to the surface by 1620 and the feeder cloud essentially lost its identity within the main storm cloud mass.

5.0 DISCUSSION

Experiments at the Alberta Research Council are now being designed to focus on the individual links in the overall precipitation process chain associated with hail growth. A schematic representation of the chain of events is shown in Figure 6. It is hoped that the measurements of the research aircraft will provide vital evidence required to relate cloud seeding effects in the cloud initiation stage to the hail initiation and growth

stages as observed by radar. The collection of hailstones at the surface represents the final link and level of observation. **This case study indicates that cloud seeding can on occasion be effective in producing ice crystal concentrations higher than natural within the time that feeder clouds grow and merge with a hailstorm.** Obviously many more controlled seeding experiments must be conducted in order to answer the important questions on the frequency and the magnitude of this result and on the conditions under which it occurs.

Figure 7 represents a conceptual model of the precipitation processes leading to the formation of hail within a severe Alberta hailstorm. The dominant hail formation mechanism involves graupel particles which are grown within feeder clouds and then transported by the wind into the main storm where they grow to hailstones along the edge of the main updraft. The conceptual model compares well with the 30 June 1982 hailstorm. The significance of this research is that direct physical evidence has been gathered to support the critical assumption in our hail suppression hypothesis of being able to increase the natural ice concentration. Although the supercooled water was depleted within the feeder cloud, it is not known whether beneficial competition was achieved within the main storm.

In the past, little success has been achieved in statistically evaluating the operational cloud seeding by comparing seeded storms with non-seeded storms. The new technique, based on in-situ observations with an instrumented research aircraft, promises to reduce some of the variability of the storms analyzed by comparing seeded feeder clouds to non-seeded feeder clouds, and add information about the degree to which a storm was seeded. The results may be useful for fine-tuning the evaluation techniques before one attempts to detect noticeable changes in the precipitation at the surface.

ACKNOWLEDGMENT

The author would like to specifically thank K. Grandia and D. Healey of INTERA and R.J. Deibert of the Alberta Research Council for their efforts in the research aircraft on the day of this experiment. Special thanks to K. Finstad for providing cloud photographs from the seeder aircraft. Grateful acknowledgement is made to all staff of the Atmospheric Sciences Department of the Alberta Research Council involved in the collection of the hailfall and radar data. This project was funded by Alberta Agriculture and the Alberta Research Council.

REFERENCES

Barge, B.L., J.H. Renick, and M. English, 1982: Forecasting and radar-derived hail measurements in evaluation of hailstorm seeding experiments. Alberta Research Council Paper presented at Conf. on Hailstorms and Hail Prevention. Cercle International Grele. Sofia, Bulgaria.

Dennis, A.S., C.A. Schock and A. Koscielski, 1970: Characteristics of hailstorms of western South Dakota. J. Appl. Meteor., 9, 127-135.

Heymsfield, A.J., A.R. Jameson and H.W. Frank, 1980: Hail growth mechanisms in a Colorado storm. Part II: Hail formation processes. J. Atmos. Sci., 37, 1779-1807.

Isaac, G.A., J.W. Strapp, R.S. Schemenauer and J.I. MacPherson, 1982: Summer cumulus cloud seeding experiments near Yellowknife and Thunder Bay, Canada. J. Appl. Meteor., 21, 1266-1285.

Krauss, T.W., 1981: Precipitation Processes in the New Growth Zone of Alberta Hailstorms. Ph.D. Thesis, Univ. of Wyoming, Laramie, 296pp.

Strapp, J.W., H.G. Leighton, and G.A. Isaac, 1979: A comparison of model calculations of ice crystal growth with observations following silver iodide seeding. Atmosphere-Ocean, 17,234-264.

Vickers, W.W., G.G. Goyer, 1966: Project Hailswath: Final Report Volume III. South Dakota School of Mines and Tech., Rept. 66-9.

Table 1: Summary of Cloud Penetration Data

No.	Time (MDT)	Cloud Width	Temperature	Average Ice Conc.	Maximum Ice Conc.
1.	154800 - 154830 (Seeding at 1549)	3 km	-8.1°C	<1 per litre	<1 per litre
2.	155230 - 155300	3	-7.4	<1	<1
3.	155450 - 155530	4	-6.6	3	146
4.	155800 - 155840	4	-5.8	4	73
5.	160130 - 160220	5	-6.2	6	32
6.	160750 - 160900	7	-3.2	5	94

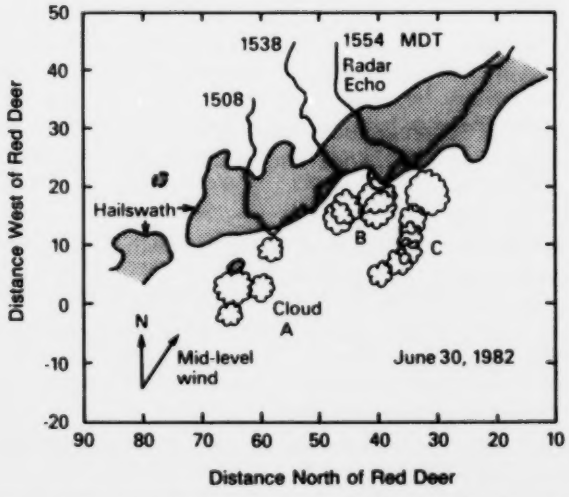

Figure 1: Successive postions of the experimental clouds A, B, and C, shown relative to the low level radar echo greater than 20 dBZ and the hailswath of the storm on 30 June 1982.

Figure 2: Two photographs of the 30 June 1982 hailstorm: (a) at 1554 looking southeast towards the southern end of the new growth zone and the seeded feeder cloud C as it appeared 5 min after seeding, and (b) at 1613 looking northwest towards feeder cloud C after it had merged with the main storm complex, 24 min after seeding.

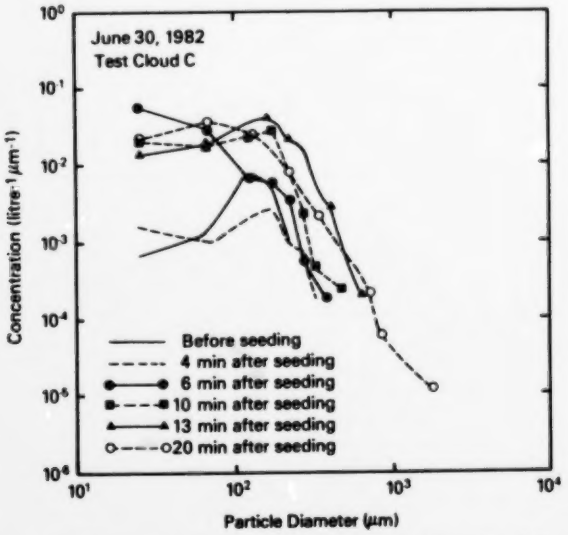

Figure 3: Evolution of the ice crystal size distribution after seeding test cloud C with AgI. The distributions are measured with a PMS 2D-C probe and are averages over the entire cloud width. The minimum detectable size is 25 μm.

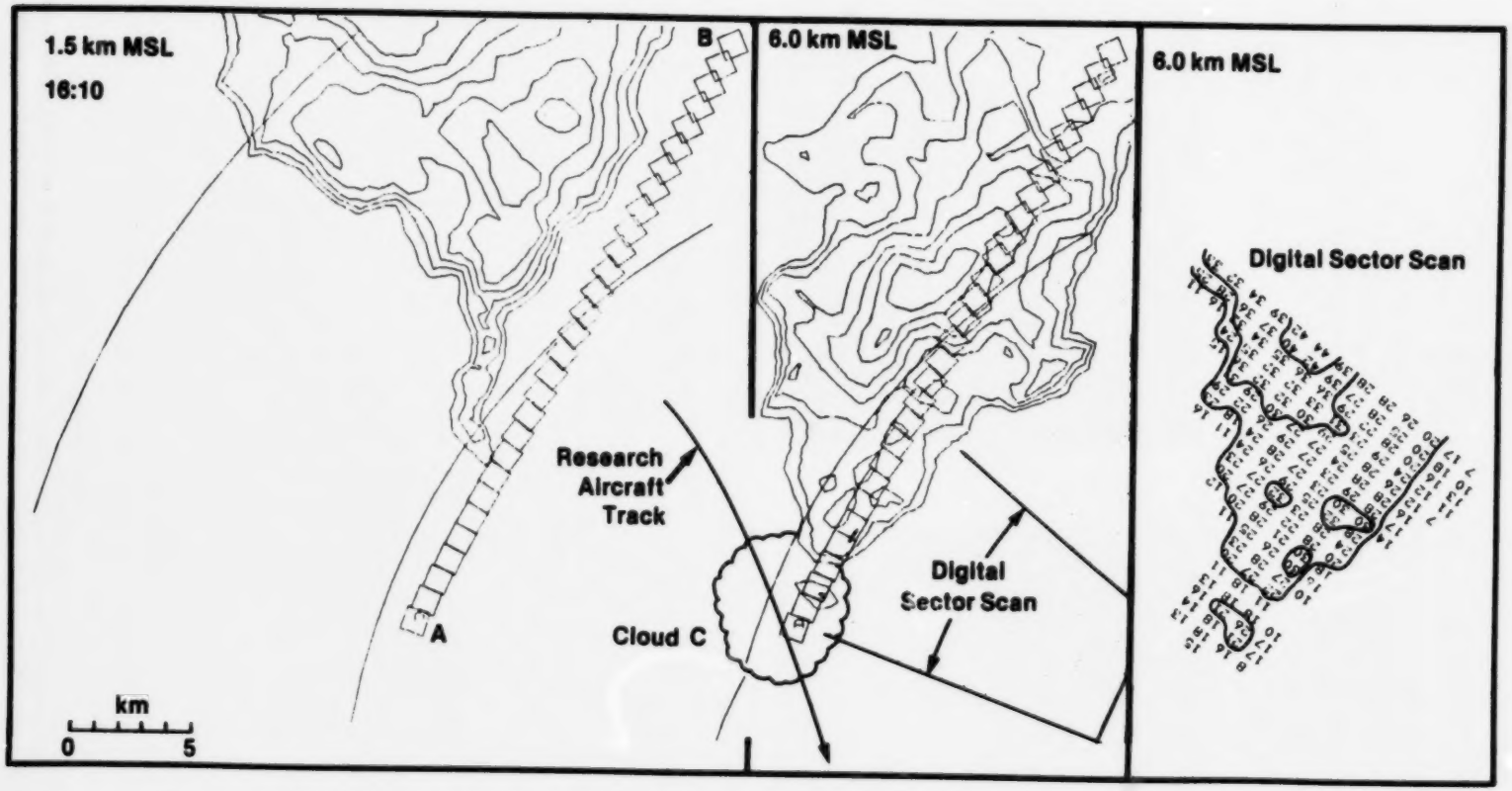

Figure 4: C-band radar reflectivity for the 30 June 1982 hailstorm at 1610 MDT. The altitude of the PPI is approximately 1.5 Km MSL in panel 1, and 6 km MSL in panels 2 and 3. Reflectivity contours are at 5 dBZ intervals starting at 20 dBZ. Panel 3 is a digital reflectivity display of the indicated sector from panel 2. The aircraft track and visual cloud outline during penetration 6 are indicated. Line AB is oriented along the mid-level wind direction and defines the vertical plane displayed in Figure 5.

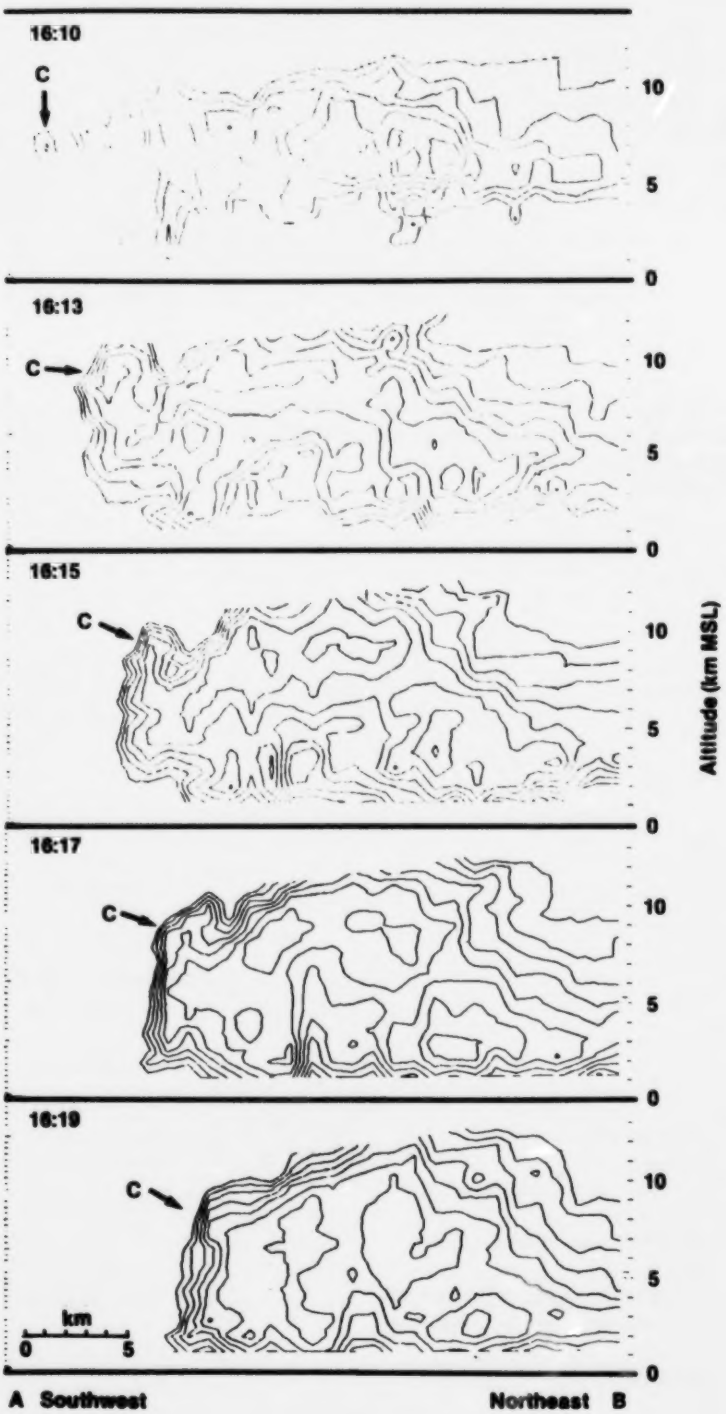

Figure 5: The sequence of radar vertical cross sections along line AB in Fig. 4 starting at 1610. Test cloud C is indicated. Radar reflectivity contours are at 5 dBZ intervals starting at 20 dBZ.

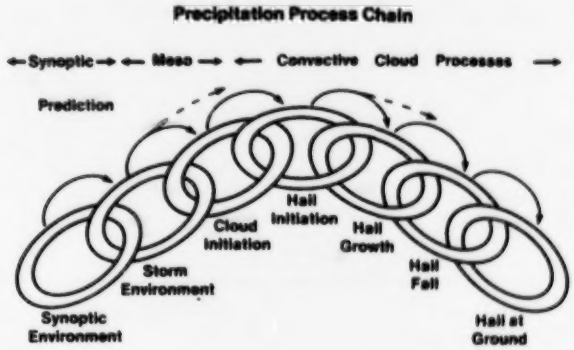

Figure 6: The 'Precipitation Process Chain' illustrating the sequence of events, not necessarily independent, which lead to precipitation at the ground. Processes within each link or event often occur on different spatial and temporal scales (from Barge et al., 1982).

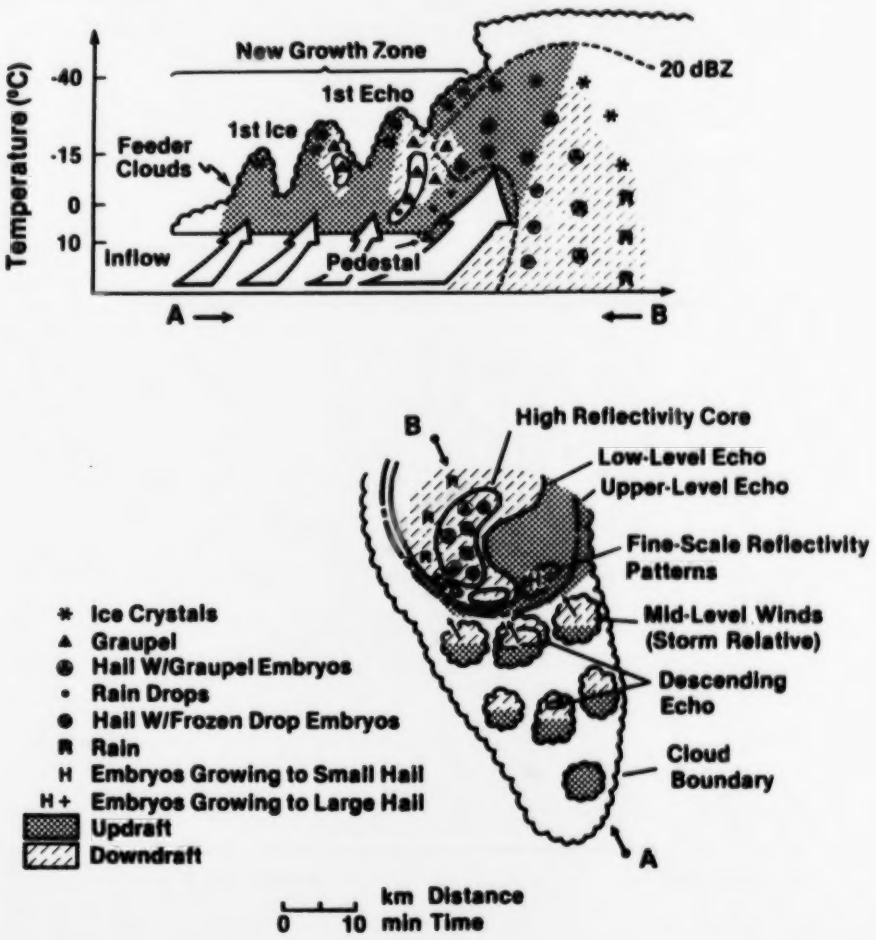

Figure 7: A conceptual model of the precipitation processes leading to the formation of hail within severe Alberta hailstorms.

POOR

QUALITY

ORIGINAL